AN ABSTRACT OF THE DISSERTATION OF

Sasha J. Rose for the degree of Doctor of Philosophy in Microbiology presented on March 15, 2016.

Title: Further Understanding Mycobacterial Biofilms and Their Interaction with the Host

Abstract approved:

_____

Luiz E. Bermudez

Respiratory infections caused by nontuberculous mycobacteria (NTM), especially *Mycobacterium avium*, can lead to progressive, recurrent disease that is refractory to therapy. Bacterial biofilms are intrinsically resistant to a variety of stressors and pressures, including host killing mechanisms and antibiotic therapy. Though it is becoming increasingly evident that NTM biofilms are important for infection, it is not currently known how these biofilms evade the immune response in an immunocompetent individual. Furthermore, what distinguishes biofilm-associated bacteria from planktonic bacteria is also mostly unknown. The main goals of this dissertation were to investigate the interaction between the host and the NTM biofilm, as well as to further identify and characterize the biofilm itself.

In Chapter 2, I developed an in vitro model to investigate the interaction between an established MAH biofilm and surveilling macrophages, mimicking a scenario of how these cells would encounter NTM in the airway. Using this model, I was able to assess multiple aspects of this interaction including bacterial killing, activation of macrophages, and apoptosis. My results show the biofilm eliciting a unique hyper-stimulation from the macrophages that results in attenuation of bacterial killing and early, atypical TNFα-driven apoptosis. Interestingly, UV-killed biofilms elicited similar responses from macrophages, suggesting that acellular biofilm matrix components could be contributing to this unique response.

In Chapter 3, I discovered that *M. avium* and other NTM can contain substantial amounts of extracellular DNA (eDNA) in their biofilm matrix and supernatant. Utilizing scanning electron microscopy and immuno-gold labelling, I was able to visualize the eDNA in these biofilms, yielding insight into the structural scaffolding-like properties the eDNA possesses. I determined that the eDNA was genomic in origin, and did not contain a specific exported sequence. By using DNA targeted enzymatic digestion with DNase I, I showed that eDNA is integral for biofilm establishment, persistence, and tolerance to clinically used antibiotics.

The work in Chapter 3 led me to hypothesize that eDNA is potentially secreted by active mechanisms, which contrasts the widely accepted idea that eDNA in bacterial biofilms results from cell autolysis. In Chapter 4, I conducted an in-depth analysis into the regulation and production of eDNA. I designed a model for fluorescently quantifying eDNA export in real time in undisturbed biofilms, which allowed investigation into triggers responsible for eDNA. When these results were combined with biofilm surface proteomics and a comprehensive transposon library screen for eDNA deficient mutants, my data suggests bicarbonate as a novel trigger for eDNA and identified many genes involved with the mechanism of eDNA export. Interesting components include an undescribed FtsK/SpoIIIE-like DNA exporting pore, multiple bicarbonate-interacting carbonic anhydrases, and a unique genomic region in MAH and other eDNA-producing NTM that could be implicated in biofilm formation and eDNA production.

Cumulatively, the work presented in this dissertation significantly advances the information known about NTM biofilms, and how they interact with and persist in the host respiratory tract. Current therapies can be ineffective at treating NTM respiratory infections, even after very long, multidrug treatment regimens. Since there is evidence to be implicated between NTM biofilms and respiratory infection, the more we can learn about the physiology of these biofilms, the more targets we can have to direct new anti-virulence therapies toward. Both bicarbonate sensing and eDNA production could become valuable anti-virulence targets for NTM infection.

Further Understanding Mycobacterial Biofilms and Their Interaction with the Host

by
Sasha J. Rose

A DISSERTATION

submitted to

Oregon State University

in partial fulfillment of
the requirements for the
degree of

Doctor of Philosophy

Presented March 15, 2016
Commencement June 2016

Doctor of Philosophy dissertation of Sasha J. Rose presented on March 15, 2016

APPROVED:

Major Professor, representing Microbiology

Chair of the Department of Microbiology

Dean of the Graduate School

I understand that my dissertation will become part of the permanent collection of Oregon State University libraries. My signature below authorizes release of my dissertation to any reader upon request.

Sasha J. Rose, Author

ACKNOWLEDGEMENTS

I would like to first thank Luiz Bermudez for all of the opportunities he has given me for my research experience and professional development. He went above and beyond to really make me learn all the aspects of science and not just the technical skills, which I believe is very important to produce a well-rounded scientist. I would also like to thank everybody in the Bermudez laboratory, both past and present, for the welcoming environment, conversations, comradery, teamwork, brain-storming, and the ever-so-important "lab day out" adventures that we embark on every summer. I want to give special thanks to Michael McNamara, who trained me initially as an undergrad and both taught me essential techniques as well as to ask questions, and Lia Danelishvili, who has been around since day one and has always been there to give her expertise and advise. I also want to thank Michael Kent, Daniel Rockey, Aleksandra Sikora, and Kari van Zee for serving on my committee during my time as a graduate student.

I want to acknowledge all of my friends that are always ready for an impromptu mountain biking trail to shred down, mountain to summit, trail to build, whitewater to paddle, project to tinker on, or music to make. All the miles, vertical feet, sore muscles, laughs, beers, and overall good times put a smile on my face and kept me going strong through this whole journey. On this subject, I am very grateful to have Amy Palmer be my partner in crime through almost every aforementioned adventure, and through everything else. Lastly, I would like to thank my parents who have been very supportive my whole life, and have encouraged me as long as I can remember to become a doctor.

CONTRIBUTION OF AUTHORS

Chapter 1: Sasha Rose wrote the general introduction.

Chapter 2: Sasha Rose helped design and perform the experiments, analyzed data, and wrote the manuscript. Luiz Bermudez helped design and perform the experiments, provided important discussion and review of the manuscript, and funded the project.

Chapter 3: Sasha Rose designed and conducted the experiments, analyzed data, and wrote the manuscript. Lmar Babrak helped perform the electron microscopy. Luiz Bermudez helped design the experiments, provided important discussion and review of the manuscript, and funded the project.

Chapter 4: Sasha Rose designed and conducted the experiments, analyzed data, and wrote the manuscript. Luiz Bermudez helped design the experiments, provided important discussion and review of the manuscript, and funded the project.

Chapter 5: Sasha Rose wrote the discussion and conclusions.

Appendix 1: Sasha Rose helped design the experiments, conducted the experiments, analyzed data, and wrote the manuscript. Mary Neville and Renu Gupta helped design the experiments, provided review of the manuscript, and funded the project. Luiz Bermudez helped design the experiments, conducted experiments, and provided important review of the manuscript.

TABLE OF CONTENTS

TABLE OF CONTENTS (Continued)

Page

TABLE OF CONTENTS (Continued)

Page

TABLE OF CONTENTS (Continued)

Page

LIST OF FIGURES

LIST OF TABLES

LIST OF APPENDIX FIGURES

LIST OF APPENDIX TABLES

Chapter 1

General Introduction

Sasha J. Rose

Overview of Mycobacteria

The genus Mycobacteria includes a wide spectrum of species, ranging from non-pathogenic environmental organisms to the one of the most studied bacterial pathogens in the world, *Mycobacterium tuberculosis*. Mycobacteria are in the Gram-positive phylum Actinobacteria, that includes other notable members such as Streptomyces, Nocardia, Rhodocossus, and Corynebacteria. Similar to other Actinobacteria, mycobacteria have a high guanine-cytosine content, typically between 60 and 70% of their genome. The defining characteristic of mycobacteria is the lipid rich atypical cell envelope. The extra layers outside of the typical Gram-positive peptidoglycan cell wall contribute to the hardiness of mycobacteria that aids in environmental protection, persistence in the host, and resistance to many selective pressures, including antibiotics. Though classified as Gram-positive phylogenetically, mycobacteria do not reliably stain Gram-positive and are referred to as acid-fast. Due to this unique property, staining procedures usually include an acidic wash component that is effective at discriminating mycobacteria from most other bacterial genera. Mycobacteria include both the slow- and fast-growing clades, though it is worth pointing out that even fast-growing mycobacteria have a slower doubling time than most commonly-studied bacteria. Growth time for visible colonies can range from 2-3 days for typical fast-growing mycobacteria all the way to 4-6 weeks for some of the slow-growing species. The most well-known mycobacteria are *M. tuberculosis, M. leprae* that are the etiological agents of tuberculosis and leprosy, respectively, and are both obligate pathogens. One third of the human population is currently infected with *M. tuberculosis* and approximately two million individuals succumb from these infections annually (WHO 2015).

Mycobacterial Cell Envelope

Many components and arrangements within the mycobacterial cell envelope make it unique from other Gram-positive bacteria (Figure 1.1). Mycobacteria possess a peptidoglycan layer containing typical N-acetyl glucosamine and N-acetyl muramic acid molecules crosslinked by peptide bridges, however these crosslinks are distinct.

In most bacterial peptidoglycan, the crosslinks are typically 4-3, but in mycobacteria, 80% of the crosslinks are 3-3, which is not found in other bacteria (Lavollay, Arthur et al. 2008). The next layer of the envelope attached to/within the peptidoglycan is arabinogalactan, which is composed of galactan bound to arabinan (Abdallah, Gey van Pittius et al. 2007; Kieser and Rubin 2014). Bound to the arabin are varying length mycolic acids, specifically alpha-meroacids, methoxy-meroacids, and keto-meroacids, that give mycobacteria their waxy, hydrophobic properties (Takayama, Wang et al. 2005). Finally, outside of the mycolic acid layer is an outer capsule, composed of surface-exposed proteins and polysaccharides (Sani, Houben et al. 2010). An additional component in environmental mycobacterial species, but absent in *M. tuberculosis*, are glycopeptidolipids that are attached within the outer capsule and are implicated with biofilm formation (Recht, Martinez et al. 2001; Carter, Wu et al. 2003; Freeman, Geier et al. 2006; Howard, Rhoades et al. 2006; Yamazaki, Danelishvili et al. 2006), sliding motility (Martinez, Torello et al. 1999; Recht, Martinez et al. 2000), and virulence (Carter, Wu et al. 2003; Howard, Rhoades et al. 2006; Yamazaki, Danelishvili et al. 2006; Nessar, Reyrat et al. 2011).

Nontuberculous Mycobacteria

The nontuberculous mycobacteria (NTM) are the grouping of mycobacteria that are essentially not in the *M. tuberculosis* complex or *M. leprae*, and include numerous opportunistic pathogens encountered in the environment. There are over 150 described species of NTM that includes both fast- and slow-growing species (Tortoli 2003). Additionally, over 90 of these NTM species are opportunistic human pathogens (Brown-Elliott, Griffith et al. 2002; Hoefsloot, van Ingen et al. 2013). The rates of NTM infection are increasing in recent years (Lai, Tan et al. 2010; Winthrop, McNelley et al. 2010; Adjemian, Olivier et al. 2012; Henkle, Hedberg et al. 2015) and the incidence of NTM infection is estimated to be between 5 to 30 per 100,000 people (Henkle, Hedberg et al. 2015). Since NTM infections are not reported nationally to the CDC (and similarly in other countries), accurate numbers for larger populations are not known, but this estimate is a fair average, as other studies have

suggested slightly lower and higher rates (Lai, Tan et al. 2010; Adjemian, Olivier et al. 2012). NTM research has mainly focused on *Mycobacterium avium* and closely related *M. intracellulare*, which are responsible for the majority of NTM human infections and collectively referred to as the *Mycobacterium avium* Complex, or MAC (Griffith, Aksamit et al. 2007). *M. avium* itself is very heterogeneous and has four subspecies including *M. avium* subsp. *hominissuis* (MAH) that is responsible for most human *M. avium* infections (Ignatov, Kondratieva et al. 2012), *M. avium* subsp. *paratuberculosis* (MAP) that causes Johne's disease in ruminants and is also loosely connected to Chron's disease in humans (Feller, Huwiler et al. 2007), and *M. avium* subsp. *avium* (MAA) and *M. avium* subsp. *sylvaticum* (MAS) that primarily infect avian species (Mijs, de Haas et al. 2002). It has been proposed that MAP, MAA, and MAS have branched evolutionarily from MAH (Turenne, Collins et al. 2008). Other notable NTM include the *M. abscessus* complex (*M. abscessus* subsp. *abscessus*, *M. abscessus* subsp. *bolletii*, and *M. abscessus* subsp. *massiliense*), that causes human respiratory infections and are notoriously difficult to treat, *M. kansasii* that also causes human infections, *M. ulcerans* that causes Buruli ulcer, and *M. marinum* and *M. chelonae* that are common fish pathogens and cause human skin infections as well. MAC is the main focus of this dissertation, as it is responsible for most human NTM infection and the primary mycobacterial species studied by the Bermudez laboratory, however *M. abscessus*, *M. chelonae*, and other NTM are also investigated in later chapters. The following sections will discuss NTM generally, with an emphasis given to MAC and the *M. abscessus* complex, as these two groups have the most clinical interest.

NTM Infection

NTM cause different pathologies depending on the species and the immune status of the host. In immunocompromised individuals, such as AIDS patients, NTM infection is predominantly MAC, can infect through the respiratory or gastrointestinal tract, and dissemination is common (von Reyn, Maslow et al. 1994; Karakousis, Moore et al. 2004). The introduction of highly active antiretroviral therapy in 1996

greatly reduced MAC disseminated disease in AIDS patients, but before this implementation the rates of MAC infection in AIDS patients ranged between 25 to 50%, depending on the specific population assessed (Falkinham 1996). One particular study in New York found that roughly 55% of deceased AIDS patients between 1981 and 1984 had disseminated MAC determined post-mortem (Kiehn, Edwards et al. 1985). Non-AIDS individuals with genetic mutations in components of the Th1 IL-12/IFNγ pathway are very susceptible to NTM infection (Figure 1.2, red highlights), and experience serious, and many times multiple NTM infections through their lives. (Wu and Holland 2015).

NTM infection in immunocompetent individuals commonly infects the respiratory tract, is also predominantly MAC, rarely disseminates, and presents as three distinct types of respiratory infection: Cavitary, hypersensitivity pneumonitis, and nodular bronchiectasis (Weiss and Glassroth 2012; Whiley, Keegan et al. 2012; Orme and Ordway 2014). Cavitary disease is seen in individuals with preexisting lung conditions such as previous tuberculosis, chronic obstructive pulmonary disease, or having a history of smoking. Cavitary disease presents similar to tuberculosis lung infection, and in addition also can be located in the upper respiratory tract. Hypersensitivity pneumonitis develops from inhalation of NTM from aerosolized water droplets from either showerheads or hot tubs. The pathology seen in hypersensitivity pneumonitis is less from the infecting NTM and more associated with the hyper immune response the host develops. Nodular bronchiectasis is the progressive widening of the bronchi that develops multiple nodules in the middle lobe of the lungs. This type of infection usually infects older women that are otherwise healthy. Underlying respiratory conditions including cystic fibrosis, chronic obstructive pulmonary disease, and bronchiectasis, do predispose individuals to NTM respiratory infection. In immunocompetent patients, though less common than respiratory infections, NTM infections can also present on the skin (Kullavanijaya, Sirimachan et al. 1997; Noguchi, Hiruma et al. 1998; Sugita, Ishii et al. 2000), in soft tissue at surgical sites (Karakousis, Moore et al. 2004), and in otherwise healthy children as cervical lymphadenitis (Thegerstrom, Friman et al. 2008).

Host Response to NTM

Whether the NTM infection is disseminated or localized to the respiratory tract, the host response is largely Th1 in nature and involves the interplay between infected monocytes and helper lymphocytes (Wu and Holland 2015; Winthrop, Rivera et al. 2016). Figure 1.2 overviews this interplay and nicely details the NTM immune response. IL-12 is an important cytokine produced by NTM-infected macrophages that signals CD4 T cells and/or natural killer cells to produce IFNγ that helps further activate killing mechanisms in infected macrophages. TNFα is also produced by infected macrophages to activate the macrophage response and can be stimulated either by IFNγ or through pathogen associated molecular patterns from the infecting bacteria. These effectors, related receptors, and transcription factors are essential for protection to NTM, as individuals with defects in many parts of this pathway are susceptible to disseminated NTM infection (Figure 1.2, red highlights). This also explains why AIDS patients are very susceptible to NTM infection, as they have diminished CD4 T cells. Furthermore, with the recent implementation of anti-TNFα monoclonal antibody therapies for various auto-immune disorders, there has been a significant increase in NTM infections in patients on these therapies (Swart, van Ingen et al. 2009; Winthrop, Chang et al. 2009). In addition to T cells and natural killer cells aiding in control of NTM, neutrophils have also been shown to be important for controlling NTM infection mainly via indirect mechanisms (Silva, Silva et al. 1989; Appelberg, Castro et al. 1995; Saunders and Cheers 1996; Bermudez, Petrofsky et al. 1998), however one study did find phagocytosed NTM inside of neutrophils (Hartmann, Becker et al. 2001).

Intracellular NTM

Pathogenic NTM are facultative intracellular pathogens that primarily reside within macrophages, but can also infect various epithelial cells of the respiratory and gastrointestinal systems (Bermudez, Petrofsky et al. 1992; Bermudez and Young 1994; Bermudez, Shelton et al. 1995; Reddy and Kumar 2000). The routes of uptake into macrophages by NTM is not completely clear, but multiple routes have been

described. Complement receptors are important for MAC and *M. kansasii* uptake in both opsonized (Swartz, Naai et al. 1988; Bermudez, Young et al. 1991; Peyron, Bordier et al. 2000) and unopsonized fashion (Roecklein, Swartz et al. 1992; Le Cabec, Cols et al. 2000; Peyron, Bordier et al. 2000). Fibronectin receptors and fibronectin binding can also be involved with NTM uptake into macrophages (Bermudez, Young et al. 1991; Rao, Ogata et al. 1993). Mannose, acting as an opsonin and potentially inducing uptake through the mannose receptor and the collectin receptor, has also been shown to influence MAC phagocytosis (Bermudez, Young et al. 1991; Roecklein, Swartz et al. 1992). Once inside the host cell, NTM reside and replicate within a modified phagosome, similar to *M. tuberculosis*. Modifications to the typical phagosomal degradation pathway include preventing acidification (Crowle, Dahl et al. 1991; Sturgill-Koszycki, Schlesinger et al. 1994; Oh and Straubinger 1996), specifically blocking vacuolar ATPases from binding (Sturgill-Koszycki, Schlesinger et al. 1994), preventing lysosomal fusion (Frehel, de Chastellier et al. 1986; Oh and Straubinger 1996), and disrupting actin filaments (Guerin and de Chastellier 2000). Importantly, these modified phagosomes still readily bind to and fuse with endosomes (Russell, Dant et al. 1996; Sturgill-Koszycki, Schaible et al. 1996), suggesting a route that intracellular NTM access iron and nutrients. *M. avium* is resistant to nitric oxide and the respiratory burst (Appelberg and Orme 1993; Bermudez 1993; Doi, Ando et al. 1993), which is interesting, as *M. tuberculosis* is sensitive to nitric oxide. Remarkably, in vivo, blocking nitric oxide actually diminished MAH levels (Gomes, Florido et al. 1999), suggesting that MAH not only is unaffected by nitric oxide, but could actually be using it to its advantage. *M. abscessus* and *M. intracellulare* have also shown resistance to nitric oxide (Doi, Ando et al. 1993; Oberley-Deegan, Lee et al. 2009), but the susceptibility of other NTM to nitric oxide has yet to be investigated, so it cannot be concluded if the resistance to nitric oxide is a shared trait among NTM. It is interesting to hypothesize, for at least the NTM that are resistant, that this adaptation could have been acquired from the environmental niches they are found in, which could help explain why *M. tuberculosis*, an obligate pathogen, is susceptible.

Treatment of NTM

Treatment of NTM is species-specific, but there are general similarities to *M. tuberculosis* therapy such as combination therapy over monotherapy and long treatment regimens (Griffith, Aksamit et al. 2007). Combination therapy for MAC includes macrolides, usually clarithromycin or azithromycin, combined with rifampin and ethambutol (Griffith, Aksamit et al. 2007; Johnson and Odell 2014). Streptomycin and amikacin can also be used with MAC unless tolerability and toxicity become an issue. *M. abscessus* pulmonary infection is typically treated with cefoxitime, imipenem, and amikacin. In addition, tigecycline and linezolid are utilized as well (Griffith, Aksamit et al. 2007). Macrolides are generally ineffective against *M. abscessus* because two of the three of its subspecies, *M. abscessus* subsp. *abscessus* and *M. abscessus* subsp. *bolletii*, contain *erm*(41), an inducible macrolide-resistance gene (Nash, Brown-Elliott et al. 2009; Griffith 2011), so are not typically part of the regimen. *M. abscessus* is the most-drug resistant of all pathogenic mycobacteria, and in some cases, surgical recession of diseased tissue is the only option, as some patient isolates are refractory to all current therapy (Griffith, Aksamit et al. 2007).

There has been a recent shift in mycobacterial respiratory therapy from systemic to topical treatment, because it delivers drug to the site of infection and reduces systemic toxicity. For example, amikacin is particularly effective against mycobacteria in vitro, including both MAC and *M. abscessus*, however the requirement of parenteral administration and the significant risk of oto- and nephrotoxicity limit its practicality for widespread use. In a recent report using a murine *M. tuberculosis* model, aerosolized amikacin had similar efficacy as parenterally injected amikacin, despite a lower dose being used and less frequent treatment (Gonzalez-Juarrero, Woolhiser et al. 2012). Inhaled dry powder containing rifampicin or capreomycin was also effective at treating *M. tuberculosis* lung infection (Garcia-Contreras, Sethuraman et al. 2006; Garcia-Contreras, Fiegel et al. 2007). Inhaled amikacin-containing liposomes have also been recently explored against NTM by our laboratory. Liposomal encapsulation of amikacin allows the drug

to achieve much higher intracellular concentrations, compared to free amikacin or powder formulations, due to the active uptake of liposomes by macrophages. In appendix 1, we describe the efficacy of this new liposomal amikacin for inhalation against MAC and *M. abscessus* both in vitro against intracellular bacteria as well as in an experimental model of lung infection in mice (Rose, Neville et al. 2014). The encouraging results from these various topical therapy studies, and ongoing clinical trials, are creating safer, more effective treatment options for mycobacterial respiratory infection.

Environmental Sources of NTM

NTM are ubiquitous in the environment and have been isolated from, but are not limited to, freshwater, seawater, potting soil, peat moss, forest soils, and swamps. (Kirschner, Parker et al. 1992; Halstrom, Price et al. 2015). It is hypothesized that NTM interact with free living protozoan hosts also found in these reservoirs, although direct evidence of NTM found inside of environmental protozoans has not been described (Salah, Ghigo et al. 2009). Experimentally, it has been shown that NTM can infect *Acanthamoeba castellanii*, *Acanthamoeba polyphaga*, and *Dictoystelium discoideum* (Cirillo, Falkow et al. 1997; Skriwan, Fajardo et al. 2002; Harriff and Bermudez 2009; Ben Salah and Drancourt 2010). Furthermore, passage through these organisms shows similarities to macrophage infection (preventing lysosomal fusion, for example) and upregulates macrophage-associated genes producing an invasive phenotype (Cirillo, Falkow et al. 1997; Harriff and Bermudez 2009).

In addition to natural sources, NTM have been isolated from municipal water pipelines, hot tubs, swimming pools, faucets, bathtub inlets, showerheads, water heaters, commercial ice, aquaculture, and bottled water (Tuffley and Holbeche 1980; Slosarek, Kubin et al. 1993; Covert, Rodgers et al. 1999; Falkinham, Norton et al. 2001; Mangione, Huitt et al. 2001; Torvinen, Suomalainen et al. 2004; Nishiuchi, Maekura et al. 2007; Falkinham, Iseman et al. 2008; Nishiuchi, Tamura et al. 2009; Falkinham 2011; Liu, Yu et al. 2012; Whiley, Keegan et al. 2012; Thomson, Tolson et al. 2013). The ubiquity of NTM in potable water systems is due to their intrinsic

resistance to commonly used water disinfection methods, such as chlorination, ozonation, and UV-treatment (von Reyn, Maslow et al. 1994; Taylor, Falkinham et al. 2000; Lee, Yoon et al. 2010). In addition, they are also resistant to temperatures found in hot water heaters and hot tubs (Schulze-Robbecke and Buchholtz 1992). A revealing study by Feazel et al. sampled the inside of showerheads throughout the United States, conducted culture-independent metagenomics from these samples, and determined that MAC and other NTM were the most abundant bacteria identified (Feazel, Baumgartner et al. 2009). The level of enrichment for MAC was over 100 times higher in the showerheads than in the running water sampled from these sources, suggesting biofilm formation on these plumbing components. Further work analyzed nutrient availability on NTM biofilm formation and found that MAC was able to form robust biofilms in potable water, but all of the other NTM tested formed better biofilms in higher-nutrient conditions, suggesting this difference as a reason why MAC, even though it is slow-growing, is the predominant NTM found in potable water sources (Williams, Yakrus et al. 2009). It is thought that NTM infections are increasing in recent years in developed areas due to the trend that that more people are showering rather than bathing and that newer environmental regulations on water heaters reduces the temperature of hot water in residences, which reduces mycobacterial killing (Schulze-Robbecke and Buchholtz 1992). Multiple studies have directly linked strains in patients to reservoirs in bathrooms in their residence or hospital room, demonstrating the connection between environmental sources of MAC and infection (Kahana, Kay et al. 1997; Lumb, Stapledon et al. 2004; Nishiuchi, Maekura et al. 2007; Falkinham, Iseman et al. 2008; Nishiuchi, Tamura et al. 2009; Falkinham 2011; Whiley, Keegan et al. 2012; Thomson, Tolson et al. 2013).

Transmission of NTM

Although environmental acquirement is widely accepted to be the primary source of NTM infection, there have been some recent instances of human to human transmission. The first evidence of transmission occurred with *M. abscessus* subsp. *massiliense* in a lung transplant and cystic fibrosis center. One patient, who was

infected and repeatedly tested positive for seven years prior to being admitted, potentially infected four other patients at the facility, who were all continually sputum-negative for mycobacteria before their stay (Aitken, Limaye et al. 2012). Another study has linked transmission of a particular strain of *M. kansasii* between a husband and wife (Ricketts, O'Shaughnessy et al. 2014). A more comprehensive bioinformatics study sequenced 168 genomes of *M. abscessus* isolates over time from 31 patients in a cystic fibrosis treatment facility and analyzed single nucleotide polymorphisms between isolates (Bryant, Grogono et al. 2013). There were two clusters of outbreaks within patients that had numerous occasions of contact, where less SNP variation was seen between patients than within a single patient over time, strongly suggesting transmission. Furthermore, environmental samples were taken throughout the study in the facility and failed to find a reservoir for infection. Recent work in our laboratory with MAH has also demonstrated transmission experimentally, using an infection model established in the round worm, *Caenorhabditis elegans* (manuscript in submission). While this is far from a human model of transmission, it is the first successful attempt at experimental MAC transmission.

NTM Biofilms

Biofilms are aggregates of cells at an interface between either a solid and a liquid, or a liquid and air that are encapsulated in an extracellular matrix (Stoodley, Sauer et al. 2002). Figure 1.3 depicts the general developmental cycle of bacterial biofilms (Stoodley, Sauer et al. 2002). Planktonic bacteria first attach to a surface, start producing biofilm matrix to increase adherence, further aggregate and/or propagate to build a more robust architecture, and then finally a subpopulation of the biofilm disperses to colonize new surfaces. Some mycobacterial species form a biofilm pellicle on the liquid/air interface, including *M. tuberculosis* and *M. smegmatis*, however the majority of NTM attach to and form biofilm on the solid surface/liquid interface. NTM readily form biofilms on common housing plumbing surfaces, including glass, galvanized steel, stainless steel, copper, and polyvinyl

chloride when grown in a biofilm flow reactor mimicking a residential potable water system (Mullis and Falkinham 2013). In most bacterial biofilms, a major component of the biofilm matrix is exopolysaccharide, but proteins, DNA, lipids and other molecules are also found (Flemming and Wingender 2010). Mycobacteria form unique, robust biofilms that lack the hallmark matrix exopolysaccharides and do not possess the genes for their synthesis (Zambrano and Kolter 2005). Studies have primarily found lipid matrix components of NTM biofilms that are generally related to the mycobacterial cell envelope: Mycolic acids in *M. smegmatis* (Ojha, Anand et al. 2005); glycopeptidolipids in MAH, *M. abscessus, and M. smegmatis* (Recht and Kolter 2001; Freeman, Geier et al. 2006; Yamazaki, Danelishvili et al. 2006; Nessar, Reyrat et al. 2011); Mycolyl-diacylglycerols in *M. smegmatis* (Chen, German et al. 2006); Lipooligosaccharides in *M. marinum* (Ren, Dover et al. 2007); Lipopeptides in MAP (Wu, Schmoller et al. 2009). Outside of these findings of cell wall components, no actual secreted products or molecules have been described in NTM biofilms, and the biofilm matrix constituents remain mostly unknown.

There are implications when treating biofilm infections, because they are usually much more drug resistant than their planktonic counterparts. In mycobacteria, there is a large disconnect between in vitro susceptibilities to antibiotics and achieving therapeutic outcomes (Kobashi, Yoshida et al. 2006; Greendyke and Byrd 2008), and in addition to this being caused from bacteria being intracellular and encased within granulomas, biofilms are likely contributing to this problem as well. Work has shown that clinical isolates of NTM do indeed form biofilms (Carter, Wu et al. 2003; Steed and Falkinham 2006; Williams, Yakrus et al. 2009; Mullis and Falkinham 2013). From the MAC strains tested, one in particular, MAH A5, stood out for forming more robust biofilm than the others tested (Carter, Wu et al. 2003). This strain has been used in most biofilm-related MAC studies conducted since this report, and is the primary strain of *M. avium* used throughout this dissertation. Research has begun to demonstrate that NTM biofilms are an important aspect of respiratory infection. Through investigating biofilm-deficient mutants in MAH A5, it was suggested that the ability to form biofilm leads to higher binding and invasion of

epithelial cells in vitro, and significantly more surviving bacteria in the lungs of mice in vivo (Yamazaki, Danelishvili et al. 2006). More recently, *M. abscessus* biofilms were visualized with immunohistochemistry and fluorescent microscopy on tissue in explanted lung sections from cystic fibrosis patients, showing directly that *M. abscessus* respiratory infection is a biofilm infection (Qvist, Eickhardt et al. 2015). Despite this reports, the exact reasons and mechanisms behind why biofilms provide benefit during respiratory infection remain unknown.

Scope of Dissertation

Mycobacterial biofilms are of particular interest because they contribute to human respiratory infection and their biology is incompletely understood. How do NTM biofilms form in the host respiratory tract and are not cleared by the immune system? What are the bacteria within these biofilms producing and exporting into the biofilm matrix and surrounding environment? What is the regulation of the mechanisms related to these biofilms? These are important questions that the work presented in the following chapters of this dissertation aim to answer. In chapter 2, I create and explore an in vitro model with *M. avium* biofilms and surveilling phagocytes to determine the specific interaction between these biofilms and the host during infection. In chapter 3, I describe the novel finding of extracellular DNA in NTM biofilms and characterize the attributes and role of eDNA within these biofilms. Finally, chapter 4 investigates the triggers of eDNA production, and uses selective proteomics and transposon mutagenesis to identify genes and proteins important for eDNA production and regulation.

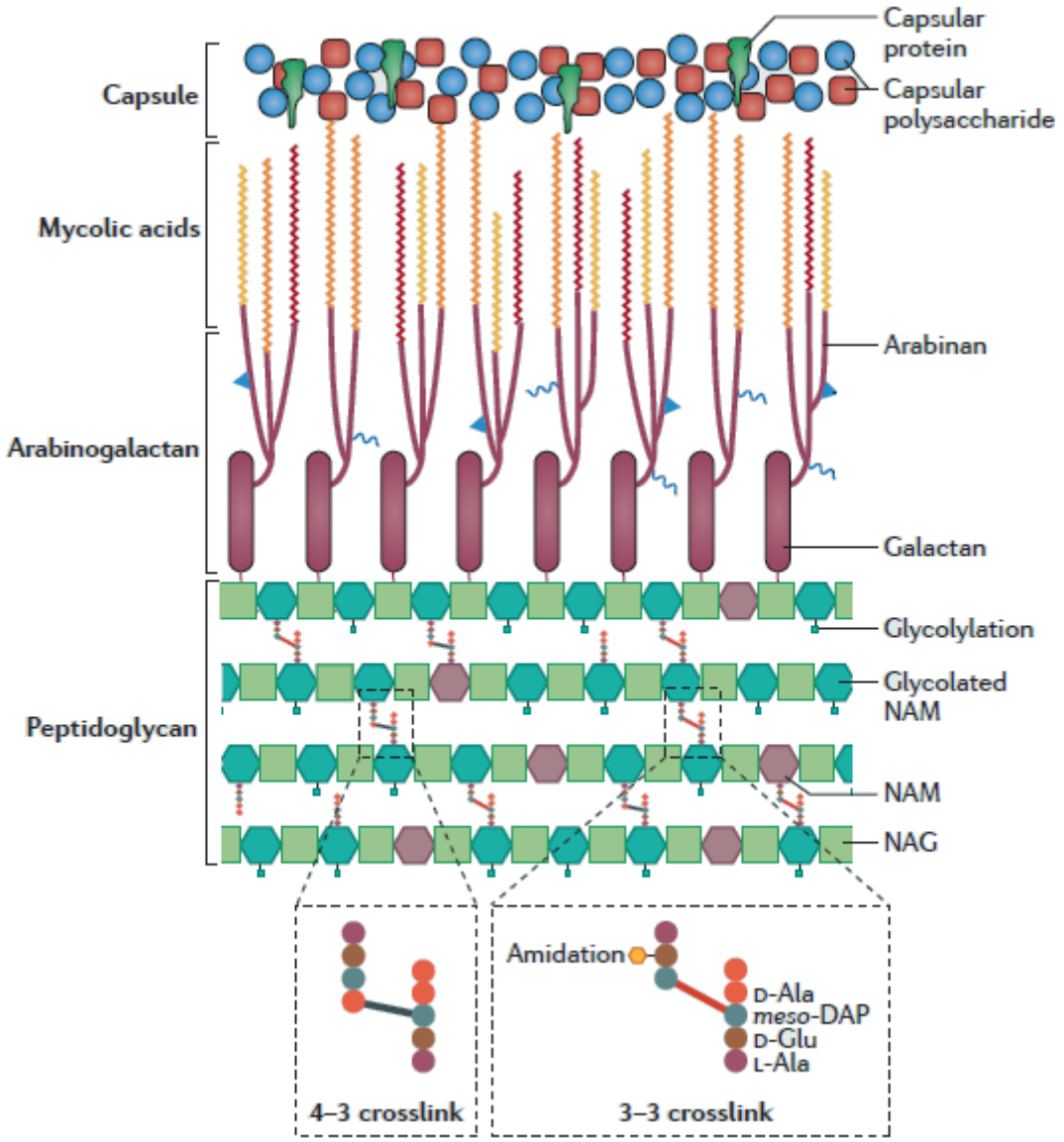

Figure 1.1. The mycobacterial cell wall. This figure illustrates the common components of the mycobacterial cell envelope including uniquely cross-linked peptidoglycan, arabinogalactan, mycolic acids, and outer capsule. Not depicted are glycopeptidolipids, which are an additional outer component of many nontuberculous mycobacterial species (Kieser and Rubin 2014).

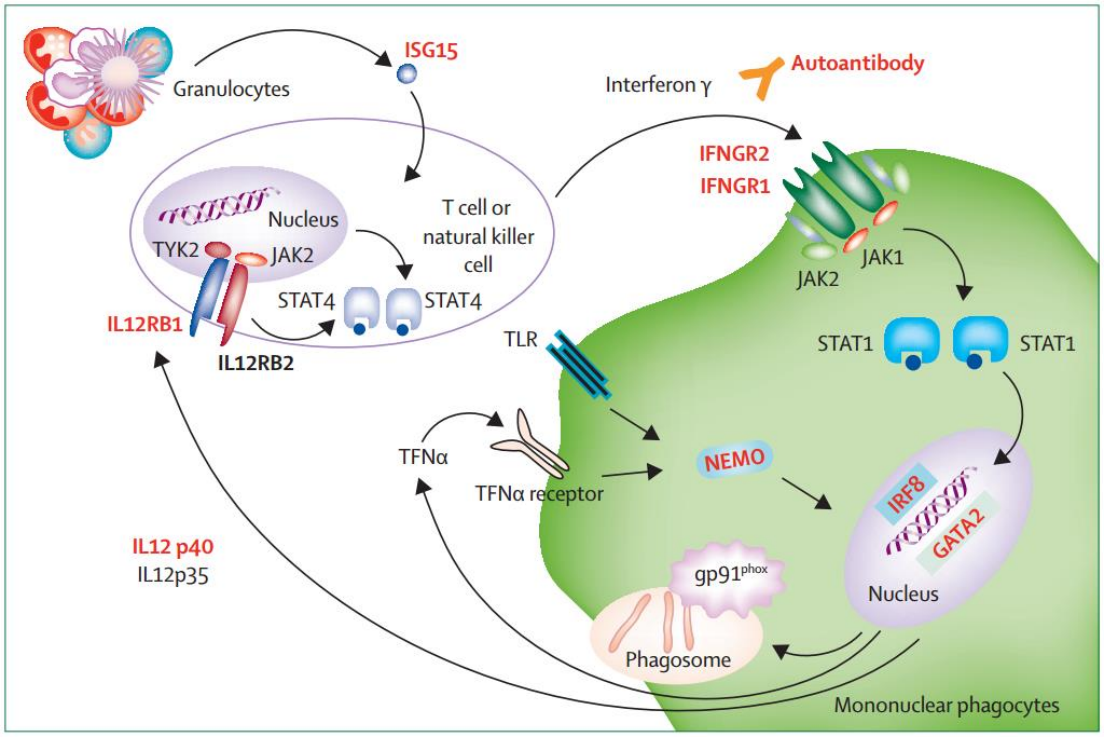

Figure 1.2. Genetic susceptibilities to NTM infection. The interaction between lymphocytes and mononuclear phagocytes is central for the immune response to NTM infection. The main axis of this response is the IL-12/IFNγ pathway. Genetic mutations (highlighted in red) in components of this pathway have been described in patients that are more susceptible to NTM infection and develop disseminated disease (Wu and Holland 2015).

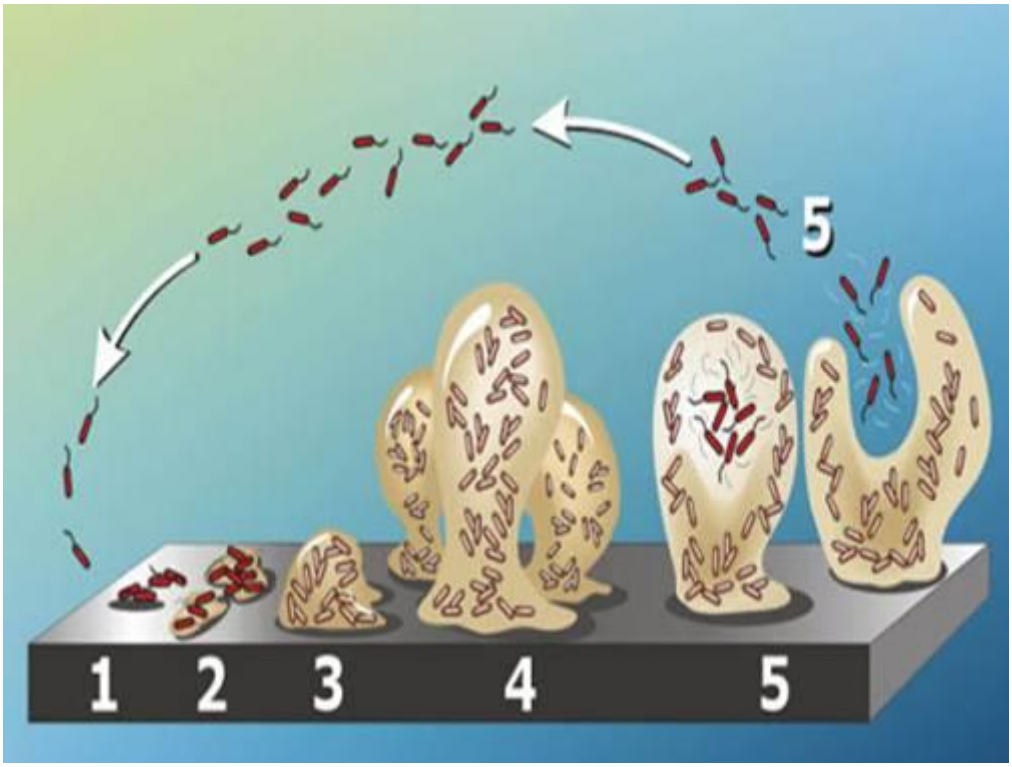

Figure 1.3. General biofilm developmental cycle. This cartoon depicts the cycle of biofilm attachment, maturation, and dispersal. Step 1 is the initial attachment of bacteria, step 2 is the initial production of biofilm matrix, step 3 is beginning to form a 3-dimensional architecture, step 4 is maturation of the architecture, and step 5 is dispersal of a portion of the biofilm to attach and colonize a new surface (Stoodley, Sauer et al. 2002).

Chapter 2

Mycobacterium avium Biofilm Attenuates Human Mononuclear Phagocyte Function by Triggering Hyper-Stimulation and Apoptosis during Early Infection

Sasha J. Rose and Luiz E. Bermudez

Infection and Immunity
2014 volume 82 (1), 405-412
PMID 24191301

Abstract

Mycobacterium avium subsp. *hominissuis* (MAH) is an opportunistic human pathogen that has been shown to form biofilm *in vitro* and *in vivo*. Biofilm formation *in vivo* appears to be associated with infections in the respiratory tract of the host. The reasoning behind how MAH biofilm is allowed to establish and persist without being cleared by the innate immune system is currently unknown. To identify the mechanism responsible for this, we developed an *in vitro* model using THP-1 human mononuclear phagocytes co-cultured with established MAH biofilm and surveyed various aspects of the interaction including phagocyte stimulation and response, bacterial killing, and apoptosis. MAH biofilm triggered robust TNF-α release from THP-1 cells as well as superoxide and nitric oxide production. Surprisingly, the hyper-stimulated phagocytes did not effectively eliminate the cells of the biofilm, even when pre-stimulated with IFN-γ or TNF-α, or co-cultured with natural killer cells (which have been shown to induce anti-MAH activity when added to THP-1 cells infected with planktonic MAH). Time-lapse microscopy and TUNEL assay determined that contact with the MAH biofilm lead to early, widespread onset of apoptosis, which is not seen until much later in planktonic MAH infection. Blocking TNF-α or TNF-R1 during interaction with the biofilm significantly reduced THP-1 apoptosis, but did not lead to elimination of MAH. Our data collectively indicate that MAH biofilm induces TNF-α driven hyper-stimulation and apoptosis of surveilling phagocytes, which prevents clearance of the biofilm by cells of the innate immune system, and allows the biofilm-associated infection to persist.

Introduction

Mycobacterium avium subsp. *hominissuis* (MAH) is a member of the *Mycobacterium avium* Complex (MAC), which also includes *M. avium* subsp. *avium* (MAA), *M. avium* subsp. *paratuberculosis* (MAP), and *Mycobacterium intracellulare.* MAH is an opportunistic human pathogen that typically infects individuals with underlying health conditions, such as AIDS and chronic pulmonary diseases such as COPD and cystic fibrosis, but can also affect immune competent individuals (Griffith, Aksamit et al. 2007).

MAH forms biofilms in the environment and is associated with diverse potable water sources including distribution pipes, bathtub inlets, faucets, showerheads, swimming pools, and hot tubs (Nishiuchi, Maekura et al. 2007; Feazel, Baumgartner et al. 2009; Nishiuchi, Tamura et al. 2009; Liu, Yu et al. 2012; Whiley, Keegan et al. 2012). MAH is ubiquitous in these environments due to intrinsic resistance against commonly used chlorination, ozonation, and UV treatment of potable water (Whiley, Keegan et al. 2012). Several studies have correlated the strain of MAH infecting a patient with a potable water source from their surroundings (Nishiuchi, Maekura et al. 2007; Falkinham, Iseman et al. 2008; Nishiuchi, Tamura et al. 2009; Whiley, Keegan et al. 2012).

The ability of MAH to form biofilm on host tissue is associated with the efficiency to infect bronchial epithelial cells and establish lung disease in mice (Yamazaki, Danelishvili et al. 2006). Mutants deficient in biofilm formation were not as efficient at invading and translocating BEAS-2b bronchial cells. Additionally, these mutants were attenuated in establishing respiratory infection in a mouse model of MAH lung disease (Yamazaki, Danelishvili et al. 2006). The reasons why MAH biofilms can be initially established in the respiratory tract, without being cleared by the innate immune system, are currently unknown.

Studies have shown that, in the case of *Pseudomonas aeruginosa* biofilm, neutrophils attracted to the site become engorged with biofilm (both cells and matrix), degranulated, immobilized, and rounded (Jesaitis, Franklin et al. 2003; Parks, Young et al. 2009). It was recently also described that polymorphonuclear leukocytes fail to

eradicate *P. aeruginosa* biofilms *in vivo* (van Gennip, Christensen et al. 2012). Another report indicates that exopolysaccharide from *Staphylococcus aureus* biofilm protects the bacterium from *Caenorhabditis elegans* immune defense (Begun, Gaiani et al. 2007). More recently, it was found that *S. aureus* biofilms attenuate a proinflammatory macrophage response *in vivo*, which could potentially explain the persistence of the biofilms in immunocompetent hosts (Thurlow, Hanke et al. 2011). Recent work with *Enterococcus faecalis* has also evidenced a diminished proinflammatory response in both macrophages and dendritic cells upon contact with biofilms, in contrast to exposure to planktonic cells (Daw, Baghdayan et al. 2012), further supporting that some biofilms may circumvent or camouflage bacteria from the traditional proinflammatory innate immune response.

One of the important questions regarding biofilms in mammalian infections relates to what appears to be the lack of the active role of the host immune system. Why don't the host cells ingest and kill biofilms? It is known that MAH inhibit inflammatory response on the mucosal surface upon colonization (Sangari, Goodman et al. 2001), however, it does not explain the inability of the host defenses to react against MAH biofilm. This study aimed to examine why MAH biofilms important for infection in the respiratory tract are not eliminated by the host innate immune system. We developed an *in vitro* model that resembles in part the *in vivo* conditions of a biofilm-associated respiratory infection. We exposed human phagocytes to established MAH biofilms in this model and assessed various aspects of interaction including activation, anti-MAH activity, and apoptosis.

Materials and Methods

Bacterial strains. MAH strains A5 and 104 were both originally isolated from the blood of AIDS patients with disseminated infection (Hellyer, Brown et al. 1991). MAH strain A5 was a generous gift from Dr. Kathleen Eisenach (Little Rock, AR). Prior to biofilm formation, bacteria were cultured on Middlebrook 7H10 agar supplemented with 10% OADC (Hardy Diagnostics, Santa Maria, CA) at 37˚C for 7-10 days until bacterial colonies were present. Pure, individual colonies were re-streaked out and used for experiments. Mutants deficient in biofilm formation were cultured as described above, except for the addition of 400 mg/ml of kanamycin supplemented in the medium to grow 6H9 and 5G4 mutants (MAH A5 biofilm deficient mutants). The mutations are in the *sucA* gene (6H9) and MAV_1565 (5G4), as previously described (Yamazaki, Danelishvili et al. 2006).

Host cells. Human THP-1 and natural killer (NK-92) cell lines were obtained from the American Type Culture Collection (Manassas, VA) and always cultured in RPMI-1640 media supplemented with heat inactivated 10% fetal bovine serum (FBS), L-glutamine and 25 mM HEPES (Cellgro, Manassas, VA) incubated at 37˚C and in an atmosphere of 5% CO_2. Additionally, NK cells used for experimentation were first cultivated alone in presence of IL-2 (50 U/ml) and washed before being added to biofilms. Prior to all cell culture experiments, viability of THP-1 and NK cells was assessed visually using trypan blue staining with a hemocytometer. Cell populations were at least 90% viable for all experiments.

Biofilm formation. Biofilms were formed statically as previously published (Carter, Wu et al. 2003), with minor modifications. Briefly, bacteria were taken from 7H10 agar plates and resuspended in Hank's Balanced Salt Solution (HBSS, Cellgro, Manassas, VA) to roughly a 5 x 10^8 CFU/ml level. Suspensions were left alone for 10 minutes to allow clumped bacteria to settle. The top half of the suspension was transferred to a new tube and adjusted down to an inoculum of 1 x 10^8 CFU/ml, using visual turbidity and optical density. Adjusted suspensions were serially diluted and plated for CFUs to verify the inoculum for each experiment. Suspensions were transferred to either 96 well polystyrene plates (BD, Franklin Lakes, NJ) or round 100

mm polystyrene tissue culture dishes (Corning, Corning, NY) depending on the experiment (round 100 mm dishes for supernatant experiment and 96 well plates for all other experiments). For 96 well plate experiments, 0.1 ml of bacterial suspension (1×10^7 bacteria) was transferred to each well. Biofilms were allowed to establish undisturbed for 14 days at room temperature (22˚C). Biofilms at this point were formed on the bottom surface of the wells.

UV-killed biofilm preparation. UV-killed biofilms were prepared by exposing mature MAH A5 biofilms to 1 minute of UV light using a UV-crosslinker (Hoefer, Holliston, MA). Wells were resuspended via pipetting, diluted, and plated to confirm UV-related killing. No viable bacteria were recovered from the UV-treated biofilms.

Planktonic bacterial immobilization. Planktonic MAH A5, first grown on 7H10 agar, and then resuspended into an inoculum of 1×10^8 CFU/ml. Bacteria were immobilized onto the surface of a 96-well plate by placing 100µl of inoculum into each well (to match with the biofilm inoculum) and then centrifuged at 2,000 x *g* for 20 minutes. The supernatant was gently removed prior to experimentation with THP-1 cells.

Biofilm supernatant preparation. For biofilm supernatant interaction experiments, supernatant was first collected from 14 day old biofilms formed as described above. Supernatants were gently aspirated from biofilms, and then centrifuged at 2,000 x *g* for 15 minutes to pellet any transferred bacteria, filtered through a 0.2 µm syringe filter (VWR, Radnor, PA) to guarantee sterilization, and then were used for experimentation. For assessing TNF-α production from interaction with the sterile biofilm supernatant, THP-1 cells were first quantified with a hemocytometer and adjusted to 1×10^6 cells/ml and the media was replaced with fresh RPMI-1640 containing 10% v/v biofilm supernatant earlier. At 4 hours, the sample supernatant was removed and ELISA was performed (Ebioscience, San Diego, CA), following the manufacturer protocol.

MAH biofilm/THP-1 cell interaction experimental design. THP-1 cells were washed once with HBSS using centrifugation (50 x g for 10 minutes), and

resuspended into fresh RPMI-1640 + 10% FBS. Cells were quantified with a hemocytometer and adjusted to 1 x 10^6 cells/ml prior to biofilm addition. The supernatant was gently aspirated from mature MAH A5 and MAH 104 biofilms (formed as described above), leaving the biofilm intact in the bottom of the well. Additional wells of biofilm were resuspended after supernatant removal, diluted, and plated for CFU to quantify the number of bacteria remaining in the well for the interaction experiments. Approximately 3 x 10^6 bacteria remained in the wells from both strains of MAH. A 0.2 ml suspension of THP-1 cells in RPMI + 10% FBS was added on top of the biofilm. Plates were allowed to incubate at 37˚C with 5% CO_2 for the respective time point for the specific experiment (which are described below). As a control, THP-1 macrophages were infected with MAH 104 and MAH A5, and NK cells (10^5 cells) were added afterwards. Monolayers were lysed after 4 days to quantify the number of intracellular bacteria.

TNF-α production and ELISA. At 0.5, 1, 2, 4, 24, and 48 hours of incubation after biofilm/THP-1 cell exposure, TNF-α production was assessed from sample supernatant using ELISA (Ebioscience, San Diego, CA). At a respective time point, plates were centrifuged at 50 x *g* for 10 minutes to pellet cells and supernatant was collected from the wells and analyzed according to the manufacturer protocol.

Superoxide anion and nitric oxide production. Supernatants were collected at time 0 and 48 hours after THP-1/biofilm interaction and superoxide anion was measured using a previously published protocol (Bermudez and Young 1990). Briefly, superoxide anion production was assayed spectrophotometrically by measuring the superoxide dismutase-inhibitable reduction of ferri-cytochrome C (Sigma-Aldrich, St. Louis, MO) after contact with the biofilm. Nitric oxide was measured using the Griess Reagent System (Promega, Madison, WI), following the manufacturer protocol.

Biofilm CFU assessment after THP-1 and NK cell exposure. Biofilms were formed and THP-1 cells were added as described above. At a respective time point, wells were mixed via pipetting (20 x) and then were serially diluted in HBSS and plated on 7H10 plates to obtain CFU/ml of recovered bacteria. THP-1 cells were also

pre-activated using either purified TNF-α and IFN-γ (Ebioscience, San Diego, CA) at a concentration of 50 and 100 ng/ml, respectively. NK cells were added to biofilms either by themselves or pre-mixed with an equal number of THP-1 macrophages. In either case, the cellular suspension was adjusted with a hemocytometer to 1 x 10^6 cells/ml and 0.2 ml of cells was added on top of the biofilm. As controls, biofilm-deficient 6H9 and 5G4 mutants were used to infect THP-1 macrophages and the survival monitored.

Microscopy. THP-1 mononuclear phagocytes were incubated with MAH A5 biofilm established on cover slips on a chamber containing RPMI-1640 medium. THP-1 cells were observed from the moment that they were added to the biofilm until 3 hours into the interaction. Time-lapse microscopy was performed on a Nikon microscope, and the images were collected with an Optronics DEI-750 camera. The experiment was repeated three times and at least 100 cells were observed each time.

Measuring apoptosis. To quantify apoptosis, biofilms were formed and THP-1 cells added as described above. At respective time points, terminal deoxynucleotidyl transferase dUTP nick end labeling (TUNEL) assay was performed (Roche, Indianapolis, IN) and visually quantified by fluorescent microscopy (Leica Microsystems, Wetzlar, Germany) following the protocol from the manufacturer. Fifty fields of view were scored for each time point and averaged.

Blocking TNF-α. To assess if TNF-α was correlated with apoptosis, antibody blocking of TNF-α was conducted using a primary monoclonal antibody (Genzyme, Boston, MA) at a concentration of 10μg/ml. Antibodies against TNF-R1 were obtained in a hybridoma suspension (Iowa University, hybridoma bank, IW) and diluted 1:10, a concentration known to inhibit TNF-α binding, before being co-cultured with the cells. Apoptosis was measured as described above. Additionally, biofilm CFU was also assessed after blocking TNF-α, following the method described earlier.

Statistical analysis. The results are represented as means of at least three repeated experiments ± standard deviation. Comparison between experimental and control groups was carried out using the Student's *t*-test. Comparisons between

multiple groups were carried out using ANOVA. In both cases, $P < 0.05$ was considered significant. Graph Pad Prism version 5.0 software was used for statistical analysis and graph creation.

Results

MAH biofilm is highly stimulatory to THP-1 mononuclear phagocytes. Previous studies have shown that MAH strain A5 forms a greater amount of biofilm *in vitro* than other clinical isolates of MAH, including strain 104 (Carter, Wu et al. 2003). It has also been reported that the ability of MAH to form biofilm increases the bacterial adherence to and invasion of BEAS-2b bronchial epithelial cells, *in vitro,* and translates into more established infection through the respiratory route *in vivo* (Yamazaki, Danelishvili et al. 2006). We first investigated whether the extent of biofilm forming ability influenced the activation of host phagocytes. Biofilms were formed using MAH A5, a previously characterized biofilm overproducing strain (Carter, Wu et al. 2003), and MAH 104, a typical biofilm forming strain, for 14 days at room temperature. THP-1 cells were then added on top of the biofilm and TNF-α production was assessed over a time course by removing culture supernatant and carrying out ELISA. When assessing TNF-α production, MAH A5 was significantly more stimulatory to THP-1 cells over the time course than MAH 104 (Figure 2.1A); however both strains appear to elicit an atypically high response compared with infection with planktonic *M. avium* infection, which typically down regulates TNF-α production (Bermudez and Young 1988; Bermudez and Young 1990; Sarmento and Appelberg 1995; Balcewicz-Sablinska, Gan et al. 1999; Danelishvilli and Bermudez 2003). Interestingly, the cell-free biofilm supernatant of strain A5 (added at 10% v/v into RPMI media) also triggered a robust TNF-α response from THP-1 cells (Figure 2.1B). To confirm that this robust TNF-α response was not simply due to the bacteria being immobilized on the bottom of the plate, an inoculum of planktonic MAH was prepared, adjusted to 1 x 10^7 per well, and immobilized onto the bottom of the plate via centrifugation, alongside mature MAH A5 biofilm. Supernatants were removed and replaced with THP-1 cells for 4 hours. Although the immobilized planktonic bacteria did elicit a TNF-α response, but it was significantly lower than the response to the biofilm (Figure 2.1C).

To further assess the role of the acellular biofilm components, mature MAH A5 biofilms were UV irradiated and then THP-1 cells were exposed to the film for 4

hours. The UV killed biofilm elicited an almost identical TNF-α response from the THP-1 cells as the non-UV treated biofilm (Figure 2.1C). Collectively, the data demonstrate that MAH biofilm is very stimulatory to phagocytes. Furthermore, the acellular biofilm constituents (both biofilm matrix in the UV killed biofilm and supernatant) could be a major stimulatory trigger of this response, since live bacteria were not required to stimulate the surveilling phagocytes. Due to the increased stimulation of phagocytes by MAH A5 (and the response to the acellular supernatant), it was chosen to further develop this model of MAH biofilm-phagocyte interaction.

Other aspects of THP-1 stimulation were assessed during exposure to MAH A5 biofilm. Superoxide anion and nitric oxide production was significantly greater in THP-1 cells in contact with the MAH A5 biofilm than biofilm-unexposed cells (Figure 2.1D and E, respectively). This data further supports that the phagocytes are becoming stimulated upon MAH biofilm exposure.

MAH A5 biofilm is unaffected by the presence of THP-1 and/or natural killer cells. The finding that MAH biofilm is highly stimulatory to phagocytes led us to investigate if this was associated with increased killing of the bacteria in the biofilm during exposure. THP-1 cells were added on top of 14 day-old MAH A5 biofilms and after 24 and 72 hours, the wells were mixed via pipetting, diluted, and plated to obtain the bacterial load of MAH. THP-1 cells were also pretreated with either IFN-γ or TNF-α to stimulate them prior to addition to the biofilm. No significant differences in the number of viable bacteria were observed with or without addition of THP-1 cells (Figure 2.2A) suggesting that macrophages are not capable of clearing established MAH biofilm. Furthermore, the pre-activation of the THP-1 cells with IFN-γ or TNF-α did not stimulate bactericidal mechanisms that can harm MAH biofilms.

Previous observations have demonstrated that addition of natural killer (NK) cells increases anti-MAH activity of macrophages (Bermudez, Wu et al. 1995; Early, Fischer et al. 2011). We examined if NK cells pre-stimulated with IL-2 and incubated in presence of THP-1 cells induced any anti-mycobacterial activity against the

biofilm. At both 24 and 48 hours after infection, neither NK cells alone nor in combination with THP-1 cells affected the CFU/ml of bacterial cells within the MAH biofilm (Figure 2.2B), but did induce bactericidal activity in THP-1 cells infected with planktonic MAH 104 and A5 (Figure 2.2C). Taken together, these results suggest that macrophages in contact with the biofilm are not capable of killing the cells within the biofilm, even if they are pre-activated or coordinated with NK cells.

To determine if mononuclear phagocytes would ingest planktonic MAH or biofilm-deficient MAH mutants 6H9 and 5G4, THP-1 cells were incubated in suspension with an MOI of 10:1 (undergoing rotation) and after 30 minutes the cells were spun down and the number of intracellular bacteria determined. THP-1 cells were able to ingest all strains and after 4 days in culture it was observed that all strains were able to grow intracellularly, showing that planktonic bacteria can replicate inside THP-1 cells (Figure 2.2D).

THP-1 cells appear grossly deformed and undergo apoptosis after exposure to MAH strain A5 biofilm. Despite the hyper-stimulation of THP-1 cells upon contact with MAH biofilm, no decrease of bacterial viability was demonstrated. THP-1 cells were added on top of MAH biofilm and microscopy was performed over a time course to assess the phagocyte morphology during biofilm exposure (Figure 2.3 A-F). After only 40 minutes of exposure, some phagocytes began to appear grossly deformed (Figure 2.3E), while others were clearly apoptotic (Figure 2.3F).

After observing apoptotic cells during the microscopy, TUNEL assay was conducted to quantify the degree of apoptosis occurring over a time course during biofilm exposure. The proportion of phagocytes undergoing apoptosis increased upon biofilm exposure over the 48 hour time course, with 79% of the host cells apoptotic at 48 hours (Figure 2.3G). Planktonic MAH infection of THP-1 macrophages does not induce rapid apoptosis seen here, as demonstrated by previous work (Early, Fischer et al. 2011).

The induction of apoptosis upon exposure is at least partly due to the TNF-α response. Due to the robust TNF-α production by biofilm-hyper-stimulated THP-1 cells and the early and surprising amount of apoptosis, we next assessed if the

two were related. THP-1 cells were exposed to MAH biofilm either with no addition or supplemented with anti-TNFR1 or anti-TNF-α antibodies and TUNEL assay was performed at 2 and 6 hours to measure apoptosis. Blocking either TNF-α itself or its receptor significantly reduced the percentage of apoptotic cells during biofilm exposure (Figure 2.4A). We then assessed if the reduction of apoptosis would result in killing of the MAH biofilm. Wells were resuspended, diluted, and plated for CFU enumeration, but there were no significant differences between the anti-TNFR1 or anti-TNF-α treated with the non-treated (Figure 2.4B). Interestingly, the CFU of antibody treated wells were increased compared to non-treated wells, indicating that engulfed MAH is replicating in the reduced apoptotic population of THP-1 cells. This data demonstrates that the significant TNF-α production is at least partially correlated with the induction of apoptosis following biofilm exposure.

Discussion

Mycobacterium avium subsp. *hominissuis* (MAH) is an opportunistic human pathogen that is ubiquitous in natural water sources, soil, and urban potable water systems. The prevalence of MAH in the environment is possibly due to its ability to form robust biofilms. Clinical isolates of MAH have been found in residential potable water systems of MAH-infected patients and genetically linked to the strains infecting the patients (Whiley, Keegan et al. 2012).

Previous work has shown that the ability to form biofilm translates into better attachment and invasiveness of bronchial epithelial cells, *in vitro,* as well as *in vivo* in a mouse model of respiratory infection (Yamazaki, Danelishvili et al. 2006). It remains unknown whether individuals get exposed to already established MAH biofilm being aerosolized into the airways or if inhaling planktonic bacteria leads to the formation of new biofilms, which was the model evaluated in mice previously. In either case, it is intriguing that these infections are allowed to persist, without innate immune clearance by the host. The same phenomenon in a few other pathogenic bacteria, including *Staphylococcus* spp. and *Enterococcus* spp., has been investigated and it has been generally suggested that biofilms circumvent the typical proinflammatory response from the innate immune system (Begun, Gaiani et al. 2007; Thurlow, Hanke et al. 2011; Daw, Baghdayan et al. 2012; van Gennip, Christensen et al. 2012). It may be explained by the fact that biofilms are usually encapsulated within exopolysaccharides (EPS). This encapsulation might reduce the exposure of pathogen-associated molecular patterns to pattern recognition receptors on host cells that planktonic bacteria would typically trigger. Physical EPS or even the genes required for its synthesis have not been found to date in any mycobacterial species (Zambrano and Kolter 2005). This is very interesting because despite lacking EPS, mycobacterial species generally still form robust biofilms. When human THP-1 mononuclear phagocytes were placed in contact with established MAH strain 104 and A5 biofilms, they responded with robust TNF-α production. This response was significantly greater with MAH A5, which has been shown previously to be a biofilm-overproducing strain (Carter, Wu et al. 2003). We have preliminary data

demonstrating that MAH A5 produces more biofilm matrix constituents than MAH 104, in both abundance and diversity (data not shown). Synthesis and secretion of TNF-α has been shown to occur upon macrophage exposure to a number of different bacterial components, and in the case of the two MAH strains tested, may be explained by the absolute amount of several biofilm components. It is interesting to point out that the ability to form biofilm at all appears be highly stimulatory to THP-1 cells, which is not observed when macrophages come in contact with planktonic MAH, which usually down regulates TNF-α production during successful infection (Bermudez and Young 1988; Bermudez and Young 1990; Sarmento and Appelberg 1995; Balcewicz-Sablinska, Gan et al. 1999; Danelishvilli and Bermudez 2003). Our current data with mycobacteria contrasts with findings obtained in systems using gram-positive and gram-negative bacteria that has concluded thus far that biofilms suppress a proinflammatory response (Thurlow, Hanke et al. 2011; Daw, Baghdayan et al. 2012).

We assessed if these hyper-stimulated phagocytes were ingesting and killing bacteria belonging to the biofilm, because of previous work showing that TNF-α stimulates anti-MAH activity in macrophages (Sarmento and Appelberg 1996). The CFU data at various time points demonstrate that the number of MAH cells in the biofilm are unaffected by the presence of THP-1 cells, even if they were pre-stimulated with TNF-α or IFN-γ (Figure 2.2A). This finding is in disagreement when compared to the effectiveness of killing of planktonic MAH by activated macrophages.

NK cells are an important part of the host innate immune response and are a component of the innate lymphoid cells in the mucosal surfaces (Bryceson, March et al. 2006). NK cells when stimulated with IL-12 or IL-2 can trigger macrophage killing of various intracellular pathogens, including MAH (Orange and Ballas 2006). In our system we hypothesize that perhaps macrophages in contact with the MAH biofilm need cooperation with NK cells to be more effective at bacterial clearance. Studies have shown that NK cells produce TNF-α and IFN-γ when stimulated, which leads to macrophage activation (Bermudez and Young 1991; Bermudez, Wu et al.

1995). Surprisingly, the addition of NK cells did not result in a decrease of bacterial CFU in the biofilm (Figure 2.2B). The observation that NK cells alone did not affect the biofilm CFU is consistent with previous work (Bermudez and Young 1991).

The observation of the significant amount of rapid apoptosis occurring in macrophages after MAH biofilm exposure is quite interesting, and atypical from planktonic MAH infection (Early, Fischer et al. 2011). Macrophages in contact with biofilm probably ingested a large amount of antigens (bacteria and biofilm matrix) and the uptake of biofilm matrix along with bacteria, and the abundance of PAMPs in the matrix could certainly trigger this response. Another consideration is that because of the large amount of matrix surrounding cells in the biofilm, macrophages are just ingesting substantial quantities of material and becoming hyper-stimulated, without having a chance to take up a significant number of bacteria, as our UV-irradiated biofilm experiment suggested (Figure 2.1C). Furthermore, there are putative secreted factors involved as well, suggested by the fact that sterile supernatant from MAH A5 biofilm was also able to induce a response from THP-1 cells (Figure 2.1B). Future work needs to be conducted to unveil what exactly in the biofilm and supernatant is responsible for the observed effects.

This study focused on the interaction of mononuclear phagocytes with established biofilms in order understand the reason for the impaired innate immune clearance of MAH biofilms. However, how does the host allow the infecting bacteria to establish biofilm in the first place? Electron microscopy of MAH in contact with BEAS-2b cells has shown aggregates of MAH A5 forming as soon as two hours post infection (Yamazaki, Danelishvili et al. 2006). More recent work has visualized matrix-like substances surrounding the aggregates as soon as 48 hours after infection (unpublished data). TNF-α production following macrophage exposure to MAH biofilm supernatant as well as preliminary experiments using extracted biofilm matrix (unpublished data) indicate that an acellular component of the biofilm is at least partially responsible for macrophage stimulation. In reviewing the literature, there has not been much research aimed at identifying constituents of mycobacterial biofilms. For example, it has been found that glycopeptidolipids and mycolic acids are

involved in the formation of MAH and *Mycobacterium tuberculosis* biofilms, respectively (Freeman, Geier et al. 2006; Yamazaki, Danelishvili et al. 2006; Ojha, Baughn et al. 2008). Perhaps the encapsulation of matrix is responsible for resistance of disease-associated host defense and therapy. Preventing or removing a specific matrix component might result in increased susceptibility of biofilm to therapy or the host response. In many pathogenic bacterial species such as *Vibrio cholerae*, *Pseudomonas aeruginosa*, *Bordetella* spp., *Enterococcus faecalis*, and *Listeria monocytogenes*, extracellular DNA (eDNA) has been found to be an important matrix component (Whitchurch, Tolker-Nielsen et al. 2002; Harmsen, Lappann et al. 2010; Conover, Mishra et al. 2011; Seper, Fengler et al. 2011; Barnes, Ballering et al. 2012). Recent work in the laboratory has shown that eDNA plays a role in MAH biofilm as well (unpublished data). Targeting matrix components of MAH biofilm might improve patient response when combined with traditional antimicrobial therapy.

To conclude, this study indicates that the reason why cells of the innate immune system are unable to clear MAH biofilm-associated infections is due to the biofilm causing hyper-stimulation of phagocytes, which leads to decreased functionality and apoptosis partially in a TNF-α dependent manner.

Acknowledgements

We thank Beth Chamblin for helping assemble the manuscript for submission. This work was supported by grant AIO43199 from the National Institutes of Health.

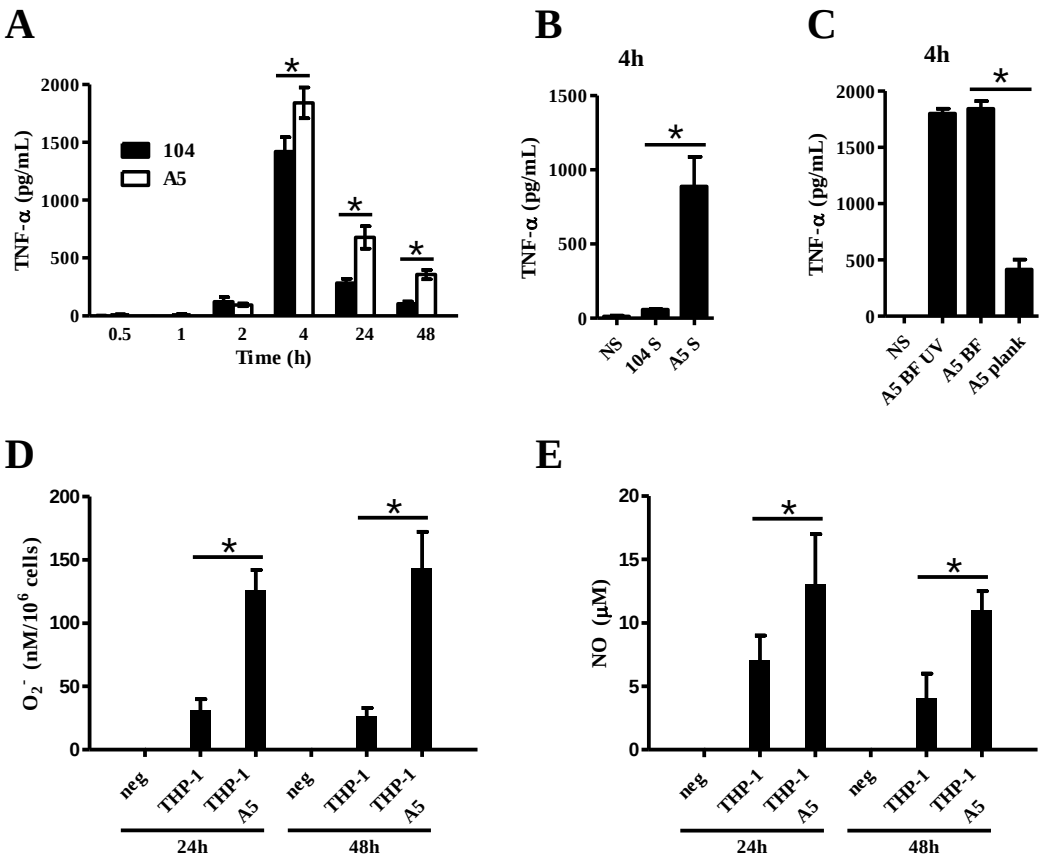

Figure 2.1. THP-1 cells are stimulated during exposure to MAH biofilms. (A) THP-1 cells were added on top of MAH strains A5 and 104 14 day-old biofilms (equal inoculum levels) and supernatant was collected at 0.5, 1, 2, 4, 24, and 48 hours. TNF-α ELISA was carried out for each time point for each strain. (B) Filter-sterilized supernatants from 14 day-old biofilms were added at a 10% concentration (v/v) in RPMI-1640 + 10% FBS with THP-1 cells for 4 hours. Culture supernatant was then collected and TNF-α ELISA was performed. Abbreviations: NS = not stimulated; 104 S = MAH 104 supernatant; A5 S = MAH A5 supernatant. (C) UV-killed MAH A5 biofilms (A5 BF UV) were compared side-by-side with non-UV treated biofilms (A5 BF) and planktonic bacteria that were immobilized on the bottom surface of the plate via centrifugation (A5 plank) for TNF-α production by THP-1 cells 4 hours after being placed on top of the bacteria. (D) THP-1 cells were placed on top of MAH A5 biofilm and O2- was assessed spectrophotometrically as described in materials and methods. (E) THP-1 cells were placed on top of MAH A5 biofilm and NO was assessed using the Griess reagent system. Abbreviations for D and E: neg = negative control for respective assay; THP-1 = THP-1 cells placed in empty wells with no bacteria present; THP-1 A5 = THP-1 cells placed in wells containing MAH A5 biofilm. Bars represent means ± SD. *$P < 0.05$.

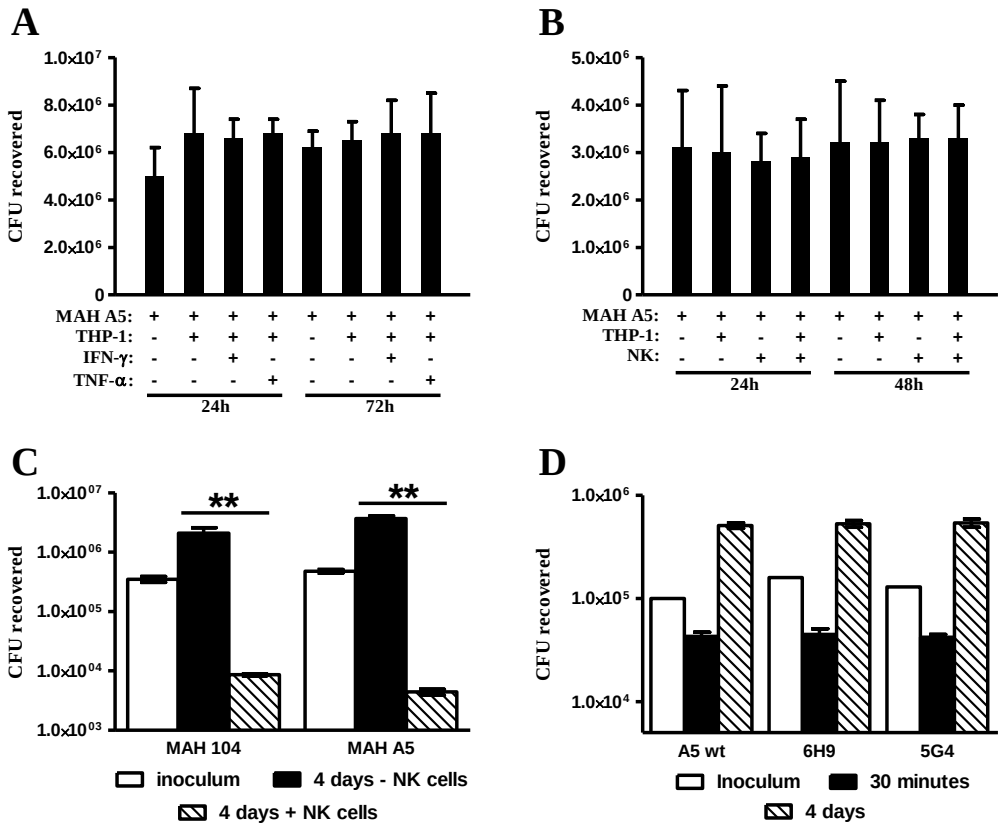

Figure 2.2. CFU of MAH A5 biofilm is unaffected by the addition of THP-1 cells, even when pre-activated or co-cultured with NK cells. (A) THP-1 cells were added on top of established MAH A5 biofilms for 24 and 72 hours. In some instances, THP-1 cells were first pre-stimulated with 50ng/ml of TNF-α or 100ng/ml of IFN-γ. At each time point, wells were resuspended, diluted, and plated to attain CFU/well of MAH A5. (B) Suspensions of THP-1 cells alone, NK cells alone, or a co-culture of both cell types were added on top of established MAH A5 biofilms for 24 and 48 hours before CFU enumeration. (C) Co-culture of NK cells and THP-1 cells infected with planktonic MAH demonstrating NK assisted bacterial killing after 4 days. (D) Infection of THP-1 with planktonic MAH A5 and two MAH A5 derived biofilm deficient mutants (6H9 and 5G4), demonstrating that planktonic MAH can grow inside of THP-1 cells. For both A and B, all comparisons to the MAH A5 control (no host cells added) for each time point were not significant. Bars represent means ± SD. $^{**}P<0.01$.

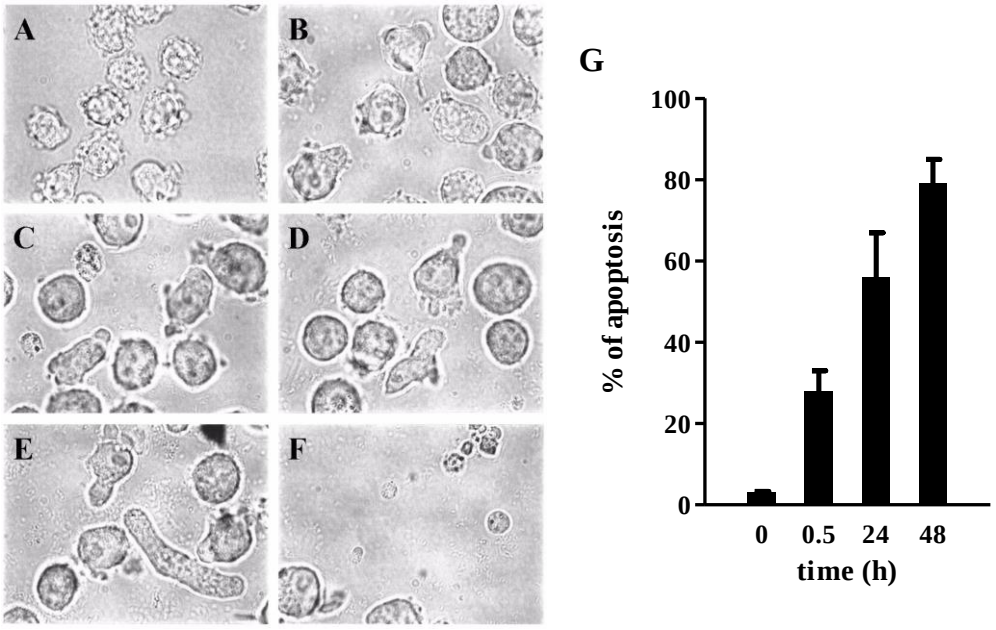

Figure 2.3. THP-1 cells rapidly undergo apoptosis after exposure to MAH A5 biofilm. (A-F) Microscopy showing THP-1 cells at 5 minutes (A), 15 minutes (B), 25 minutes (C-D), and 40 minutes (E-F). (G) THP-1 cells were placed on top of established MAH A5 biofilm and TUNEL assay was performed at 0, 0.5, 24, and 48 hours. In each field of view, apoptotic cells were counted microscopically and divided by the total number of counted cells counted to attain percent of apoptosis. Fifty fields of view were counted for each time point and averaged. The bars represent the mean of each time point ± SD.

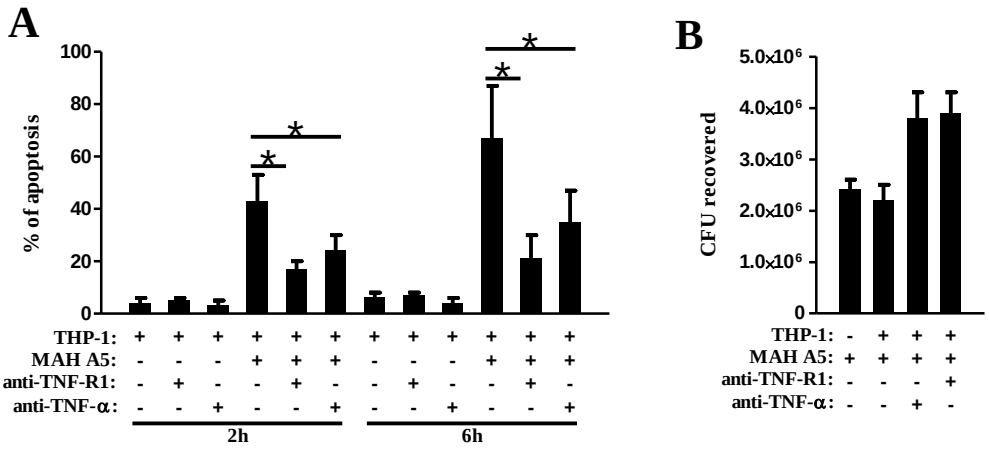

Figure 2.4. Blocking TNF-α reduces apoptosis of THP-1 cells during MAH A5 biofilm exposure. THP-1 cells were placed on top of established MAH A5 biofilms with or without anti-TNF-R1 (1:10 dilution of a hybridoma suspension) or anti-TNF-α (10 μg/ml). (A) TUNEL assay was performed at 2 and 6 hours after exposure. The ratio of apoptotic to total cells was counted in 50 fields of view microscopically and was averaged for each time point. (B) THP-1 cells were lysed at 24 hours after exposure and wells were resuspended, diluted, and plated for CFU of MAH. Bars represent the mean ± SD. **P* < 0.05.

Chapter 3

Mycobacterium avium Possesses Extracellular DNA that Contributes to Biofilm Formation, Persistence, and Tolerance to Antibiotics

Sasha J. Rose, Lmar M. Babrak, and Luiz E. Bermudez

PLOS ONE

2015, volume 10 (5), e0128772-e0128772

PMID 26010725

Abstract

Mycobacterium avium subsp. *hominissuis* is an opportunistic pathogen that is associated with biofilm-related infections of the respiratory tract and is difficult to treat. In recent years, extracellular DNA (eDNA) has been found to be a major component of bacterial biofilms, including many pathogens involved in biofilm-associated infections. To date, eDNA has not been described as a component of mycobacterial biofilms. In this study, we identified and characterized eDNA in a high biofilm-producing strain of *Mycobacterium avium* subsp. *hominissuis* (MAH). In addition, we surveyed for presence of eDNA in various MAH strains and other nontuberculous mycobacteria. Biofilms of MAH A5 (the high biofilm-producing strain) and MAH 104 (reference strain) were established at 22°C and 37°C on abiotic surfaces. Acellular biofilm matrix and supernatant from MAH A5 7 day-old biofilms both possess abundant eDNA, however very little eDNA was found in MAH 104 biofilms. A survey of MAH clinical isolates and other clinically relevant nontuberculous mycobacterial species revealed many species and strains that also produce eDNA. RAPD analysis demonstrated that eDNA resembles genomic DNA. Treatment with DNase I reduced the biomass of MAH A5 biofilms when added upon biofilm formation or to an already established biofilm both on abiotic surfaces and on top of human pharyngeal epithelial cells. Furthermore, co-treatment of an established biofilm with DNase 1 and either moxifloxacin or clarithromycin significantly reduced the tolerance of the bacteria within the biofilm to these clinically used antimicrobials. Collectively, our results describe an additional matrix component of mycobacterial biofilms and a potential new target to help treat biofilm-associated nontuberculous mycobacterial infections.

Introduction

Mycobacterium avium subsp. *hominissuis* (MAH) is an opportunistic human pathogen that typically infects individuals with underlying health conditions, such as AIDS, chronic obstructive pulmonary disease, and cystic fibrosis. Pulmonary infections with MAH and other nontuberculous mycobacteria are also increasing in incidence in patients without underlying conditions (Griffith, Aksamit et al. 2007). MAH is ubiquitous in the environment and is commonly found in potable water systems, presumably persisting in biofilms (Feazel, Baumgartner et al. 2009; Liu, Yu et al. 2012; Whiley, Keegan et al. 2012). Studies have linked potable water reservoirs of MAH directly to infection in patients (Nishiuchi, Maekura et al. 2007; Falkinham, Iseman et al. 2008; Nishiuchi, Tamura et al. 2009). Previous work in our laboratory has suggested that the ability to form biofilm is associated with the efficiency to establish lung disease in mice (Yamazaki, Danelishvili et al. 2006). Furthermore, we recently reported that MAH biofilm formed *in vitro* induces rapid, atypical TNF-α-dependent apoptosis of phagocytes exposed to the biofilm, which could explain how MAH biofilms formed *in vivo* establish and persist without host clearance (Rose and Bermudez 2014). This report additionally found that UV-sterilized biofilm was just as stimulatory to macrophages as non-sterilized live biofilm, suggesting that an acellular component of the biofilm matrix could be responsible for this rapid cell death upon interaction.

Little is currently known about the constituents of the extracellular polymeric substance (EPS) composing the matrix of *M. avium* biofilms. In most bacterial species, a major component of EPS are exopolysaccharides, however mycobacteria do not produce them, and lack the genes necessary for synthesis (Zambrano and Kolter 2005). Studies have primarily found lipid EPS components of mycobacterial biofilms including free mycolic acids in *M. tuberculosis* and *M. smegmatis* (Ojha, Anand et al. 2005; Ojha, Baughn et al. 2008), glycopeptidolipids in *M. avium, M. abscessus,* and *M. smegmatis* (Recht and Kolter 2001; Freeman, Geier et al. 2006; Yamazaki, Danelishvili et al. 2006; Nessar, Reyrat et al. 2011), mycolyl-diacylglycerols in *M. smegmatis* (Chen, German et al. 2006), lipooligosaccharides in

M. marinum (Ren, Dover et al. 2007), and lipopeptides in *M. avium* subsp. *paratuberculosis* (Wu, Schmoller et al. 2009).

In addition to exopolysaccharides, another important component of the EPS in bacterial biofilms is extracellular DNA (eDNA). It was first discovered in *Pseudomonas aeruginosa* biofilms by Whitchurch *et al.* in 2002 (Whitchurch, Tolker-Nielsen et al. 2002). Since this report, eDNA has been described in many gram negative (Jurcisek and Bakaletz 2007; Lappann, Claus et al. 2010; Conover, Mishra et al. 2011; Grande, Di Giulio et al. 2011; Seper, Fengler et al. 2011) and gram positive (Moscoso, Garcia et al. 2006; Qin, Ou et al. 2007; Rice, Mann et al. 2007; Thomas, Thurlow et al. 2008; Vilain, Pretorius et al. 2009; Harmsen, Lappann et al. 2010; Hymes, Randis et al. 2013) bacteria. eDNA in these biofilms contribute to surface attachment and colonization (Moscoso, Garcia et al. 2006; Harmsen, Lappann et al. 2010; Lappann, Claus et al. 2010; Seper, Fengler et al. 2011), biofilm recruitment (Qin, Ou et al. 2007; Seper, Fengler et al. 2011), structural integrity (Jurcisek and Bakaletz 2007; Rice, Mann et al. 2007; Thomas, Thurlow et al. 2008; Vilain, Pretorius et al. 2009; Conover, Mishra et al. 2011; Hymes, Randis et al. 2013), nutrient acquisition (Godeke, Heun et al. 2011; Seper, Fengler et al. 2011), and a source of DNA for horizontal gene transfer (Hannan, Ready et al. 2010; Grande, Di Giulio et al. 2011). eDNA has also been shown to protect biofilms against antibiotics, biocides, and chemicals (Allesen-Holm, Barken et al. 2006; Tetz, Artemenko et al. 2009; Kaplan, LoVetri et al. 2012; Hymes, Randis et al. 2013). Additionally, it was recently determined that eDNA facilitates cellular aggregation within *P. aeruginosa*, *Streptococcus mutans*, and *Staphylococcus epidermidis* biofilms (Das, Krom et al. 2011; Das, Kutty et al. 2013), and assists in spatial self-organization in expanding *P. aeruginosa* biofilms (Gloag, Turnbull et al. 2013).

The source of eDNA in bacterial biofilms is a controversial and ongoing issue. In *Pseudomonas aeruginosa*, *Staphylococcus* spp., and *Enterococcus* spp., eDNA has been connected to cell lysis (Allesen-Holm, Barken et al. 2006; Qin, Ou et al. 2007; Rice, Mann et al. 2007; Thomas, Thurlow et al. 2008; Das and Manefield 2012). Mechanisms of cell lysis contributing to eDNA production have included autolysin

proteins (Qin, Ou et al. 2007; Rice, Mann et al. 2007; Thomas, Thurlow et al. 2008), pyocyanins leading to H_2O_2 production and lysis (Das and Manefield 2012), and quorum sensing resulting in prophage-mediated lysis (Allesen-Holm, Barken et al. 2006).There has also been a growing body of research suggesting active export in the absence of cell lysis as an alternative source of eDNA. One report investigating eDNA in *Enterococcus faecalis* early biofilms found no evidence of cell lysis and moreover the eDNA producing cells had elevated membrane potential (Barnes, Ballering et al. 2012). Another study recently described early competence genes involved with eDNA production in *Bacillus cereus*, which also suggests a defined mechanism and not a mass cell die off as a trigger (Vilain, Pretorius et al. 2009). Secreted membrane vesicles are another mechanism that has been demonstrated to export eDNA outside of bacteria within biofilms (Sahu, Iyer et al. 2012; Liao, Klein et al. 2014). Other groups investigating eDNA production in *Helicobacter pylori* and an aquatic bacterium strain F8 also suggest eDNA release to be independent of cell lysis (Bockelmann, Janke et al. 2006; Grande, Di Giulio et al. 2011; Sahu, Iyer et al. 2012).

Prior work with *M. avium* biofilms has highlighted their importance for environmental persistence and possibly infection (Carter, Wu et al. 2003; Yamazaki, Danelishvili et al. 2006). MAH A5, in particular, has shown to be a strain that produces very robust and resistant biofilms (Carter, Wu et al. 2003), which induce very atypical host responses when compared to their planktonic counterparts (Rose and Bermudez 2014). Currently, little is known about the physical makeup of the MAH biofilm and the mechanisms responsible for it. In this study, we observed and characterized eDNA in MAH strain A5, which is the first report to date of eDNA as a biofilm matrix component in pathogenic mycobacteria. We also identified other clinically relevant nontuberculous mycobacteria that possess eDNA as a biofilm matrix component.

Materials and Methods

Bacterial strains and growth. *Mycobacterium avium* subsp. *hominissuis* (MAH) strains A5 and 104 were originally isolated from the blood of AIDS patients. MAH strains 3386, 3388, and 3393 as well as *M. intracellulare* strain 3387 were generous gifts from Barbara Brown-Elliott (University of Texas Health Science Center). MAH Cl-3, MAH Cl-4, *M. intracellulare* Cl-2, and *M. abscessus* subsp. *bolletii* 26 were kindly provided by Steven Holland (National Institutes of Health). *Mycobacterium chelonae* strain h1e2 and *M. marinum* Harvard were gifted from Michael Kent (Oregon State University). *M. abscessus* subsp. *abscessus* strain 19977 was obtained from the American Type Culture Collection (Manassas, VA). The other mycobacteria used are strains isolated by our laboratory. All mycobacteria were grown on Middlebrook 7H10 agar plates containing 10% oleic acid, albumin, dextrose, and catalase (OADC; Hardy Diagnostics, Santa Maria, CA). MAH, *M. intracellulare*, and *M. abscessus* strains were grown at 37˚C. All other mycobacterial species were grown at 30˚C.

Host cells. Human HEp-2 pharyngeal epithelial cells (CCL-23) were obtained from the American Type Culture Collection and cultured in RPMI-1640 media containing 2 mM L-glutamine and 25 mM HEPES (Cellgro, Manassas, VA) further supplemented with 10% heat inactivated fetal bovine serum (FBS, Gemini Bio-Products, Sacramento, CA) at 37˚C with 5% CO_2. Confluent monolayers of cells were removed using TrypLE (Life Technologies, Carlsbad, CA), washed, resuspended in fresh media, counted with a hemocytometer, and seeded into 96-well plates for later biofilm formation experiments.

Biofilm formation. Static biofilms were used in this study, formed similarly to previous reports (Carter, Wu et al. 2003; Rose and Bermudez 2014), with minor modifications. Briefly, log-phase bacteria were transferred from 7H10 agar into Hank's Balanced Salt Solution (HBSS; Cellgro) to create a mid-10^8 bacteria/ml suspension, using visual turbidity. This suspension was left alone for 10 minutes to allow clumped bacteria to sediment. The top half of the suspension was withdrawn, and adjusted to 3 x 10^8 bacteria per ml, using a McFarland #1 standard as a reference.

This suspension was transferred into an appropriate polystyrene vessel (listed for each experiment) and incubated at 22˚C, 30˚C, or 37˚C for the time point indicated by the specific experiment.

Scanning electron microscopy. Biofilms visualized via scanning microscopy were prepared as described above and processed for microscopy as previously described (Barnes, Ballering et al. 2012). Briefly, biofilms were prepared on top of round coverslips in the bottom of wells of a 24-well culture plate. At 7 days of biofilm maturation, the supernatant was removed and the coverslips were gently rinsed three times with HBSS and then blocked with 2% bovine serum albumen. Samples were labeled with a primary mouse antibody against dsDNA (Abcam, Cambridge, MA) and then after three washes, a donkey anti-mouse secondary antibody conjugated to 12 nm colloidal gold particles (Abcam). Labeled samples were fixed in a solution of 150 mM sodium cacodylate, 2% formaldehyde, 2% glutaraldehyde, 4% sucrose, and 0.15% Alcian blue 8GX (Sigma Aldrich, St. Louis, MO) at room temperature for 22 hours. Samples were then dried in graded ethanol concentrations (25%, 50%, 70%, 85%, 95%, 95%, 100%, 100%), further dried in a CO_2 critical point dryer, and sputter coated with 10-15nm of gold palladium. Electron micrographs were captured using a FEI Quant 600F FE scanning electron microscope at the Oregon State University Electron Microscopy Facility.

Biofilm matrix and supernatant preparation. Seven day-old biofilms grown in 75 cm^2 flasks were gently removed using a sterile swab, collected, and centrifuged at 2,500 x *g* for 15 minutes to pellet the biomass. The biofilm supernatant was poured off, collected, and filtered through a 0.2µm syringe filter. The supernatant was then concentrated 30x using 30 kDa pore size centrifugal filter (Pall Corporation, Port Washington, NY). The remaining biomass pellet after supernatant removal was resuspended into 1 ml of sterile dH_2O and physically agitated in a Mini-Beadbeater-1 (Biospec Products, Bartlesville, OK) at 4,800 oscillations per minute for 1 minute without beads, to not lyse the bacteria. Samples were centrifuged 12,000 x *g* for 5 minutes to pellet the bacteria, but keep the solubilized matrix in suspension. The

liquid was withdrawn, and filtered through a 0.2µm syringe filter to sterilize the extracted matrix.

Quantification of eDNA. 25 µl of biofilm matrix or supernatant was added into 4 replicate wells of a black walled 96-well plate and then 25 µl of 6 µM propidium iodide (in deionized H_2O) was added to each well. The plate was briefly vortexed, incubated at room temperature in the dark for 15 minutes, and then fluorescently quantified using an Infinite F200 microplate reader (Tecan, Männedorf, Switzerland) with an excitation filter at 535 nm and an emission filter at 620 nm. As a background control, deionized H_2O was mixed with the propidium iodide to attain the background fluorescence of the stain. The mean of the background value for each plate was subtracted from the sample values obtained, thus fluorescent signal reported is directly correlated to presence of DNA.

RAPD PCR, cloning, and sequencing of eDNA. Genomic DNA (gDNA) from log-phase MAH A5 was extracted using the DNeasy Blood and tissue kit (Qiagen, Venlo, Netherlands). eDNA was extracted in the matrix described above and further purified using a DNA Clean & Concentrator kit (Zymo Research, Irvine, CA). RAPD (Randomly Amplified Polymorphic DNA) PCR was conducted on eDNA and gDNA using previously published random primers that worked successfully with *M. avium*: primer set 1, 5'-AACGCGCAAC-3' (Ramasoota, Chansiripornchai et al. 2001); primer set 2, 5'-AAGAGCCCGT-3' (Ramasoota, Chansiripornchai et al. 2001); and primer set 3, 5'-AACGGTGACC-3' (Pillai, Jayarao et al. 2001). The reaction was as follows: 92˚C for 1 minute, 35˚C for 1 minute, and 72˚C for 1 minute for 45 cycles followed by a final extension period of 7 minutes. RAPD products were separated and visualized using 2% agarose gel electrophoresis containing 0.5 µg/ml of ethidium bromide in the gel. For cloning and sequencing of random eDNA fragments, purified eDNA was double-digested for 2 hours at 37˚C with BamHI and BglII, PCR purified (Qiagen), ligated into a similarly digested pMV261 mycobacterial shuttle vector, and then electroporated into *Escherichia coli* DH10B (Life Technologies). Inserts from 7 random transformants were sequenced at the Center for Genome Research and Biocomputing at Oregon State University. BLAST

from NCBI was used to identify the returned sequences and the *M. avium* 104 annotated genome (NCBI Reference Sequence: NC_008595.1) was used as a reference genome for gene identifications.

DNase I experiments. Recombinant DNase I (Roche, Penzberg, Germany) was used at 100 Kunitz units per ml in all experiments to analyze biofilm prevention, removal, and tolerance. These experiments were carried out in 96-well polystyrene plates. To assess the effect of DNase on biofilm formation, biofilms were formed, as described earlier, with the addition of 10% v/v 10x DNase buffer (400 mM Tris-HCl, 100 mM NaCl, 60mM MgCl2, 10 mM CaCl2; pH 7.9) into the inoculum with or without DNase. After 1 day of biofilm formation, supernatants were withdrawn, serially diluted, and plated to attain CFU of non-adherent bacteria.

For established biofilm removal experiments, biofilms were formed in HBSS as described earlier on abiotic surfaces and for the HEp-2 experiments, the bacterial inoculum was created in RPMI media instead of HBSS and the plates were incubated only at 37˚C with 5% CO_2. At 7 days of biofilm formation the supernatant was gently removed and replaced with 1x DNase buffer in HBSS with or without DNase for 2 hours at 37˚C (even for 22˚C biofilms). For both experiments, supernatant was withdrawn, serially diluted, and plated to determine CFU of removed bacteria.

For antibiotic tolerance experiments, stock solutions of moxifloxacin (Sigma) and clarithromycin (TCI, Tokyo, Japan) were made at 20 mg/ml in dH_2O and acetone, respectively. Moxifloxacin and clarithromycin were used at 16 μg/ml for experiments. Biofilms were formed in HBSS for 7 days, and then supernatants were gently removed and replaced with 1x DNase buffer with antibiotic with or without DNase and incubated at 37˚C for 48 hours (even for 22˚C biofilms). This experiment was unique from the others, in that after treatment, supernatant was not removed from the wells; instead, the entire population of bacteria (both unadhered and adhered) were mixed, diluted, and plated for CFU. Wells were mixed well by pipetting 50x, diluted, and plated to attain CFU of surviving bacteria.

Statistical analysis. Statistical comparisons were made using an unpaired homoscedastic t-test. Definitions of statistical significance, where shown in figures by

asterisks, are described in the corresponding Figure caption. Microsoft Excel and GraphPad Prism were used for statistics and graphical outputs, respectively.

Results

Extracellular DNA is abundant in the MAH A5 biofilm matrix and supernatant. Despite the growing body of research suggesting eDNA as a major component of microbial biofilms, there have been no reports to date of eDNA as a constituent of mycobacterial biofilms. We first assessed if MAH 104 and MAH A5 possess eDNA when grown in biofilms *in vitro*. Previous work has characterized MAH A5 as a high biofilm producing strain, when compared to other MAH clinical isolates (Carter, Wu et al. 2003) and MAH 104 is the genome-sequenced reference strain. Macroscopically, surface-attached biofilms from MAH 104 (Figure 3.1A) and MAH A5 (Figure 3.1B) have differing phenotypes. Additionally, MAH A5 has a distinct wrinkling pattern, which is consistent with other reports of eDNA-producing biofilms (Asally, Kittisopikul et al. 2012). To visualize if eDNA was present in these biofilms, scanning electron microscopy with dsDNA-specific immunogold labeling was carried out on 7 day MAH A5 and 104 biofilms formed in HBSS on abiotic surfaces at 22˚C (Figure 3.1 C-F). A network of fibrous structures are seen in the MAH A5 biofilm with immunogold particles being localized on these structures (Figure 3.1 D-F), which is consistent with eDNA recently visualized in *Enterococcus* biofilms (Barnes, Ballering et al. 2012). Though the biofilm as not as intact after preparation, biofilm matrix was seen in the MAH 104 biofilm, but it was not fibrous and did not contain any bound immunogold particles (Figure 3.1C).

Due to the observation suggesting eDNA in MAH A5 biofilms, next we quantitatively assessed eDNA in acellular biofilm components. Biofilms were statically formed on abiotic surfaces both at 22˚C and 37˚C, to represent environmental and human host associated biofilms, respectively. After 1 and 7 days of biofilm formation, supernatant was collected and concentrated, and the water soluble biofilm matrix was extracted. The acellular matrix and supernatant were quantified with a fluorescent plate reader after mixing with propidium iodide, a stain specific for DNA. When comparing day 1 to day 7, there is a significant increase in eDNA production over the time course (Figure 3.2 A and B). At day 7 of biofilm formation, MAH A5 possesses abundant eDNA in its acellular matrix and supernatant

formed at both 22˚C and 37˚C, whereas MAH 104 produced significantly less eDNA at both temperatures (Figure 3.2B). Taken together, these data suggest that eDNA is a major component of MAH A5 biofilms.

To assess how the number of viable bacteria in the biofilm correlated with eDNA production, CFU of MAH A5 and 104 were enumerated over the course of biofilm formation (Figure 3.2C). There is a slight drop in CFU for both strains between the original inoculum and days 1 and 7, but the drop is larger in MAH 104, which produces significantly less eDNA. Furthermore, eDNA measured from day 1 MAH A5 biofilms is substantially less than day 7 (Figure 3.2 A and B), which indicates that the minor drop in CFU does not correlate with presence of eDNA, since day 1 and 7 MAH A5 CFU recovered are similar (Figure 3.2C).

eDNA is found among MAH and other nontuberculous mycobacteria. To survey if eDNA production was specific to MAH A5, or more widespread among MAH, we extracted acellular biofilm matrix from other MAH clinical isolates and quantified eDNA. Though MAH A5 possesses more eDNA in its biofilm matrix than other MAH strains tested, the data shows that other MAH strains do produce eDNA (Figure 3.3A). Due to the known heterogeneity of the species, it is not unexpected that the eDNA concentrations are variable among strains. We further expanded the assessment of eDNA production beyond MAH to other clinically relevant, biofilm forming nontuberculous mycobacteria (Figure 3.3B). Similar to *M. avium*, eDNA levels are variable in different species, but it does appear that *M. abscessus* and *M. chelonae*, regardless of strain, produce considerably more eDNA than the other mycobacterial species tested. Since MAH A5 produces the most eDNA of the mycobacterial species tested, it being characterized previously as a high biofilm producer, and our interest in its pathogenesis, we chose to concentrate on MAH A5 for the rest of the study.

Characterization of eDNA in MAH A5. To investigate if eDNA found in the biofilm matrix is genomic in origin or an eDNA-specific sequence, it was directly compared to genomic DNA (gDNA) from log-phase MAH A5. Random amplified Polymorphic DNA (RAPD) PCR was used to gauge the similarity between extracted

eDNA and gDNA with the rationale that a specific secreted sequence of DNA (not containing the entire genome) will produce a RAPD fingerprint distinct from genomic DNA. The RAPD fingerprint between eDNA and gDNA using three proven RAPD primers were all indistinguishable (Figure 3.4), suggesting eDNA is genomic in origin. To corroborate this, extracted eDNA was digested with BamHI and BglII, ligated into a similarly digested pMV261 mycobacterial-*E. coli* shuttle vector, electroporated into *E. coli*, and plasmid insertions from 7 transformants were sequenced. The returned sequences were distributed randomly throughout the MAH genome (Table 3.1), further confirming that the eDNA is genomic in origin and not a particular sequence unique to eDNA.

eDNA has a structural role in MAH A5 biofilms. Previous work describing MAH A5 as a biofilm overproducer (Carter, Wu et al. 2003), the robustness of the biofilm (Figure 3.1B), and the fibrous eDNA matrix (Figure 3.1 D-F) led us to hypothesize that eDNA could participate in a structural role in the A5 biofilm. To investigate this, DNase I was used to prevent biofilm formation as well as to destabilize established biofilms. After 1 day of biofilm formation with the addition of DNase buffer with or without DNase I to the biofilm inoculum, the supernatants were removed to quantify the amount of unadhered bacteria. The combination of DNase buffer and DNase significantly inhibited the establishment of MAH biofilms after 1 day of formation, when compared to the addition of DNase buffer by itself (Figure 3.5A). This effect was observed in biofilms formed both at 22˚C (48% more bacteria removed) and 37˚C (37% more bacteria removed). DNase did not have any significant differences from buffer alone at 3 or 7 days (data not shown) presumably due to the enzyme degrading or quenching over the longer courses of incubation.

To assess the structural contribution of eDNA to established A5 biofilms, DNase was added after 7 days of biofilm formation by gently removing the biofilm supernatant and replacing with DNase buffer with or without DNase. DNase buffer with DNase was also significantly more effective at removing MAH A5 established biofilms than DNase buffer by itself (48% and 41% more bacteria removed from 22˚C and 37˚C biofilms, respectively) after a 2 hour digestion period (Figure 3.5B).

To further determine the structural contribution of eDNA to host-associated biofilms, MAH A5 biofilms were formed on top of a HEp-2 pharyngeal cell monolayer for 7 days and then subjected to a 2 hour DNase digestion. Similar to biofilms formed on top of abiotic surfaces, DNase also significantly removed more bacteria from established biofilms on top of HEP-2 cells, when compared with DNase buffer by itself (Figure 3.5B). The effect was more pronounced in these experiments (268% more bacteria removed), which suggests that the biofilms formed on top of host cells could be different from biofilms formed on abiotic surfaces. Collectively, these data demonstrate that eDNA plays a considerable structural role in MAH A5 biofilms.

eDNA aids in tolerance of the MAH A5 biofilm to antibiotic treatment. MAH biofilms have been shown to be more resistant to antimicrobials than their planktonic counterpart (McNabe, Tennant et al. 2011). Since the DNase prevention and removal work demonstrated the structural role of eDNA in these biofilms (Figure 3.5), we further assessed if co-treatment of DNase with an antimicrobial would reduce the tolerance of the biofilm. Moxifloxacin and clarithromycin, which are both used clinically against MAH (Griffith, Aksamit et al. 2007), were used in these experiments. Biofilms were formed for 7 days on an abiotic surface, and then the supernatant was removed and replaced with 16 μg per ml of moxifloxacin or clarithromycin in DNase buffer with or without DNase and incubated at 37˚C for 48 hours. Without washing away or removing any bacteria first, entire biofilm wells (containing both unadhered and adhered bacteria) were resuspended and plated to attain CFU of surviving bacteria. Bacteria in the biofilms co-treated with DNase were significantly more sensitive to both moxifloxacin and clarithromycin than ones in biofilms that were co-treated with DNase buffer only (Figure 3.6 A and B, respectively). For moxifloxacin, there were 48% less viable bacteria at 22˚C and 37% less at 37˚C. For clarithromycin, there were 43% less at 22˚C and 24% less at 37˚C. Taken together, these data show that eDNA in the biofilm contributes to the tolerance of MAH to commonly used antibiotics for MAH treatment.

Discussion

Extracellular DNA (eDNA) has been described in many bacterial biofilms in recent years, but until this point, has not been identified in mycobacterial biofilms. We found and characterized eDNA in a previously reported high biofilm forming strain of *Mycobacterium avium* subsp. *hominissuis*, MAH A5. Furthermore, we report that eDNA in mycobacterial biofilms is more widespread and not just unique to MAH A5, even though of the species and strains tested, it appears to be the largest producer. The eDNA in MAH A5 biofilms appears to be of genomic origin, aids in the structural integrity, and contributes to antimicrobial tolerance.

The source of eDNA, whether it be a result of cell lysis or is actively secreted, is a controversial subject. Multiple reports have described lysis as the mechanism (Allesen-Holm, Barken et al. 2006; Qin, Ou et al. 2007; Rice, Mann et al. 2007; Thomas, Thurlow et al. 2008; Das and Manefield 2012), but in recent years, growing evidence is suggesting that in some organisms, eDNA production could result from non-lytic mechanisms (Bockelmann, Janke et al. 2006; Vilain, Pretorius et al. 2009; Grande, Di Giulio et al. 2011; Barnes, Ballering et al. 2012; Sahu, Iyer et al. 2012; Liao, Klein et al. 2014). We assessed if the numbers of viable bacteria correlated with was responsible for eDNA production in MAH A5 by tracking CFU of MAH in the biofilm over the experimental time course. At day 1 and 7 there are similar minor reductions in the MAH A5 CFU from the initial inoculum, but this can be attributed to insufficient removal of all of the bacteria out of the microplate due to the lipid rich biofilm and visual confirmation of residue left in the wells. Interestingly, there was very little difference between CFU recovered between day 1 and day 7, even though the eDNA quantified increased dramatically between these two time points. Barnes *et al.* described lysed cells and subsequently released eDNA in electron micrographs and that in their early biofilm micrographs, lysed cells were infrequently encountered (Barnes, Ballering et al. 2012). Our electron micrographs agree with this in that we largely observe intact bacilli within the A5 biofilm (Figure 3.1F). More research will be needed to answer if MAH eDNA is a result of mass cell lysis, but our data presented gives preliminary evidence that other mechanisms could be contributing to

eDNA production, such as membrane vesicle secretion (Sahu, Iyer et al. 2012; Liao, Klein et al. 2014). Secreted membrane vesicles have been found in mycobacteria, including *M. avium*, but eDNA in these vesicles has not been reported (Marsollier, Brodin et al. 2007; Prados-Rosales, Baena et al. 2011).

When comparing the fibrous or strand-like eDNA structures observed in MAH A5 with other reports (Bockelmann, Janke et al. 2006; Barnes, Ballering et al. 2012), there are visual similarities. The fibrous eDNA network in the environmental strain F8 from Böckelmann *et al*. is very similar to our observations. The strands seen in Barnes *et al.* do not form a network as complex as ours or in Böckelmann *et al*., but these were early biofilms studied (2-8 hours), compared with ours (7 days) and Böckelmann *et al*. (4 days). We are confident that the fibrous matrix observed in the A5 biofilm is, at least partly, composed of eDNA, but there were limitations in the immunogold labeling. When comparing the MAH A5 biofilm with the *Enterococcus* biofilm in Barnes *et al*., there is reduced antibody labeling. It can be assumed that the matrix of early *Enterococcus* biofilms is less complex than of our 7 day MAH A5 biofilms, which could yield more accessible eDNA targets for antibody binding. It is plausible that the complex, lipid rich matrix of MAH A5 either making the eDNA inaccessible to the antibody, or that a component in the matrix is non-specifically binding the antibody and inactivating it. Interestingly, the labeling occurred most frequently at biofilm wrinkles or breaks, which there were possibly more exposed portions of eDNA.

It is important when studying environmental opportunistic pathogens to discern environmental mechanisms and processes from host-specific ones. A goal of this study was to investigate this newly found eDNA under conditions representing environmental and host-related biofilms, to help elucidate if eDNA production in *M. avium* is an environmental adaptation, a mechanism used for virulence, or possibly used for both. When quantifying eDNA from acellular A5 supernatant and matrix (Figure 3.2A), there were differences between biofilms grown at 22˚C and 37˚C (less eDNA in the matrix than 22˚C but more in the supernatant). When analyzing the effect of DNase on MAH A5 biofilm structure and antimicrobial tolerance, there were

consistently greater reductions at 22˚C than at 37˚C, but due to the differing matrix/supernatant eDNA quantifications between the temperatures, a conclusion cannot be reached from this. Interestingly, the biofilm formed at 37˚C on top of HEp-2 cells had a much more significant reduction from DNase treatment than either the biofilm formed at 22˚C or 37˚C on abiotic surfaces. eDNA production might be regulated by factors not related to heat-shock, but instead environmental and/or host signals. It is important to note however, that the biofilms formed on top of the cells were in RPMI media supplemented with FBS (compared to the abiotic biofilms formed in HBSS), which could contribute to a different biofilm and resulting DNase treatment efficacy.

Another possible link of eDNA to infection is a recent report with *M. tuberculosis* producing extracellular DNA during intracellular infection that exits the perforated phagosome and stimulates the cytosolic surveillance pathway to promote infection (Manzanillo, Shiloh et al. 2012). The authors found that the extracellular DNA was mycobacterial in origin and hypothesized that it was secreted, though the mechanism remains elusive. We published a recent manuscript looking at the interaction of MAH biofilms with host surveilling phagocytes, and found that A5 was significantly more stimulatory to phagocytes than MAH 104 (Rose and Bermudez 2014). To distinguish if the cells themselves or an acellular component was responsible for this hyper stimulation, we UV-sterilized biofilms prior to infection (Rose and Bermudez 2014). The sterilized biofilm elicited an almost identical effect on the phagocytes. Similarly, the acellular supernatants of MAH A5 and 104 biofilms were cultured with phagocytes, and A5 (but not 104) elicited a large response (Rose and Bermudez 2014). It is well known that CpG bacterial DNA is a substrate for toll-like receptor 9 in host phagocytes and other cells. When combining those phagocyte stimulation results with the findings of this current report, we speculate that the eDNA could, at least partly, explain the uniquely high TNF-α production elicited from MAH A5. The contribution, if any, of MAH eDNA to virulence still needs to be investigated.

The significant effect of DNase I on the biofilms was intriguing. Biofilm-associated infections with MAH, especially of the respiratory tract, are difficult to treat clinically. We recently published a report establishing the efficacy of a novel inhaled liposomal amikacin for inhalation (Rose, Neville et al. 2014). Topical therapy delivered by liposomes was effective at reducing the MAH burden in the respiratory tract of mice. It would be worthwhile to investigate the added benefit of possibly combining this topical therapy with an inhaled DNase adjuvant, which is already an FDA approved as an inhaler for cystic fibrosis patients (Pulmozyme®). Reducing the tolerance of MAH biofilms *in vivo*, as we demonstrated with DNase *in vitro* in this study, could create more effective treatment options clinically.

Acknowledgements

We thank Zachary Rose for his assistance with the CFU experiments and Michael McNamara for helping sequence the eDNA fragments. We acknowledge Teresa Sawyer and the Oregon State University Electron Microscopy Facility for their expertise and the use of their facility. This work was supported by grant AI041399 from the National Institutes of Health.

Figure 3.1. Gross morphology and scanning electron microscopy of MAH 104 and A5 7 day-old biofilms. Log-phase bacteria were resuspended into HBSS and were incubated statically for 7 days at room temperature to allow biofilm formation on an abiotic surface at the surface-liquid interface. (A and B) Gross morphology of a biofilm formed in a 6-well polystyrene plate. (C-F) Biofilms formed on top of coverslips were fixed, labeled with an anti-dsDNA primary antibody, labeled with a secondary antibody conjugated to gold particles, and visualized with scanning electron microscopy. MAH 104 (C) and MAH A5 (D-F) both have biofilm matrix, but the eDNA is only observed in MAH A5 (fibrous structures). Gold particles bound to eDNA, appearing as white spots, were only visualized in MAH A5 biofilms and were localized to the filamentous structures. Asterisks are placed in the micrographs to demonstrate locations of immunogold particles.

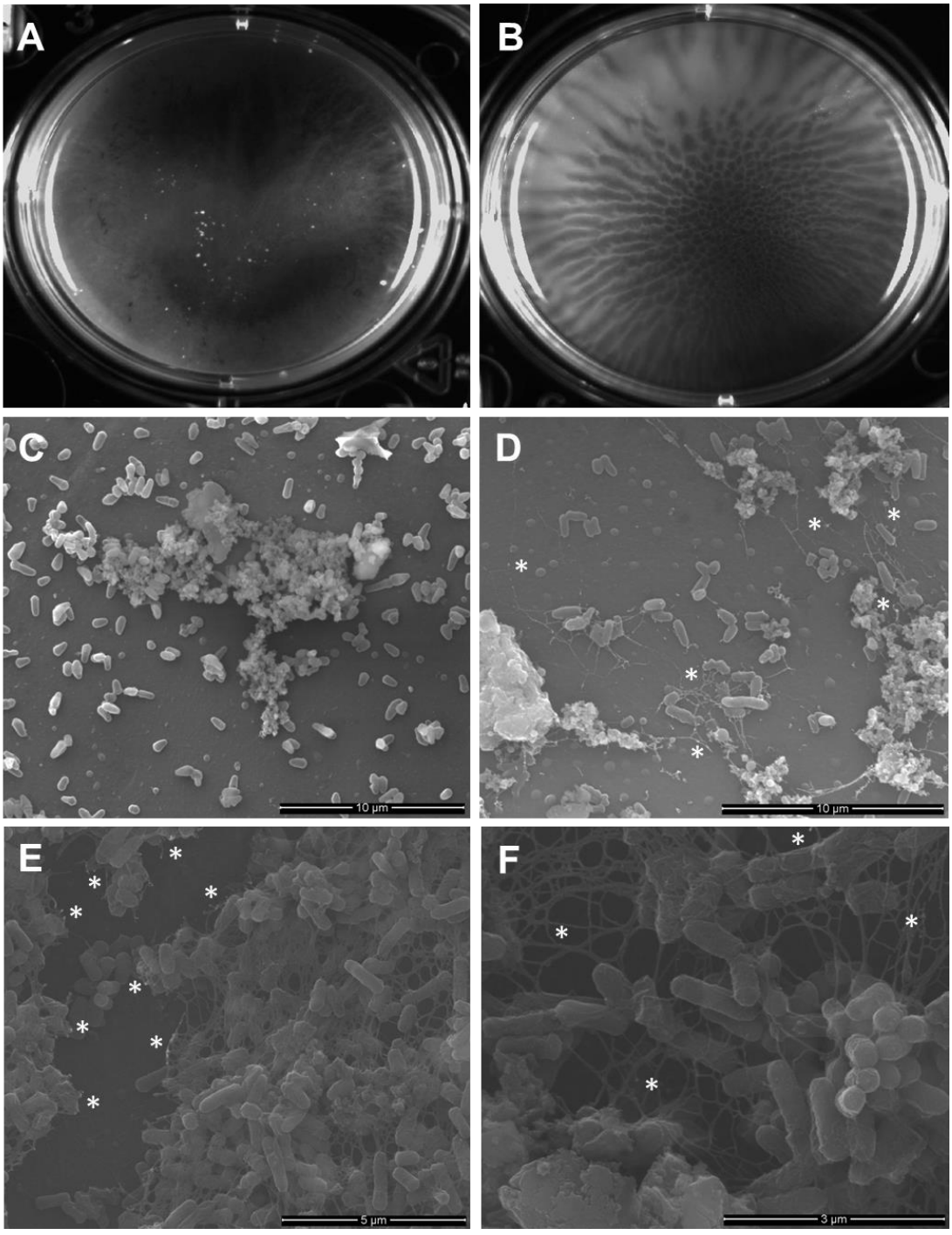

Figure 3.1. Gross morphology and scanning electron microscopy of MAH 104 and A5 7 day-old biofilms.

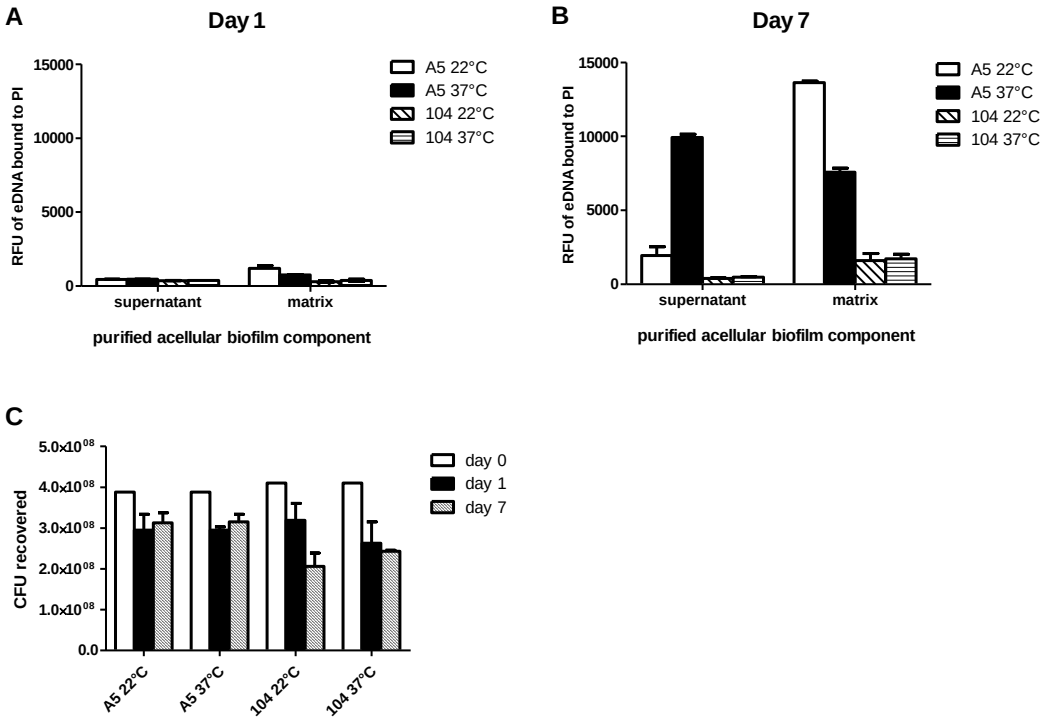

Figure 3.2. Quantitative assessment of eDNA and CFU in MAH A5 and 104 biofilms. MAH A5 and 104 static biofilms were formed in 75 cm^2 flasks in HBSS at both 22˚C and 37˚C to represent environmental and host-associated biofilms, respectively. (A and B) After 1 and 7 days of biofilm formation, acellular matrix and supernatant was collected from the biofilms and quantitatively assessed for eDNA using propidium iodide. Bars represent the mean of three biological replicates ± the standard error of the mean (day 7) and the mean of two biological replicates ± the standard error of the mean (day 1). RFU: Relative fluorescence units. PI: Propidium iodide. (C) As biofilms formed over 7 days, wells were mixed thoroughly to remove adhered bacteria and samples were processed for CFU. Day 0 represents the CFU of the inoculum prior to seeding wells for biofilm production. Bars represent the average of three wells of biofilm processed independently ± the standard deviation. The data shown is representative of three biological replicates.

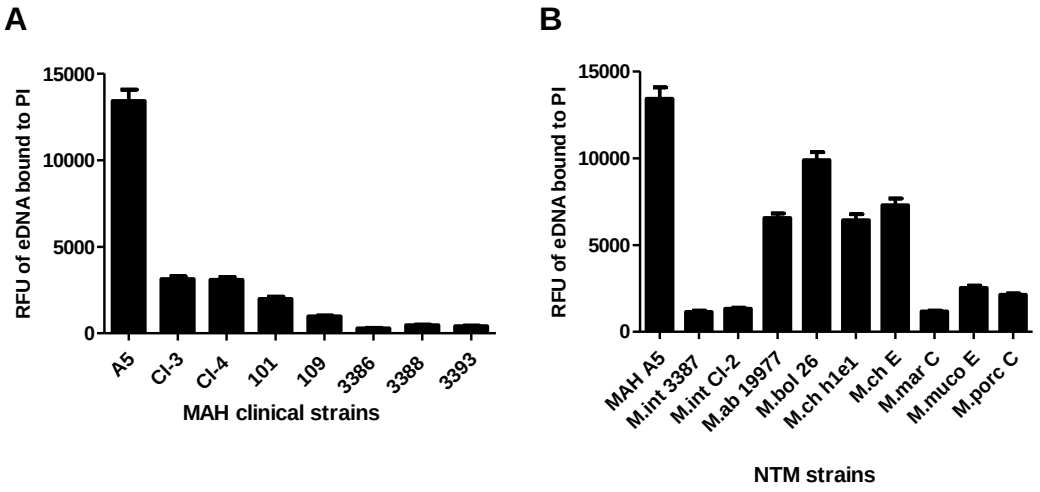

Figure 3.3. Survey of eDNA in other MAH strains and nontuberculous mycobacteria. To assess if eDNA was widespread throughout mycobacteria and not an artifact of MAH A5, biofilms were formed in (A) other *M. avium* strains and (B) other nontuberculous mycobacteria. Biofilms were formed in 75 cm^2 flasks (20 ml volume) and after 7 days of formation at 30˚C, acellular biofilm matrix was extracted and quantified for eDNA. Abbreviations used: M.int = *M. intracellulare*; M.ab = *M. abscessus* subsp. *abscessus*; M.bol = *M. abscessus* subsp. *bolletii*; M.ch = *M. chelonae*; M.mar = *M. marinum*; M.muco = *M. mucogenicum*; M.porc = *M. porcinum*; E = environmental isolate; C = clinical isolate; RFU = relative fluorescence units; PI = propidium iodide.

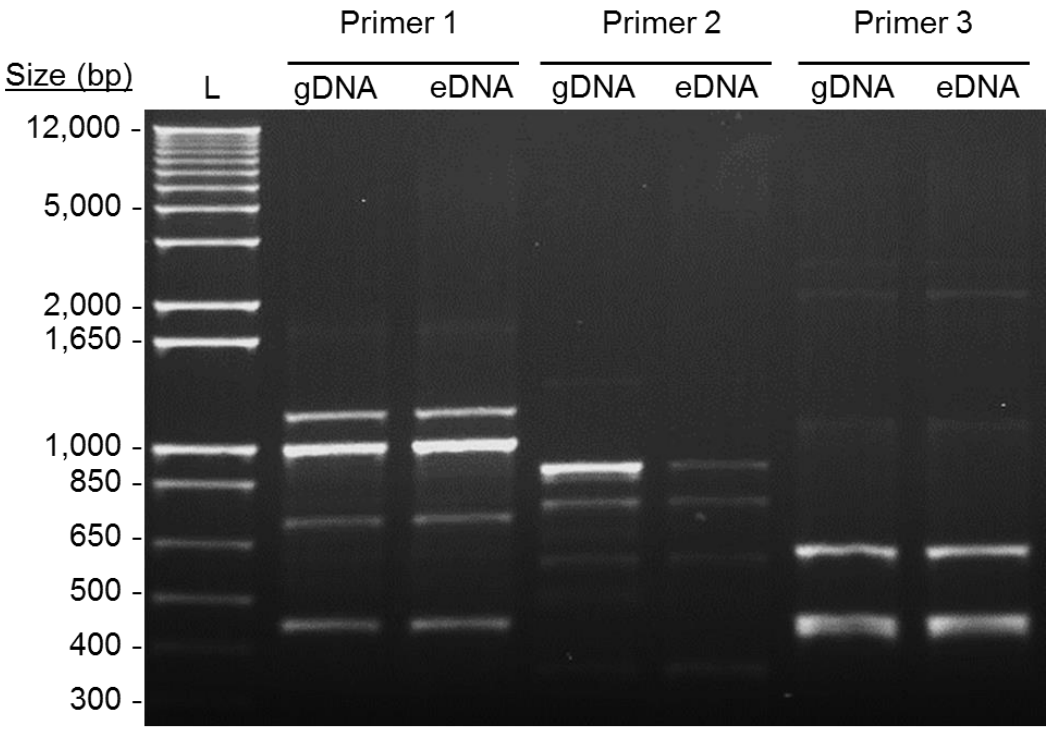

Figure 3.4. Characterization of eDNA in the MAH A5 biofilm. To compare the similarities of eDNA with genomic DNA (gDNA), side-by-side fingerprinting was done. eDNA extracted from the A5 biofilm matrix was purified and gDNA was extracted from log-phase A5 using a commercial kit. RAPD PCR was conducted from these DNA templates using three sets of random primers that have already been confirmed to work with *M. avium*.

Table 3.1. Sequence results from 7 random pieces of eDNA that were extracted from the MAH A5 biofilm matrix, digested, purified, cloned into a shuttle plasmid, and sequenced.

Sample ID	Gene ID*	Gene description
1	MAV_0734	Hypothetical protein
	MAV_0735	Phosphoribosylformylglycinamidine synthase, PurS
	MAV_0736	Phosphoribosylformylgylcinamidine synthase I
2	MAV_2472	Isochorismatase family protein
	MAV_2473	Nuclear transport factor 2 (NTF2) domain family
3	MAV_5173	Putative acyl-CoA dehydrogenase
	MAV_5174	ZbpA protein
4	MAV_4973	MmpL11 protein
5	MAV_4859	Trans-aconitate 2-methyltransferase
6	MAV_4893	Hypothetical protein
	MAV_4892	Nitrite transporter
7	MAV_4541	Cyclopropane-fatty-acyl-phospholipid synthase
	MAV_4542	Exodeoxylribonuclease V, gamma subunit

* The MAH 104 annotated genome (NCBI Reference Sequence: NC_008595.1) was used as a reference genome for gene identifications.

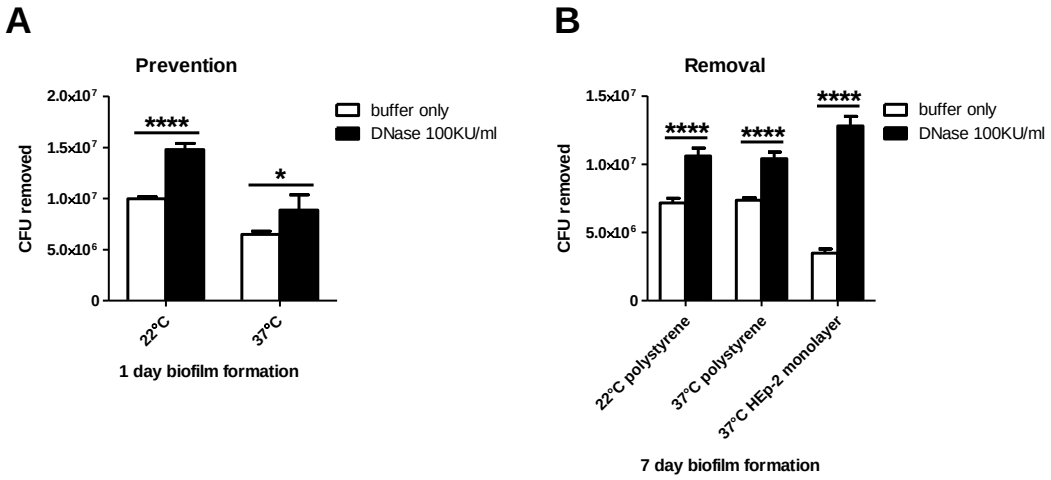

Figure 3.5. Effect of DNase treatment on preventing and removing MAH A5 biofilms. (A) Biofilms inoculums were made in HBSS supplemented with 1x DNase buffer ± 100 Kunitz units per ml of recombinant DNase I. After 1 day of static biofilm formation at both 22˚C and 37˚C, supernatants were removed to enumerate the CFU of non-adhered bacteria. (B) For abiotic surface removal, biofilms were formed in 96-well plates in HBSS for 7 days at both 22˚C and 37˚C. For HEp-2 surface removal, biofilms were formed in RPMI media supplemented with 10% FBS on top of already established HEp-2 monolayers in 96-well plates. At 7 days, supernatants were gently removed and replaced with HBSS supplemented with 1x DNase buffer ± 100 Kunitz units per ml of DNase. Biofilms were incubated for an additional 2 hours and then supernatants removed to enumerate CFU of detached bacteria. For both A and B, bars represent the average of 4 wells of biofilm processed independently ± standard deviation. Data sown are representative of three biological replicates. Statistical comparisons: * $P < 0.05$; **** $P < 0.0001$.

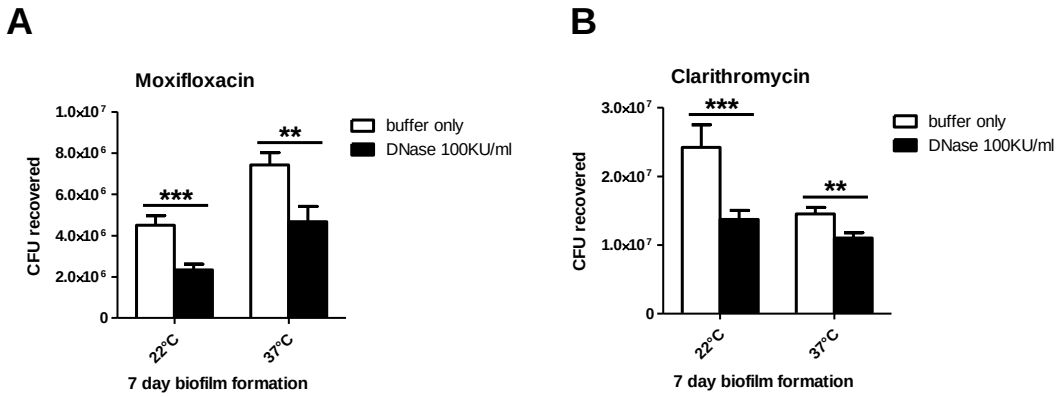

Figure 3.6. Effect of DNase co-treatment with antimicrobials on the MAH A5 biofilm. Biofilms were formed in HBSS in 96-well plates and incubated at 22˚C and 37˚C for 7 days. Supernatants were gently removed and replaced with HBSS containing 16 µg/ml of (A) moxifloxacin or (B) clarithromycin further supplemented 1x DNase buffer ± 100 Kunitz units per ml of recombinant DNase. All biofilms (including 22˚C) were incubated for 48 hours at 37˚C. Wells were mixed 50 times via pipetting to remove attached bacteria and samples were diluted and plated to obtain total viable bacteria. For both A and B, bars represent the average of 4 wells of biofilm processed independently ± standard deviation. Data shown are representative of three biological replicates. Statistical comparisons: ** $P < 0.01$; *** $P < 0.001$.

Chapter 4

Identification of Bicarbonate as a Trigger and Genes involved with Extracellular DNA Export in Mycobacterial Biofilms

Sasha J. Rose and Luiz E. Bermudez

Submitted to the journal mBio

Abstract

Extracellular DNA (eDNA) is an integral biofilm matrix component of numerous pathogens, including nontuberculous mycobacteria (NTM). Cell lysis is the source of eDNA in certain bacteria, but the mechanism remains unanswered for NTM, as well as other eDNA producing bacterial species. In this study conditions affecting eDNA production were investigated, and genes involved with the eDNA export mechanism were identified. After establishing a method for monitoring eDNA in real-time in undisturbed biofilms, different conditions affecting eDNA were investigated. Bicarbonate positively influenced eDNA export in a pH-independent manner in *M. avium*, *M. abscessus*, and *M. chelonae*. The surface-exposed proteome of *M. avium* in eDNA-containing biofilms revealed abundant carbonic anhydrases. Chemical inhibition of carbonic anhydrases with ethoxzolamide significantly reduced eDNA production. An unbiased 4,048 mutant transposon library screen for eDNA export in *M. avium* identified many severely eDNA-attenuated mutants including one not expressing a unique FtsK/SpoIIIE-like DNA transporting pore, two with inactivation of carbonic anhydrases, nine mutants with inactivation of genes belonging to a unique genomic region, as well as numerous mutants involved in metabolism and energy production. Complementation of nine mutants including the FtsK/SpoIIIE and carbonic anhydrase significantly restored eDNA production. Interestingly, several attenuated eDNA mutations are in genes encoding proteins that were found with the surface proteomics, and many more are localized in potential operons with surface proteins. Collectively, our data strengthens the evidence of eDNA export being an active mechanism, activated by the bacteria responding to bicarbonate.

Importance

Many bacteria produce extracellular DNA (eDNA) in their biofilm matrix, as it has many biological and physical functions. We recently reported that nontuberculous mycobacteria (NTM) can contain significant quantities of eDNA in their biofilms. In some bacteria eDNA is derived from dead cells, but it does not appear to be the case for all eDNA-producing organisms, including NTM. In this paper, we found that eDNA production in NTM is conditional depending on what molecules the bacteria are exposed to and that bicarbonate positively influences eDNA production. We also identified genes and proteins important for eDNA production, which begins to piece together the mechanism behind eDNA. Better understanding eDNA production can give new targets to develop anti-virulence drugs against, which are attractive as resistance to classical antibiotics is a significant problem currently.

Introduction

Nontuberculous mycobacteria (NTM) are opportunistic pathogens that are ubiquitous in the environment and are enriched in urban potable water systems (Griffith, Aksamit et al. 2007). Even though NTM infections are not reported in many countries, analysis of smaller populations has shown that the prevalence of NTM infections is increasing, with infections caused by *Mycobacterium avium* (MAH) being the most common (Winthrop, McNelley et al. 2010; Adjemian, Olivier et al. 2012; Henkle, Hedberg et al. 2015; Shao, Chen et al. 2015). Though MAH infects individuals with immunosuppression through the gastrointestinal route and often leads to disseminated disease, infections in immunocompetent patients and are typically localized to the respiratory tract (Griffith, Aksamit et al. 2007; Honda, Knight et al. 2015). Underlying respiratory conditions such as cystic fibrosis, chronic obstructive pulmonary disease, and bronchiectasis increase susceptibility for infection, but otherwise normal individuals can also develop disease (Winthrop, McNelley et al. 2010; Honda, Knight et al. 2015).

How these infections establish and persist in the respiratory tract of immunocompetent patients is not completely understood, but growing evidence supports the hypothesis that, in addition to the well-described intracellular lifestyle in macrophages, NTM also colonize the airway through microaggregate and biofilm formation. Microscopy conducted on explanted lung sections from cystic fibrosis patients found *M. abscessus* biofilms on tissues, demonstrating the direct role of biofilms during these infections (Qvist, Eickhardt et al. 2015). In MAH, biofilm formation augments infection of epithelial cells in vitro and significantly influences respiratory infection in vivo (Yamazaki, Danelishvili et al. 2006). Furthermore, MAH forms mircoaggregates once in contact with respiratory epithelial cells, and once formed, the bacteria are more proficient at binding to and invading other cells (Yamazaki, Danelishvili et al. 2006; Babrak, Danelishvili et al. 2015; Babrak, Danelishvili et al. 2015). Surveilling macrophages that encounter MAH in vitro become hyper-stimulated and undergo early, rapid apoptosis in a TNFα-dependent manner (Rose and Bermudez 2014), which could explain why the aggregates and

biofilms are not cleared by the immune system. Interestingly, UV-sterilized biofilms elicited a similar TNFα response from the phagocytes as the live biofilm, suggesting that an acellular matrix component of the biofilm could be responsible for the atypical macrophage response (Rose and Bermudez 2014).

The biofilm matrix of most bacteria is composed of exopolysaccharides (EPS), proteins, lipids, and nucleic acids (Flemming and Wingender 2010). Mycobacteria form unique biofilms compared to most other biofilm forming pathogens, in part because they do not produce EPS (Zambrano and Kolter 2005). Studies have identified some of the components of the unique mycobacterial biofilm matrix, including free mycolic acids (Ojha, Anand et al. 2005; Ojha, Baughn et al. 2008), glycopeptidolipids (Recht and Kolter 2001; Freeman, Geier et al. 2006; Yamazaki, Danelishvili et al. 2006; Nessar, Reyrat et al. 2011), and other lipid-containing molecules (Chen, German et al. 2006; Ren, Dover et al. 2007; Wu, Schmoller et al. 2009) in the matrix. Additionally, we recently reported the novel finding of extracellular DNA (eDNA) in both fast and slow growing NTM biofilms, including MAH, *M. abscessus*, *M. intracellulare*, and *M. chelonae*, among others (Rose, Babrak et al. 2015). Treatment with DNase I reduced biofilm colonization in vitro, aided in removing established biofilms, and, when co-treated with various clinically-used antibiotics, reduced the MAH tolerance to the antimicrobials. Since this report, another study also recently described effective co-treatment of *M. chelonae* and *M. fortuitum* biofilms with DNase I and antimicrobial agents (Aung, Hoong et al. 2015), further demonstrating the importance of eDNA in NTM biofilms.

eDNA has been found in the biofilm matrix of many bacterial genera, including numerous pathogens (Okshevsky, Regina et al. 2015). In *Staphylococcus* spp., *Enterococcus* spp., and *Pseudomonas aeruginosa*, lytic events release eDNA, including autolysins, H_2O_2-induced lysis, and prophage-mediated lysis have been reported (Allesen-Holm, Barken et al. 2006; Qin, Ou et al. 2007; Rice, Mann et al. 2007; Thomas, Thurlow et al. 2008; Das and Manefield 2012). Contrary to these findings however, there is a growing number of examples of non-lytic eDNA production in bacterial biofilms. Work with *Enterococcus faecalis* biofilms has

presented convincing data for active secretion including the lack of lysed cells, distinct eDNA morphologies between the fibrous eDNA and lysis-based DNA, bacteria possessing elevated membrane potentials, and no biochemical detection of intracellular components (Barnes, Ballering et al. 2012). Work with *Bacillus cereus* described early competence genes associated with eDNA production (Vilain, Pretorius et al. 2009). A report on an aquatic bacterium, F8, described distinct differences between the fibrous eDNA in the biofilm matrix and genomic DNA (Bockelmann, Janke et al. 2006). In addition, reports with *Streptococcus mutans* and *Acinetobacter baumannii* have identified eDNA in secreted membrane vesicles (Sahu, Iyer et al. 2012; Liao, Klein et al. 2014). These reports of lysis-independent eDNA in biofilms agrees with our finding of eDNA in MAH, in which we did not observe mass cell lysis microscopically or by monitoring CFU (Rose, Babrak et al. 2015). Importantly, despite this growing evidence of lysis-independent eDNA in bacterial biofilms, the actual mechanism(s) of eDNA production have yet to be identified.

In this study, we investigated the triggers of eDNA production and to begin to elucidate a mechanism of lysis-independent eDNA export in MAH. We determined that exogenous bicarbonate induces eDNA production in a pH-independent manner, and by studying the biofilm surface proteome and screening transposon mutants, we have unveiled genes associated with eDNA production including a DNA extrusion pore, a carbonic anhydrase, and a novel genomic region.

Materials and Methods

Bacterial strains and growth. *Mycobacterium avium* subsp. *hominissuis* strain A5 (MAH A5) was originally isolated from the blood of an AIDS patient. *M. abscessus* subsp. *abscessus* strain 19977 was obtained from the American Type Culture Collection (Manassas, VA). The *M. chelonae* isolate used is an environmental strain from Corvallis, Oregon that was isolated by our laboratory and used previously (Rose, Babrak et al. 2015). Unless otherwise noted, bacteria for experiments were grown and maintained on 7H10 agar supplemented with 10% oleic acid, albumin, dextrose, and catalase (OADC; Hardy Diagnostics, Santa Maria, CA) at 37˚C.

Biofilm formation. Static biofilms were formed as described previously (Rose and Bermudez 2014), with minor modifications. Briefly, a 10^9 CFU/ml suspension was prepared in deionized H_2O (DI H_2O) from log-phase bacteria grown on 7H10 agar. After allowing 10 minutes for the clumps to sediment, the top half of the suspension was transferred and adjusted by diluting a sample of the suspension 1:10 and then assessing visual turbidity using a McFarland #1 standard (3×10^8 CFU/ml). Once adjusted, biofilm inoculums were formed by mixing 10% v/v of the 3×10^9 suspension with 90% v/v of appropriate diluent. For the initial experiments, the diluent was 90% DI H_2O or Hank's balanced salt solution (HBSS) with calcium and magnesium (Corning, Corning, NY). Biofilms were incubated for up to 7 days for experimentation at room temperature, unless otherwise noted.

Live tracking of eDNA production. Upon biofilm formation, propidium iodide was added to the inoculum to 3 µM, from a 20 mM stock in DMSO. Fluorescence of propidium iodide bound to eDNA was quantified at 535/620 nm with an Infinite F200 microplate reader (Tecan, Männedorf, Switzerland). Readings were taken at time 0 (upon plate inoculation) and then over a 7 day time course. For a respective experiment, a specific manual gain was used for each time course, to standardize time points to each other.

HBSS component addition and subtraction. The formulation of HBSS with calcium and magnesium used has the following components: Anhydrous $CaCl_2$ 0.14 g/L; KCl 0.4 g/L; KH_2PO_4 0.06 g/L; anhydrous $MgSO_4$ 0.0977 g/L; NaCl 8 g/L;

anhydrous Na_2HPO_4 0.0477 g/L; $NaHCO_3$ 0.35 g/L; and D-glucose 1 g/L. 10x stock solutions of each of the 8 ingredients were made individually in DI H_2O. For individual ingredient additive experiments, 10% v/v of the 3 x 10^9 bacterial suspension (prepared as described above) was mixed with 10% v/v of a single 10x component, 80% v/v DI H_2O, and propidium iodide to 3 µM. Paired component additive experiments were set up similarly, with the exception that two 10x components were added, and only 70% v/v DI H_2O was used. For subtractive experiments, 10% v/v of the 3 x 10^9 bacterial suspension was mixed with different combinations of 7 of the 8 components (all at 10% v/v) and 20% v/v DI H_2O. Real-time quantification of eDNA production was fluorescently measured as described above.

Biotinylation and purification of surface-exposed and biofilm matrix proteins. The procedures used for biotin labelling and streptavidin purification from MAH A5 biofilms were adapted from McNamara *et al* (McNamara, Tzeng et al. 2012). Seven day-old biofilms were resuspended with a cell scraper, and then centrifuged at 2,000 x *g* for 15 minutes. Supernatants were removed and pellets were gently resuspended in HBSS containing 1 mg of EZ-Link Sulfo-NHS-LC biotin (ThermoFisher, Waltham, MA). Samples were incubated at 4˚C for 30 minutes under rotation. Glycine was added to 10 mM for 10 minutes to quench the excess reagent. Samples were washed three times in HBSS via centrifugation and resuspended in a guanidinium lysis buffer (6 M guanidine HCl 10 mM EDTA, 2 mM EGTA, 0.1% tween-20, in PBS, adjusted to pH 7.2) with 0.2 ml of 0.1 mm glass beads and homogenized. Samples were centrifuged at 12,000 x *g* for 10 minutes, and supernatants were collected and filtered through a 0.2 µm syringe filter. Eighty (80) µl of C1 streptavidin-coupled Dynabeads (ThermoFisher) was added to each sample and incubated, under rotation, at room temperature for 1 hour. The beads were then washed (using a magnetic separation stand) twice using the guanidinium lysis buffer and then twice using PBS + 0.05% tween-20. Beads were resuspended in 35 µl of 0.1% SDS in H_2O and incubated at 65˚C for 10 minutes. An equal volume of 2x Laemmli buffer (Bio-Rad) was added, and samples were incubated at 95˚C for 10

minutes and then 72˚C for 10 minutes. Samples were centrifuged for 2 minutes at 200 x *g* to pellet the beads, and then supernatant collected for downstream analysis.

Protein purification and mass spectrometry. Biotin-labelled protein samples were submitted to electrophoresis until they travelled 1 cm into a 12% polyacrylamide gel, and then the whole 1cm piece was excised. Samples were prepared and digested using Protease Max surfactant (Promega, Madison, WI) in combination with Trypsin Gold (Promega) following the manufacturer's protocol, with minor modifications including multiplying all volumes by 5 prior to the digestion step and the digestion was carried out with 100 µl of Protease Max containing 300 ng of trypsin for the 10 minute rehydration followed by overlaying with 500 µl of Protease Max. Digested samples were submitted to the Environmental Health Science Center Mass Spectrometry Facility at Oregon State University for mass spectrometric protein identification, following their established protocols. Briefly, samples were further purified with a C18 column and analyzed with a LTQ-TF mass spectrometer (Thermo) coupled with a NonoAcquity UPLC system (Waters). Proteome Discoverer v1.3.0, Mascot v2.3, and Scaffold were used for data analysis. The uniprot_MAV104 database was used for database search. Proteomics data is displayed as total spectrum count with the following parameters: 95% peptide threshold using the Scaffold Local FDR algorithm and 95% protein threshold with a two peptide minimum for protein identity.

MycomarT7 transduction and transposon library creation. MycomarT7 (Mmt7) is a temperature sensitive transposon-containing phagemid (Sassetti, Boyd et al. 2001) that was kindly provided by Eric Rubin (Harvard T.H. Chan School of Public Health, Boston, MA). Mmt7 stock was propagated and titered in *M. smegmatis* strain mc^2155 as previously described (Bardarov, Kriakov et al. 1997). To transduce MAH A5, bacteria were first grown at 37˚C in 7H9 broth supplemented with 10% OADC and 0.1% tween-80 shaking at 200 rpm. Bacteria were washed 2x with 37˚C MP buffer (150 mM NaCl, 50 mM pH 7.5 Tris HCl, 10 mM Mg_2SO_4, 2 mM $CaCl_2$), then resuspended in 37˚C MP buffer and diluted to 6 x 10^8 CFU/ml using visual turbidity. Five (5) ml of this suspension (3 x 10^9) was infected with Mmt7 at an MOI

of 2. Bacteria were transduced at 37˚C for 4 hours with intermittent mixing. After transduction, aliquots were plated on 7H10 agar containing 400 µg/ml kanamycin to obtain individual transposon mutants. Sixty kanamycin resistant colonies were screened for presence of Mmt7 with PCR and all colonies tested were positive for presence of Mmt7, even after re-plating and confirming with PCR a second time.

Transposon library screen for eDNA production. 4,048 transposon mutants were individually picked into 250 µl of 7H9 supplemented with OADC and 400 µg/ml kanamycin and grown for 5 days in deep, round bottom 96-well plates at 37˚C under 210 rpm of rotation. Plates were centrifuged at 2,000 x *g* for 15 minutes to pellet bacteria. Supernatants were removed and pellets were resuspended into HBSS containing 3 µM of propidium iodide and transferred into flat bottom polystyrene 96-well plates. Initial optical density of plates was measured with a 595 nm filter. Biofilms were formed statically at 30˚C and eDNA production was measured in real-time at day 0, 3, 5, and 7, as described earlier.

Transposon location identification. Transposon insertion locations on mutants of interest were identified utilizing a previously reported ligation mediated PCR technique (LMPCR), with minor modifications (Prod'hom, Lagier et al. 1998; Abdallah, Verboom et al. 2006). Cell lysate was produced by resuspending bacteria into DI H_2O, adding 0.2 ml of 0.1 mm glass beads, and homogenized. Samples were centrifuged at 10,000 x *g* for 2 minutes to pellet cell debris, and then the DNA was purified from the supernatant using a DNA Clean and Concentrate kit (Zymo Research, Irvine, CA) following the manufacturer's protocol. 100-150 ng of DNA was single digested with SalI or double digested with BamHI and BglII (all enzymes were Thermo fast digest enzymes) for 20 minutes at 37˚C. LMPCR adapters were made for both SalI (Salgd+Salpt adapter, Supplemental Table 4.1) and BamHI/BglII (Salgd+Bampt adapter, Supplemental Table 4.1) by mixing equal molar amounts of each oligo with 1x Taq DNase buffer + $MgCl_2$ and ligating by decreasing the temperature from 80˚C to 4˚C over the course of 1 hour in a thermal cycler. 25 ng of digested DNA was ligated with 0.5 µl of freshly prepared 100 µM adapters using the T4 DNase ligase system (Life Technologies). 0.5 µl of this ligation was used as

template in the LMPCR reaction, which used the Fidelitaq system (Affymetrix, Santa Clara, CA). Two sets of primers were used for each sample that shared the reverse primer (complementary to the adapter) and either had the forward primer at the inverted repeat of the transposon, or 150 base pairs upstream into the transposon (Supplemental Table 4.1). The LMPCR reaction was: 97˚C for 7 minutes, 40 cycles of 97˚C for 30 seconds, 58˚C for 1 minute, and 72˚C for 1:45, and then a final step of 72˚C for 10 minutes. PCR products were visualized using ethidium bromide and agarose gel electrophoresis. Bands of interest were excised using a Gene Jet gel extraction kit (ThermoFisher) following the manufacturer's protocol. Purified samples were submitted to the Center for Genome Research and Biocomputing at Oregon State University for DNA sequencing. Transposon locations were determined by using CLC Sequence Viewer software (CLC Bio, Aarhus, Denmark) with the MAH A5 annotated genome and the MycomarT7 sequences downloaded from NCBI.

Complementation of mutants. Genes and up to 500 bp of upstream sequence were complemented via the integrative pMV306 plasmid as described before (Stover, de la Cruz et al. 1991) with minor modifications. Since the transposon mutants already possess kanamycin resistance, an apramycin resistance gene was cloned into the pMV306 plasmid, producing the pMV306-Apr plasmid. Coding sequences and up to 500bp of upstream DNA were cloned into pMV306-Apr using primers listed in Supplemental Table 4.1. Electrocompetent MAH A5 mutant cells were prepared by washing plate-grown bacteria 5x via centrifugation at 4˚C for 15 minutes at 2,000 x *g* in a chilled 10% glycerol and 0.1% tween-80 solution, followed by resuspension in a small volume of chilled 10% glycerol to concentrate the competent cells. PCR and double restriction digest verified constructs were electroporated into their respective MAH A5 electrocompetent mutants in a 0.2 cm cuvette using 2500 V, 1000 Ω, and 25 µF. Bacteria were recovered in 7H9 broth supplemented with 10% OADC overnight, followed by plating on 7H10 plates containing 400 µg/ml kanamycin and 400 µg/ml apramycin. Colonies were PCR screened using the same primers as described above to confirm positive clones.

Statistics. Statistical comparisons between groups were made using a two-tailed homoscedastic t-test in Microsoft Excel. Detailed information about data presentation and *p* value definitions are listed in each applicable figure legend. Graphical outputs were created with GraphPad Prism software.

Results

Production of eDNA in *M. avium* is conditional. We previously reported that nontuberculous mycobacteria (NTM) produce extracellular DNA when biofilms are formed in HBSS. Importantly, signs of massive cell lysis in MAH A5 biofilms were not observed, which led to the hypothesis that a non-lytic mechanism could be responsible for eDNA in NTM biofilms. Due to this, we wanted to investigate variables that could affect eDNA production. In that study, and prior work, biofilms were formed in HBSS. For this work, we created a method for quantifying eDNA in undisturbed NTM biofilms as they form using the cell-impermeable fluorescent dye, propidium iodide. Agreeing with previous work (Rose, Babrak et al. 2015), MAH A5 biofilms formed in HBSS produce a significant amount of eDNA over 7 days of biofilm formation (Figure 4.1A). Interestingly, biofilms formed in deionized H_2O (DI H_2O) appear to produce very little or no eDNA through the time course (Figure 4.1A). To ensure that this result was not an artifact of the assay, cell-free biofilm matrix was extracted from 7 day old biofilms and then quantified fluorescently, as reported recently (Rose, Babrak et al. 2015). Similar to the live-tracking, MAH A5 biofilms formed in DI H_2O produce significantly less eDNA than the identical inoculum formed in HBSS (Figure 4.1B). This stark difference suggests that eDNA is conditionally produced and that a specific trigger could influence eDNA production.

Bicarbonate positively influences eDNA production in nontuberculous mycobacteria independent of pH. Considering the significant differences in eDNA production between HBSS and DI H_2O, the ingredients of our HBSS were further analyzed for their individual involvement with eDNA production in both an additive and subtractive manner (refer to the materials and methods for HBSS formulation). When tracking eDNA in MAH A5 biofilm formed in single components in DI H_2O, sodium phosphate partially restored eDNA to the levels produced in HBSS and sodium bicarbonate and D-glucose both increased eDNA to a level higher than in HBSS (Figure 4.2A, black bars). When analyzing individual components in a subtractive manner (each mix is 7 components minus the one listed), sodium bicarbonate is the only component that reduces eDNA below the level produced in

HBSS (Figure 4.2B, black bars). When either D-glucose or sodium chloride was removed, eDNA production was markedly increased over HBSS levels (Figure 4.2B, black bars), suggesting that those components impede the effect of bicarbonate. When comparing paired interactions between bicarbonate and the other individual components, D-glucose and sodium chloride reduced eDNA production compared to other tested components (Figure 4.2C, black bars). All of the other possible pairs of components were tested and agree with their respective single component data (data not shown). Taken together, this data suggests that sodium bicarbonate positively influences eDNA production and it itself is negatively affected by D-glucose and sodium chloride. Since the pH of sodium bicarbonate by itself is the only ingredient more alkaline than HBSS (Figure 4.2A, grey bars), pH was analyzed for all other experiments to assess the role of pH with eDNA production. There does not appear to be a correlation between eDNA and pH, as there are many instances where pH is similar between two samples, but the level of quantified eDNA differs significantly (Figure 4.2B and C, grey bars). To directly assess if sodium bicarbonate facilitates eDNA production due to pH, biofilms were formed with HEPES to keep the pH buffered (Figure 4.2D). When analyzing eDNA production in these HEPES buffered sodium bicarbonate solutions, there was significantly more eDNA produced at all concentrations of HEPES used than in solutions lacking sodium bicarbonate (Figure 4.2D). There does appear to be a correlation of more eDNA production with lessening HEPES concentrations, but there are perhaps unseen interactions between the HEPES and the sodium bicarbonate. To assess if bicarbonate influenced eDNA production in other NTM, *M. abscessus* and *M. chelonae*, that were already shown to produce substantial eDNA (Rose, Babrak et al. 2015), were examined. In agreement with MAH A5, bicarbonate buffered in HEPES elicited significantly more eDNA in *M. abscessus* and *M. chelonae* than in HEPES alone (Figure 4.2E and F, respectively). Taken together, this demonstrates that bicarbonate triggers eDNA production in NTM, and that this is occurring independent of pH.

Surface proteomics of bicarbonate-exposed biofilm reveal abundant carbonic anhydrases. It has been described that the surface-exposed proteins of

MAH vary depending on the environment the bacteria is in, including different states of infection (McNamara, Tzeng et al. 2012). To investigate the MAH surface-exposed and biofilm matrix proteins of MAH A5, mature HBSS incubated biofilms were labelled using a cell-impermeable Sulfo-NHS-LC-biotin reagent followed by streptavidin purification and mass spectrometric protein identification. Between two independent biological replicates, a total of 100 proteins were identified (Supplemental Table 4.2). Interestingly, a carbonic anhydrase (MAVA5_02375) was among the most abundant proteins identified (Table 4.1).

Chemical inhibition of carbonic anhydrase reduces eDNA production. Due to the direct effect of bicarbonate on eDNA production and abundant surface-exposed carbonic anhydrases, chemical inhibition of carbonic anhydrase was explored to see it affects eDNA export. Ethoxzolamide is a sulfonamide carbonic anhydrase inhibitor that has previously been demonstrated to have activity against *M. tuberculosis* carbonic anhydrases (Carta, Maresca et al. 2009; Johnson, Colvin et al. 2015). Biofilms were formed and live-tracked with wildtype MAH strain A5 incubated in HBSS with either 100 nM ethoxzolamide (from a 2mM stock solution in ethanol) or ethanol vehicle diluted similarly. Ethoxzolamide treatment significantly reduced eDNA production compared to the ethanol vehicle over the time course (Figure 4.3).

Transposon library screen for eDNA attenuation identified mutants putatively involved with bicarbonate, an eDNA secretion mechanism, metabolism, and a novel genomic region. To identify genes involved with eDNA export and, potentially, the bicarbonate sensing mechanism, a mycobacteriophage based transposon library was created in MAH A5 and 4,048 mutants were individually screened for eDNA using the propidium iodide live-tracking method. To help control for variations in starting optical density of mutants, four wild-type controls for each screened plate were differentially diluted to obtain starting optical densities that represented the range of mutants in that particular plate. From the 4,048 mutants screened, 238 were found to be deficient in eDNA production using graphical and numerical analysis from each plate. Out of the 238 deficient mutants,

further mathematical comparisons were made and 173 mutants were cumulatively chosen to sequence transposon insertion locations. Sequence analysis of 158 of the 173 mutants gave definitive transposon locations, and 15 either gave ambiguous or negative results. Of the 158 mutants identified, 126 insertions were directly in genes and 32 were intergenic, though 20 of the intergenic insertions were located within 100 bp upstream of annotated genes (Supplemental Table 4.3). Summary statistics for every mutant and wild type MAH A5 clone analyzed in the library screen were calculated by normalizing day 7 eDNA measurements to starting optical densities and averaging these values for subsets of clones from the screen (Table 4.2). There was significant reduction in this average value between all mutants screened and the 238 eDNA deficient mutants (17,609 average normalized eDNA RFU compared to 12,004, respectively). Furthermore, the 173 clone subset of mutants chosen cumulatively to sequence had a lower normalized eDNA measurement compared to the 81 deficient mutants not chosen for identification (10,760 average normalized eDNA measurement versus 14,416, respectively). There were four occasions of mutations identified in multiple independent clones: MAVA5_03165, GntR transcriptional regulator (19d12, 26e9); MAVA5_05585, transcriptional-repair coupling factor (16e4, 41c1); MAVA5_10275, metal-dependent hydrolase (26e12, 29b11, 7d3); and MAVA5_10310, monooxygenase (43f8, 5d3) (Supplemental Table 4.3). In all of these instances, the mutations within a single gene are all located in unique locations. In addition, there were 30 instances of mutants in close genomic proximity with other mutants (within 10 genes), and of that, 10 of these associations are potentially in the same operon (Supplemental Table 4.3).

To assess functional groups of the sequence identified mutants, functional categories (downloaded from the J. Craig Venter Institute) were applied to the 126 mutants directly interrupting genes, revealing metabolism and energy production (35 mutants, 28%) and hypothetical (29 mutants, 23%) as the most abundant categories (Figure 4.4 and Supplemental Table 4.3). The large number of mutants involved with metabolism and energy production further suggest active processes involved with eDNA in MAH A5.

To quantitatively compare the eDNA deficiency between the 126 sequenced mutants directly interrupting genes, the day 7 fluorescent measurement of PI bound to eDNA for each mutant was normalized to its starting optical density (Supplemental Table 4.3). The most eDNA attenuated mutant found was 11e7 (MAVA5_03380), a FtsK/SpoIIIE-like DNA transporter (Table 4.3). 40c10 (MAVA5_19945), a carbonic anhydrase, was also among the most deficient (Table 4.3). There were mutants in two separate genes encoding SAM-dependent methyltransferases as well as six hypothetical proteins among the most deficient mutants (Table 4.3). Conserved domain searches on these hypotheticals found that 2e3 contains a WXG100 domain, 42c3 contains a major facilitator superfamily domain, 24d3 contains a Rossmann NAD binding fold and a dehydrogenase domain, 40h2 contains a MaoC dehydrogenase domain, 35c4 contains mycobacterial 19 kDa lipoprotein antigen domain, and 14g4 contains a DUF domain. It is also interesting that 35c4 (oxidoreductase) and 39d19 (cytochrome P450) are among the most deficient, and they are located in the same operon (Table 4.3).

The genome of MAH A5 was recently sequenced by our laboratory (GenBank accession: GCA_000696715.1). The MAH A5 genome is ~500 kbp smaller than the MAH 104 reference genome, and contains only small amounts of genetic material that MAH 104 is missing. Notably, there is a ~50 kbp genomic region (MAVA5_10140 through MAVA5_10380, Supplemental Table 4.4) flanked by a tRNA. When BLASTed, the region is unique to mycobacteria and has homology to some other MAH strains, some *M. intracellulare* strains, and most *M. abscessus* strains. The region contains open reading frames for an AraC transcriptional regulator (MAVA5_10195) and an FtsK/SpoIIIE DNA pore (MAVA5_10375). Nine eDNA deficient mutants identified were located within this genomic region: 23d4 (MAVA5_10205), a N5,N10-methylene tetrahydromethanopterin reductase; 40h2 (MAVA5_10220), a hypothetical protein; three mutants (7d3, 26e12, 29b11) in different locations in MAVA5_10275, a metal-dependent hydrolase; 37h6 (MAVA5_10295), a Flavin-binding monooxygenase; two mutants (43f8 and 5d3) in

different locations in MAVA5_10310, a 4-hydroxyacetophenone monooxygenase; and 37d4 (MAV_10315), a cytochrome P450 protein (Supplemental Table 4.4).

To further confirm that eDNA deficient mutants were directly related to eDNA export, nine mutants were chosen to complement a functional copy of the respective mutated gene along with up to 500bp upstream of the gene into the integrative pMV306-Apr Plasmid. The 126 mutants were narrowed down first by functional analysis (excluding metabolism and energy production mutants). Genes from remaining mutants were analyzed against MAH 104 (produces very little or no eDNA), *M. tuberculosis*, and *M. abscessus* (both of which have been shown to produce eDNA) (Manzanillo, Shiloh et al. 2012; Rose, Babrak et al. 2015). Mutants with homologs in MAH 104 that were genetically identical were excluded and inversely mutants that shared homology with *M. tuberculosis* and/or *M. abscessus* were included. The narrowed down mutants were re-confirmed for eDNA deficiency (data not shown) and analyzed for availability of upstream sequence (containing a native promoter) before the next upstream gene. Mutants that met the above criteria were selected for complementation and included the FtsK/SpoIIIE pore (11e7), the carbonic anhydrase (40c10), a metal dependent hydrolase from the 50 kb region (29b11), a hypothetical membrane protein (8e7), TetR and GntR transcriptional regulators (38h12 and 26e9, respectively), a precorrin-3B synthase (26b3), and two hypotheticals (27c4 and 16g11). Every complemented mutant significantly restored eDNA export compared to its non-complemented counterpart (FIG 4.5), further demonstrating the direct role of genes found in the eDNA transposon screen in eDNA regulation and export.

Connection between eDNA-producing surface proteome and eDNA deficient mutants. To corroborate the proteins identified in the bicarbonate exposed biofilm surface proteome with eDNA production, the identified proteins were analyzed against the sequenced eDNA deficient mutants. In total, 43 of the 99 identified surface proteins were in close proximity (5 genes) with identified eDNA mutants (Table 4.4). An additional 12 identified proteins were located within 10 genes of eDNA deficient mutants (data not shown). Five identified proteins match

actual eDNA deficient mutants, two are directly overhanging with eDNA deficient mutants, and 24 are located in potential operons with eDNA deficient mutants (Table 4.4). Interestingly, there were seven groupings of adjacent identified proteins that are located in close proximity to eDNA deficient mutants (Table 4.4). Collectively, this suggests that a significant number of proteins encoded by genes important for eDNA in MAH A5 are localized extracellularly in these biofilms.

Discussion

The ability of nontuberculous mycobacteria (NTM) to form biofilm creates challenges for treatment efficacy and host clearance (Yamazaki, Danelishvili et al. 2006; Rose and Bermudez 2014; Babrak, Danelishvili et al. 2015; Qvist, Eickhardt et al. 2015). We recently reported that NTM contain extracellular DNA (eDNA) in their biofilm matrix that significantly contributes to colonization, persistence, and drug tolerance, suggesting a novel anti-virulence target for NTM (Rose, Babrak et al. 2015). Since this report, another group demonstrated the effectiveness of DNase in combination with antimicrobials against NTM biofilm (Aung, Hoong et al. 2015). In the current work we describe bicarbonate as a trigger for eDNA export in *M. avium* and identified genes and extracellular proteins that are involved with the mechanism(s) of eDNA production. Work with other eDNA producing organisms has found elevated membrane potentials (Barnes, Ballering et al. 2012), early competence genes (Vilain, Pretorius et al. 2009), and secreted membrane vesicles containing eDNA (Sahu, Iyer et al. 2012; Liao, Klein et al. 2014), but the genes and proteins involved with the actual mechanisms remain largely unknown. The method presented in this work for monitoring eDNA as it is exported allowed us to screen a large transposon library to identify genes associated with eDNA. Multiple mutants were found in ATPases, ABC transporters, transcriptional regulators, and energy production and metabolism genes. This strengthens the idea of active processes involved with eDNA production.

Host organisms contain elevated carbon dioxide and bicarbonate concentrations compared to environmental sources, and pathogens have developed sensing mechanisms to these molecules. *Cryptococcus*, *Bacillus*, and *Streptococcus* species respond to carbon dioxide to regulate gene expression (Mogensen, Janbon et al. 2006; Hammerstrom, Roh et al. 2011; Burghout, Zomer et al. 2013). The AraC transcriptional regulators RegA in *Citrobacter rodentium*, PerA in *Enterococcus faecalis*, and ToxT in *Vibrio cholerae* directly respond to bicarbonate stimulation (Yang, Hart et al. 2008; Abuaita and Withey 2009; Maddox, Coburn et al. 2012). We did not find any AraC mutants in our transposon screen, however nine mutants were

found in a unique genomic region in MAH A5 that contains an AraC regulator (MAVA5_10195), and eDNA deficient mutants were identified two and four genes downstream from this regulator. *M. tuberculosis* contains six AraC regulators, but interestingly, Rv1395 is the only homolog to MAVA5_10195 (which on its own is unique from the other *M. avium* annotated AraC regulators). A Rv1395 mutant was attenuated during respiratory infection of mice using a signature tagged mutagenesis screen (Camacho, Ensergueix et al. 1999). We have preliminary tested a Rv1395 mutant for eDNA from the culture supernatant and found a 3-fold reduction in eDNA levels compared to the wild type (unpublished data). In addition, it lacked the wildtype *M. tuberculosis* biofilm pellicle formed at the air/liquid interface during growth in culture media, even though it grew in the liquid at a comparable rate (unpublished data). Ongoing work in our laboratory is looking at the genes this AraC is influencing in both MAH A5 and *M. tuberculosis.*

One of the most abundant proteins identified through analysis of the extracellular biofilm proteome was the DNA binding protein HU (MAVA5_16770). Similar DNA binding proteins have been found extracellularly within other eDNA-containing biofilms (Goodman, Obergfell et al. 2011; Novotny, Amer et al. 2013). Antisera targeting DNA binding proteins effectively disrupted eDNA architecture and biofilm integrity in various pathogens (Goodman, Obergfell et al. 2011; Novotny, Amer et al. 2013). In our experience, treatment with trypsin destabilized MAH A5 biofilms and released eDNA into the biofilm supernatant (unpublished data), agreeing that protein component is participating with eDNA in these biofilms. Extracellular DNA binding proteins have also been shown to bind to host cells (Winters, Ramasubbu et al. 1993; Boleij, Schaeps et al. 2009; Kunisch, Kamal et al. 2012) and stimulate inflammatory responses from macrophages (Zhang, Ignatowski et al. 1999). MAH A5 elicited a robust proinflammatory response from macrophages that were exposed to biofilm (Rose and Bermudez 2014), and the extracellular DNA binding protein HU could have contributed to that role. Further work will be needed to determine the specific function of MAVA5_16770.

Due to the surface exposed carbonic anhydrase, MAVA5_02375, abundant in the MAH A5 biofilm, we investigated eDNA production while using the carbonic anhydrase inhibitor ethoxzolamide. This sulfonamide has been described previously to have activity against *M. tuberculosis* carbonic anhydrases (Carta, Maresca et al. 2009; Johnson, Colvin et al. 2015). Even though we observed significant reduction of eDNA co-incubated with EZA, complete inhibition of eDNA was not achieved, which could be due to multiple reasons. There are at least four carbonic anhydrases annotated in the MAH A5 genome, and perhaps EZA did not inhibit all of them, inhibition was temporary, or EZA could not access all of the functioning carbonic anhydrases. This agrees with the carbonic anhydrase eDNA deficient mutants 40c10 (MAVA5_19945) and 20e5 (MAVA5_22765) found in our library screen, while although significantly eDNA deficient, complete elimination of eDNA was not observed. Recent work has shown that in *M. tuberculosis*, EZA inhibition interrupts both the PhoPR regulatory system as well as ESX-1 secretion (Johnson, Colvin et al. 2015). This is interesting, because the ESX-1 secretion system has been shown necessary for intracellular *M. tuberculosis* to permeabilize the phagosomal membrane and allow eDNA produced in the phagosome to access cytosolic DNA receptors (Manzanillo, Shiloh et al. 2012; Wassermann, Gulen et al. 2015). The MAH A5 genome does not contain a complete ESX-1 region, but does contain ESX-2 through ESX-5 (manuscript in review). Our screen did find eDNA deficient mutants located in ESX-2 (23a3, MAVA5_00710), ESX-3 (8c10, MAVA5_21435) and ESX-5 (39f5, MAVA5_12405). The roles these ESX systems have directly in eDNA production, if any, need to be further studied.

The most eDNA deficient mutant found in our screen was 11e7, which carries a mutation in MAVA5_03380, an FtsK/SpoIIIE-like DNA translocation protein. These proteins were first described in *E. coli* to localize on the divisome during cell division and translocate copied chromosomal DNA into the daughter cell (Begg, Dewar et al. 1995). Mycobacteria contain numerous proteins that are annotated as FtsK/SpoIIIE. Each of the five mycobacterial ESX regions contain one of these proteins. We compared all of the FtsK/SpoIIIE genes in the MAH A5 genome with

other mycobacteria and found the only one that is conserved was MAVA5_15915 (Rv2748c, MAV_3639), which is more than likely the FtsK/SpoIIIE protein that participates in cell division. Even though 11e7 was the most deficient mutant, eDNA was still observed. There could be multiple proteins responsible for eDNA translocation. When analyzing all of the FtsK/SpoIIIE proteins in MAH A5, the only one that shares identity with MAVA5_03380 is MAVA5_10375, which is located in the unique 50 kbp region also identified as important for eDNA due to deficient mutants identified from it. We did not find a MAVA5_10375 mutant in our screen, but since this gene has not been directly studied, it is unknown if it is essential for growth, and our screen was limited to non-essential genes. The LMPCR method was very successful at sequencing mutants (158 out of 173), but did not work for all mutants. We PCR screened the 15 eDNA deficient mutants that did not work with LMPCR via regular PCR for intact MAV_10375 and did not find any mutants. Alternatively, MAVA5_10375 could have been less deficient, and as a result been in the subpopulation of deficient mutants identified that were not sequenced. Additionally, it could have not been deficient at all, or just not included in the library screen.

Identifying nine mutants deficient in eDNA that have mutations in genes located in the unique 50 kb genomic region was remarkable. In our initial report on mycobacterial eDNA (Rose, Babrak et al. 2015), the NTM species that produced similarly high amounts of eDNA were *M. abscessus* and *M. chelonae*. Furthermore, in the current work we demonstrated that these two mycobacterial species export eDNA when stimulated by bicarbonate, strengthening the idea that the mechanism of eDNA production in MAH A5 could be shared by other mycobacteria. When we first found this unique genomic region in MAH A5, we analyzed it against other mycobacteria and it is mainly found in various strains in *M. abscessus*, *M. chelonae*, *M. avium*, and *M. intracellulare*. The GC content of this region (64%) matches that of *M. abscessus* and *M. chelonae*, but is different than *M. avium* and *M. intracellulare* (both 69%). This suggests that the region could have been introduced horizontally into the *M. avium* complex from the *M. abscessus/chelonae* complex. Flanking the

region is a tRNA, which furthers the possibility of horizontal transfer. Further work on this interesting region will help determine the specific role it has with bicarbonate sensing and/or eDNA production.

Acknowledgements

We are grateful to Zachary Rose for his technical assistance. The authors acknowledge the Environmental Health Science Center Mass Spectrometry Facility at Oregon State University. This work was supported by grant AI041399 from the National Institutes of Health. The mass spectrometry facility was supported, in part, by award P30ES000210 from the National Institute of Environmental Health Sciences at the National Institutes of Health.

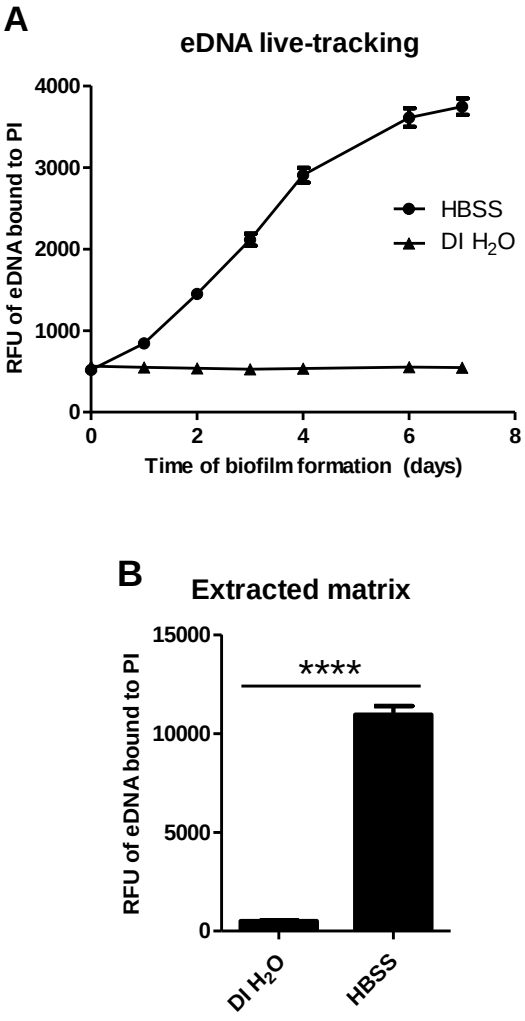

Figure 4.1. Conditional production of eDNA in MAH A5 biofilms. MAH biofilms were formed in HBSS and DI H_2O, and eDNA was quantified. (A) Biofilm were formed with 3µM cell-impermeable propidium iodide and incubated for a week. Undisrupted biofilms were fluorescently measured over the time course to measure eDNA bound to propidium iodide. Data points represent the average of 6 separate biofilms ± SD. (B) Biofilms were formed without propidium iodide for 7 days, then biofilm matrix was extracted, filter sterilized, mixed with propidium iodide, and fluorescently read to quantify eDNA in the extract, as previously published (Rose, Babrak et al. 2015). Bars represent the average of 4 technical replicates ± SD. Data shown for both A and B are representative of three independent biological replicates. Statistical comparisons: **** $p < 0.0001$.

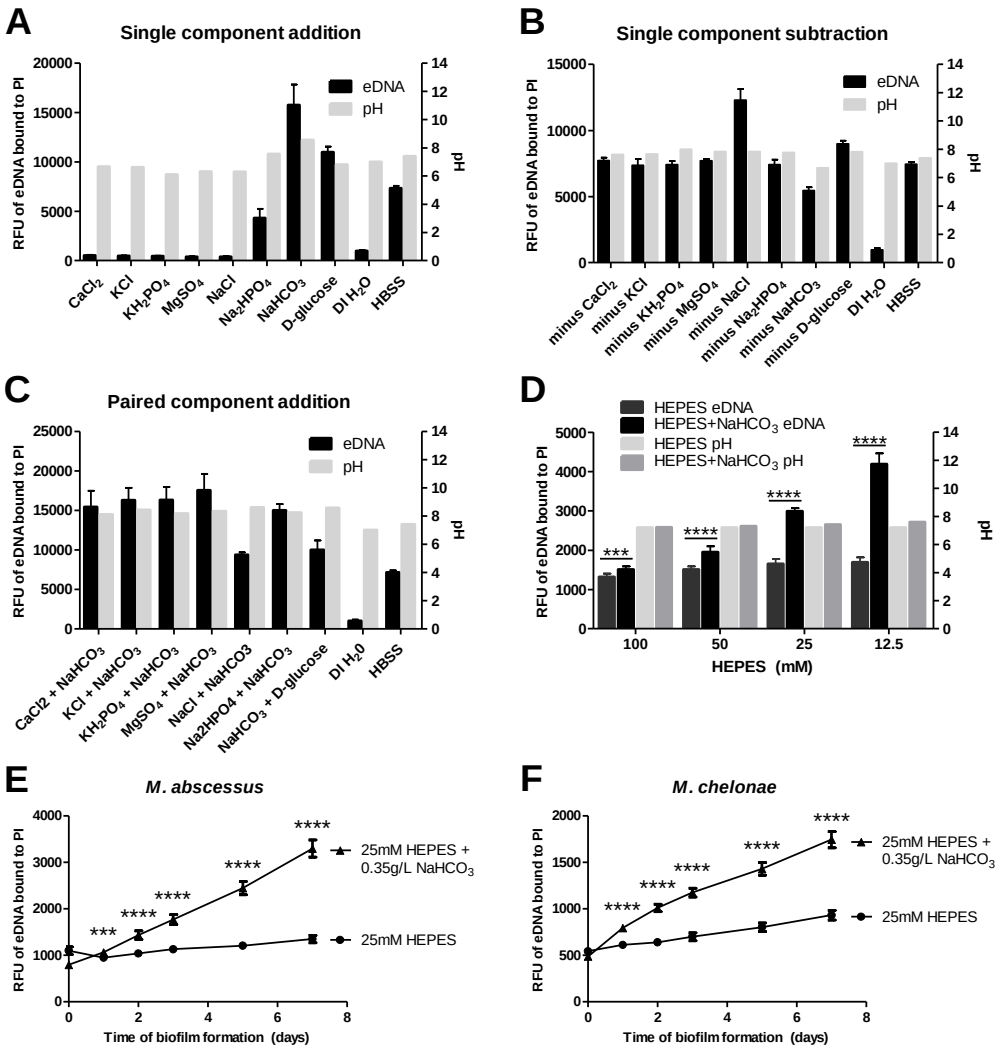

Figure 4.2. Bicarbonate influences eDNA production in NTM biofilms. Biofilm inoculums were made in different diluents with propidium iodide, incubated for 7 days, and fluorescently measured eDNA over the time course. Data shown for A-D is day 7 eDNA fluorescence and pH of the respective solutions. Refer to the materials and methods for concentrations of HBSS components. (A) Biofilms were formed in individual HBSS components in DI H_2O. (B) Biofilms were formed in 7 of the 8 HBSS components except for the listed component. (C) Biofilms were formed in individual HBSS component paired with bicarbonate in DI H_2O. (D) Biofilms were formed in DI H_2O buffered with different concentrations of HEPES ± 0.35g/L bicarbonate. (E and F) biofilms were formed in 25 mM HEPES ± bicarbonate in *M. abscessus* subsp. *abscessus* strain 19977 (E) and an environmental *M. chelonae* isolate (F) and live-tracked for eDNA production. For eDNA measurements, bars are averages of 6 separate biofilms ± SD. Data shown is representative of two independent biological replicates. Statistical comparisons: ***p<0.001; ****p<0.0001.

Table 4.1. Ten most abundant surface-exposed proteins identified from a 7 day MAH A5 HBSS biofilm.

Protein	A5 gene	Total spectrum count
Wag31 protein	MAVA5_10120	29
ATP synthase subunit beta	MAVA5_07195	27
Elongation factor Tu	MAVA5_19500	22
Superoxide dismutase	MAVA5_00855	22
Carbonic anhydrase	MAVA5_02375	20
Antigen 85-B	MAVA5_22455	18
Glutamine synthetase	MAVA5_09755	15
Catalase-peroxidase	MAVA5_11495	14
MoxR protein	MAVA5_14195	11
DNA-binding protein HU	MAVA5_16770	10

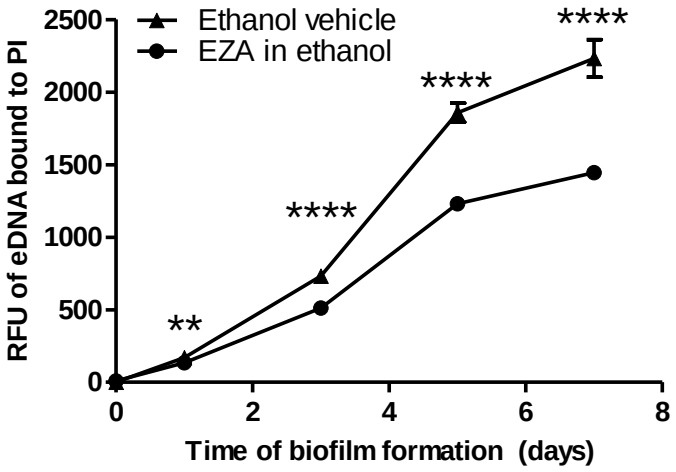

Figure 4.3. Carbonic anhydrase inhibition reduces eDNA in MAH A5 biofilms. Biofilms were formed in HBSS with either 0.1 µM ethoxzolamide (EZA) from a 2 mM stock in ethanol, or with the equivalent dilution of ethanol vehicle and eDNA was measured over a 7 day time course with propidium iodide. Data points represent the mean of 6 biofilms ± SD. Statistical comparisons: $^{**}p < .01$; $^{****}p < 0.0001$.

Table 4.2. Summary statistics for MAH A5 Mmt7 transposon library eDNA screen.

Description	Number of samples	Avg eDNA/OD[a]
Wild type MAH A5	154	21,884
All Mmt7 mutants	4,048	17,609
eDNA- all mutants	238	12,004
eDNA- no sequence attempt	65	14,416
eDNA- all sequence attempt	173	10,760
eDNA- yes sequence in-gene	126	10,712
eDNA- yes sequence intergenic	32	10,697

[a]The eDNA/OD value for each sample was calculated by normalizing the day 7 RFU bound to PI fluorescent reading to the starting O.D. of the respective sample.

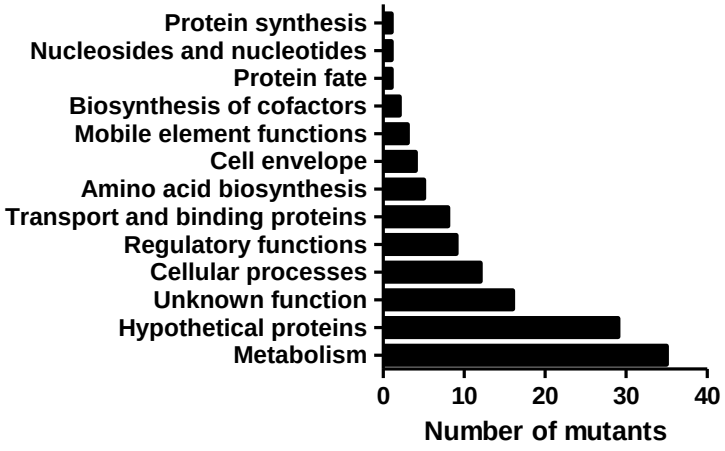

Figure 4.4. Functional analysis of eDNA deficient MAH A5 mutants. Biofilms were formed with 4,048 individual clones from a MAH A5 transposon library and eDNA was quantified over the time course. Functional roles were assigned to the 126 sequenced eDNA deficient mutants directly interrupting genes and are shown as percentage of the total 126 mutants (see Supplemental Table 3 for individual mutant functional assignments).

Table 4.3. Fifteen most eDNA-deficient mutants from MAH A5 Mmt7 library screen.

Encoded protein	Name	A5 gene	eDNA/OD[a]
FtsK/SpoIIIE	11e7	MAVA5_03380	6,177
Hypothetical protein	2e3	MAVA5_19115	6,432
ABC transporter permease	29e7	MAVA5_10575	6,619
Hypothetical protein	42c3	MAVA5_13685	6,654
SAM-dependent methyltransferase	39e5	MAVA5_20295	6,798
Carbonic anhydrase	40c10	MAVA5_19945	6,941
Hypothetical protein	24d3	MAVA5_13900	7,105
Transcription-repair coupling factor	41c1	MAVA5_05585	7,184
(2Fe-2S)-binding protein	36d7	MAVA5_05310	7,469
Hypothetical protein	40h2	MAVA5_10220	7,581
SAM-dependent methyltransferase	1e5	MAVA5_10615	7,871
Oxidoreductase	36f9	MAVA5_13185	7,932
Hypothetical protein	35c4	MAVA5_01245	7,960
Cytochrome P450	39d10	MAVA5_13215	8,000
Hypothetical protein	14g4	MAVA5_07205	8,077

[a]The eDNA/OD value for each sample was calculated by normalizing the d7 RFU bound to PI fluorescent reading to the starting O.D. of the respective sample.

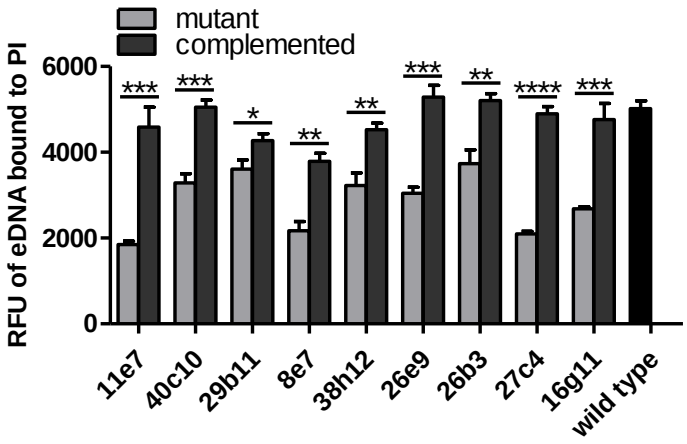

Figure 4.5. Complementation of eDNA deficient mutants. Nine eDNA deficient mutants were selected to complement their respective genes using the integrative pMV306-Apr plasmid. Bacteria were grown in 7H9 broth with OADC containing either no antibiotic (wild type), kanamycin (deficient mutants), or kanamycin and apramycin (complemented mutants). Biofilms were formed with propidium iodide and eDNA was measured over a time course. Bars are averages ± SD at day 7 of three separate biofilms that were grown separately in broth beforehand as well. Data shown is representative of at least two independent biological replicates. Statistical comparisons: *$p < 0.05$; **$p < .01$; ***$p < 0.001$; ****$p < 0.0001$.

Table 4.4. Overlap of identified biofilm surface proteins with sequenced eDNA deficient mutants.

Gene of identified biofilm protein	eDNA deficient mutant within close proximity of identified protein (MAVA5_gene#)	Exact proximity of identified protein from deficient mutant[a]	Adjacent identified proteins?
MAVA5_00730	23a3 (_00710)	4 genes downstream	
MAVA5_00855	11g6 (_00880)	5 genes away	
MAVA5_00885	11g6(_00880)	1 gene away	
MAVA5_02995	13d3 (_03020)	5 genes downstream	
MAVA5_03155	19d12/26e9 (both _03165)	2 genes away	
MAVA5_03760	9b11 (_03755)	24bp downstream	
MAVA5_03945	25d12 (_03920-_03925)	4 genes downstream	Yes
MAVA5_03950	25d12 (_03920-_03925)	5 genes downstream	Yes
MAVA5_04770	30e5 (_04775)	Overhanging	
MAVA5_05225	36h9 (_05210)	3 genes downstream	
MAVA5_05665	45e4 (_05645)	4 genes upstream	
MAVA5_05780	12h10 (_05775)	1 gene away	
MAVA5_07180	14g4 (_07205)	5 genes upstream	Yes
MAVA5_07185	14g4 (_07205)	4 genes upstream	Yes
MAVA5_07190	14g4 (_07205)	3 genes upstream	Yes
MAVA5_07195	14g4 (_07205)	2 genes upstream	Yes
MAVA5_09565	18b11 (_09590)	5 genes downstream	Yes
MAVA5_09570	18b11 (_09590)	4 genes downstream	Yes
MAVA5_09575	18b11 (_09590)	3 genes downstream	Yes
MAVA5_09755	41e1 (_09740)	3 genes away	
MAVA5_11495	46a1 (_11495)	Same gene	
MAVA5_11885	16g11 (_11885)	Same gene	
MAVA5_12085	6g5 (_12060)	5 genes away	
MAVA5_12110	30e6/44b10 (_12130/_12135)	4/5 genes away	
MAVA5_12185	34g9 (_12185-_12190)	directly upstream	
MAVA5_13360	7b10 (_13345)	3 genes away	
MAVA5_13390	7b5 (_13410)	4 genes away	
MAVA5_14395	6f4 (_14420)	5 genes away	Yes
MAVA5_14400	6f4 (_14420)	4 genes away	Yes
MAVA5_16150	7e2 (_16155)	23bp upstream	
MAVA5_16825	13f3 (_16800)	5 genes away	
MAVA5_19500	5d9 (_19495)	1 gene upstream	Yes
MAVA5_19510	5d9 (_19495)	3 genes upstream	Yes
MAVA5_19940	40c10 (_19945)	1 gene upstream	
MAVA5_20590	11d3 (_20565)	5 genes away	
MAVA5_21610	29c4 (_21610)	Same gene	Yes
MAVA5_21615	29c4 (_21610)	Overhanging	Yes
MAVA5_21640	29f12 (_21635)	1 gene downstream	Yes
MAVA5_21645	29f12 (_21635)	2 genes downstream	Yes
MAVA5_21745	26a3 (_21745)	Same gene	
MAVA5_21745	4c2 (_21735)	2 genes away	
MAVA5_22265	31g1 (_22270)	1 gene downstream	
MAVA5_22890	45c6 (_22890)	Same gene	

[a] "downstream/upstream" indicate that all genes within the given proximity are all in the same orientation. "Away" indicates that genes within proximity are in different orientations.

Supplemental Table 4.1. Primers used in this Study.

Description	Sequence (5' to 3')
Saldg (for both adapters)	TAGCTTATTCCTCAAGGCACGAGC
Salpt (for SalI adapter)	TCGAGCTCGTGC
Bampt (for BamHI/BglII adapter)	GATCGCTCGTGCC
pSalg R (for LMPCR reaction)	GCTTATTCCTCAAGGCACGA
pMyco F1 (for LMPCR reaction)	CCGGGGACTTATCAGCCAAC
pMyco F2 (for LMPCR reaction)	ACCCGTGATATTGCTGAAGAG
11e7 MAVA5_03380 F	AAAAAAgaattcCCCGTAGTACCTAGCGATCC
11e7 MAVA5_03380 R	TTTTTTaagcttGGTGTTGATGCCGAGAGTTG
27c4 MAVA5_15290 F	AAAAAAgaattcCAAACGGCCTTGATGACGG
27c4 MAVA5_15290 R	TTTTTTaagcttCGCTCGGCCAATATAACTCC
8e7 MAVA5_21960 F	AAAAAAgaattcGACCCCAATCCCGTGCATAT
8e7 MAVA5_21960 R	TTTTTTaagcttGCGACCGAAAGTGGATCAG
26b3 MAVA5_10770 F	AAAAAAgaattcAGGGTTTAGGTCTGGCTGAA
26b3 MAVA5_10770 R	TTTTTTgtcgacATAGATCTCCGCCGCATCG
38h12 MAVA5_03425 F	AAAAAAtctagaTCGTCGTCCAAGTAAGAGCA
38h12 MAVA5_03425 R	TTTTTTaagcttCGTGGTCGGCGAATTAGC
26e9 MAVA5_03165 F	AAAAAAtctagaCGCCAATATTTCCGCCTACC
26e9 MAVA5_03165 R	TTTTTTaagcttGCCACCGAAGAATCTGTTGA
40c10 MAVA5_19945 F	AAAAAAtctagaCTTTGCGTTCTCTATGGGCC
40c10 MAVA5_19945 R	TTTTTTaagcttATTGCACATCAGGATCGACG
16g11 MAVA5_11885 F	AAAAAAgaattcTGAGAGCCGGAACAGACG
16g11 MAVA5_11885 R	TTTTTTgtcgacGAACGGTCGAGGGGTTATCC
29b11 MAVA5_10275 F	AAAAAAgaattcGGACAGCCCGCCATAAACA
29b11 MAVA5_10275 R	TTTTTTgtcgacCCGCACTTCCGCATCTTTG

Supplemental Table 4.2. All identified surface-exposed proteins from 7 day old MAH A5 biofilm

Description	MAH A5 gene	Total Spectrum Count
Wag31 protein	MAVA5_10120	29
ATP synthase subunit beta	MAVA5_07195	27
elongation factor Tu	MAVA5_19500	22
superoxide dismutase	MAVA5_00855	22
carbonic anhydrase	MAVA5_02375	20
Antigen 85-B	MAVA5_22455	18
glutamine synthetase	MAVA5_09755	15
Catalase-peroxidase	MAVA5_11495	14
MoxR protein	MAVA5_14195	11
DNA-binding protein HU	MAVA5_16770	10
malate dehydrogenase	MAVA5_06685	10
35kd antigen	MAVA5_15895	9
oxidoreductase	MAVA5_21645	9
peroxisomal multifuctional enzyme type 2	MAVA5_22265	9
putative uncharacterized protein	MAVA5_00730	9
universal stress protein family protein	MAVA5_13390	9
ATP synthase subunit alpha	MAVA5_07185	9
electron transfer flavoprotein	MAVA5_16965	8
cluster of Retinol dehydrogenase 13	MAVA5_05545	8
DNA-directed RNA polymerase subunit alpha	MAVA5_03950	8
putative uncharacterized protein	MAVA5_08060	8
acetyl-CoA acetyltransferase	MAVA5_05780	8
glycerol-3-phosphate dehydrogenase	MAVA5_19940	8
fructose-bisphosphate aldolase class-I	MAVA5_22890	7
Putative uncharacterized protein	MAVA5_11885	7
heparin binding hemagglutinin hbha	MAVA5_20430	7
malate synthase G	MAVA5_12185	6
transaldolase	MAVA5_14335	6
two component transcriptional regulator trcr	MAVA5_05665	5
immunogenic protein MPT64	MAVA5_18240	5
30S ribosomal protein S7	MAVA5_19510	5
isocitrate lyase	MAVA5_11710	5
transcriptional regulator, Crp/Fnr family protein	MAVA5_01985	5
thiol peroxidase	MAVA5_11660	5
PPE family protein	MAVA5_12310	5
ABC transporter, ATP-binding protein	MAVA5_19575	5
30kDa chaperonin 2	MAVA5_20590	4
acetyl-/propionyl-coenzyme A carboxylase	MAVA5_18840	4
putative thiosulfate sulfurtransferase	MAVA5_18830	4
10 kDa chaperonin	MAVA5_19365	4
prephenate dehydratase	MAVA5_00885	4
acetyl-CoA acetyltransferase	MAVA5_21640	4
Lsr2 protein	MAVA5_02325	4
putative molybdenum cofactor synthesis protein	MAVA5_05225	4
glutamine synthetase, type I	MAVA5_09735	4
phosphotriesterase-like protein	MAVA5_21745	4
ATPase family protein (AAA+)	MAVA5_01770	3
dienelactone hydrolase family protein	MAVA5_10805	3
enoyl-CoA hydratase	MAVA5_19725	3

Supplemental Table 4.2 (Continued)

Description	MAH A5 gene	Total Spectrum Count
uncharacterized oxidoreductase	MAVA5_16675	3
ModD protein	MAVA5_12085	3
30S ribosomal protein S5	MAVA5_03700	3
putative acyl-CoA dehydrogenase	MAVA5_09940	3
enoyl-CoA hydratase	MAVA5_16150	3
50S ribosomal protein L3	MAVA5_03585	3
short chain dehydrogenase	MAVA5_12110	3
ATPase family protein (AAA+)	MAVA5_01770	3
D-3-phosphoglycerate dehydrogenase	MAVA5_16825	3
aldo/keto reductase	MAVA5_18060	3
major membrane protein 1	MAVA5_08920	3
glyceraldehyde-3-phosphate dehydrogenase	MAVA5_14400	3
MihF protein	MAVA5_14605	3
saccharopine dehydrogenase	MAVA5_08150	3
HpcH/HpaI aldolase/citrate lyase family protein	MAVA5_17490	3
acyl carrier protein	MAVA5_09575	3
ATP synthase gamma chain	MAVA5_07190	3
PPE family protein	MAVA5_18930	3
putative uncharacterized protein	MAVA5_16665	3
nitroreductase family protein	MAVA5_19205	3
putative uncharacterized protein	MAVA5_20165	3
[NADH]enoyl-[acyl-carrier-protein] reductase	MAVA5_14170	3
MaoC family protein	MAVA5_19685	3
gamma-glutamyl phosphate reductase	MAVA5_08270	2
ATP synthase subunit b-delta	MAVA5_07180	2
aspartate transaminase	MAVA5_01615	2
phosphoribosylformyglycinamidine synthase I	MAVA5_03155	2
30S ribosomal protein S2	MAVA5_16425	2
aconitate hydratase 1	MAVA5_14215	2
HIT domain protein	MAVA5_02995	2
naphthoate synthase	MAVA5_20035	2
3-oxoacyl-[acyl-carrier-protein] synthase 1	MAVA5_09570	2
branched-chain-amino-acid aminotransferase	MAVA5_09815	2
quinone oxidoreductase	MAVA5_14320	2
transketolase	MAVA5_14330	2
succinate dehydrogenase	MAVA5_21615	2
30S ribosomal protein S4	MAVA5_03945	2
hydrolase, alpha/beta hydrolase fold family protein	MAVA5_06485	2
6-phosphogluconolactonase	MAVA5_14350	2
methyltransferase type 12	MAVA5_13360	2
putatuve uncharacterized protein	MAVA5_04770	2
triosephosphate isomerase	MAVA5_14390	2
succinate dehydrogenase	MAVA5_21610	2
phosphoribosylaminoimidazole carboxylase	MAVA5_18785	2
cluster of 2-oxoacyl-[acyl-carrier-protein]	MAVA5_09565	2
nitrogen regulatory protein P-II	MAVA5_16575	2
putative uncharacterized protein	MAVA5_03760	2
60 kDa chaperonin 1	MAVA5_19360	2
putative uncharacterized protein	MAVA5_05150	2
LprG protein	MAVA5_14525	2
phosphoglycerate kinase	MAVA5_14395	2

Supplemental Table 4.3. All sequenced eDNA deficient A5 transposon mutants.

Mutant	d7/ O.D.	A5 gene	Description	JCVI functional category
3f4	10261	MAVA5_00150	conserved hypothetical protein	Hypothetical proteins
18c7	11217	MAVA5_00260	leucyl-tRNA synthetase	Protein synthesis
33c5	13970	intergenic	20bp upstream from MAVA5_00320	N/A
23a3	11238	MAVA5_00710	Hypothetical protein	Hypothetical proteins
11g6	9615	MAVA5_00880	conserved hypothetical protein	Hypothetical proteins
35c4[b]	7960	MAVA5_01245	lipoprotein LpqH	Unknown function
34c12[b]	10730	MAVA5_01250	metallo-beta-lactamase superfamily protein	Unknown function
17g10	9598	MAVA5_01565	dihydrodipicolinate reductase, N-terminus domain protein	Amino acid biosynthesis
29b4	12617	MAVA5_01820	formate dehydrogenase, alpha subunit	Energy metabolism
28f5	10995	MAVA5_02140	conserved hypothetical protein	Hypothetical proteins
27g3	12966	MAVA5_02215	hypoxanthine phosphoribosyltransferase	Nucleosides, and nucleotides
45f8	9153	MAVA5_02520	putative flavin reductase	Fatty acid and phospholipid metabolism
24e5	12324	MAVA5_02785	thiamine pyrophosphate enzyme	Unknown function
42f6	10863	intergenic	40bp upstream from MAVA5_02875	N/A
8d10	9211	intergenic	7bp upstream from MAVA5_02950	N/A
13d3	19340	MAVA5_03020	cytochrome P450	Fatty acid and phospholipid metabolism
19d12[a]	8090	MAVA5_03165	transcriptional regulator, GntR family protein	Regulatory functions
26e9[a]	9351	MAVA5_03165	transcriptional regulator, GntR family protein	Regulatory functions
27c6	11684	MAVA5_03295	phosphate ABC transporter, permease protein PstA	Transport and binding proteins
11e7[b]	6177	MAVA5_03380	cell divisionftsk/spoiiie	Cellular processes
2f5[b]	8209	MAVA5_03410	conserved hypothetical protein	Hypothetical proteins
38h12[b]	8469	MAVA5_03425	putative transcriptional regulator	Regulatory functions
3d1	15062	MAVA5_03655	conserved hypothetical protein	Hypothetical proteins
9b11	10560	MAVA5_03755	carbohydrate kinase, FGGY family	Unclassified
25d12	11285	intergenic	103bp upstream from MAVA5_03920	N/A
13g9	14096	MAVA5_04105	transposase	Mobile element functions
29d11	9105.7	MAVA5_04290	4-carboxymuconolactone decarboxylase domain protein	Energy metabolism
30e5	8420	MAVA5_04775	conserved hypothetical protein	Hypothetical proteins
4e12	12293	intergenic	non-CDS region. Nearest is MAVA5_04940	N/A

[a] the same gene is interrupted between these mutants, however the locations are unique

[b] this mutant is within 10 genes proximity of the mutant before and/or after it

[c] the mutants and all genes between them are in the same orientation, potentially in an operon

Supplemental Table 4.3 (Continued)

Mutant	d7/ O.D.	A5 gene	Description	JCVI functional category
36h9[b]	13436	MAVA5_05210	mycobacterial persistence regulator mrpa	Regulatory functions
15b11[b]	15837	MAVA5_05260	acetyltransferase, GNAT family	Unknown function
36d7[b]	7469	MAVA5_05310	rieske [2Fe-2S] domain protein	Energy metabolism
37c1[b]	12110	MAVA5_05580	diaminopimelate decarboxylase	Amino acid biosynthesis
16e4[a,b]	11954	MAVA5_05585	transcriptional-repair coupling factor	DNA metabolism
41c1[a,b]	7184	MAVA5_05585	transcription-repair coupling factor	DNA metabolism
45e4	6972	MAVA5_05645	K+-transporting ATPase, A subunit	Transport and binding proteins
31g7[b,c]	11779	MAVA5_05750	cysteine dioxygenase type I superfamily	Energy metabolism
12h10[b,c]	13861	MAVA5_05775	permease of the major facilitator superfamily	Transport and binding proteins
37h10	12264	MAVA5_05920	3-beta hydroxysteroid dehydrogenase/isomerase family	Energy metabolism
39f10[b]	6872	MAVA5_06175	conserved hypothetical protein	Hypothetical proteins
25a2[b]	8759	MAVA5_06190	Mcr protein	DNA metabolism
33f11[b]	9850	intergenic	10bp upstream from MAVA5_06230	N/A
33g10	13703	MAVA5_06285	nitrate reductase, alpha subunit	Energy metabolism
18e8	8853	intergenic	90bp upstream from MAVA5_06615	N/A
29b2	19306	intergenic	20bp upstream from MAVA5_06690	N/A
33g2	10496	intergenic	2bp upstream from MAVA5_06800	N/A
10e8[b]	22099	MAVA5_06930	StaS protein	Protein fate
36h7[b]	9107	MAVA5_06955	TrkA-N domain family	Transport and binding proteins
40h7	9553	MAVA5_07075	gp13 protein	Mobile element functions
14g4	8077	MAVA5_07205	conserved hypothetical protein	Hypothetical proteins
28g12	11671	intergenic	23 bp upstream from MAVA5_07680	N/A
45e7	8405	MAVA5_07915	Carboxyl transferase domain	Fatty acid and phospholipid metabolism
33c10	10554	MAVA5_08200	transcriptional regulator, TetR family protein	Regulatory functions
15c6[b]	13021	MAVA5_08465	sulfate/thiosulfate import ATP-binding protein CysA	Transport and binding proteins
36d5[b]	7616	MAVA5_08485	conserved hypothetical protein	Hypothetical proteins
36h6	6382	intergenic	257 bp upstream from MAVA5_08600	N/A

[a] the same gene is interrupted between these mutants, however the locations are unique

[b] this mutant is within 10 genes proximity of the mutant before and/or after it

[c] the mutants and all genes between them are in the same orientation, potentially in an operon

Supplemental Table 4.3 (Continued)

Mutant	d7/ O.D.	A5 gene	Description	JCVI functional category
24b6	8505	MAVA5_08785	conserved hypothetical protein	Hypothetical proteins
27b6	13623	intergenic	100bp upstream from MAVA5_09125	N/A
38c1[b]	9816	MAVA5_09320	LppO protein	Unclassified
1c5[b]	14295	MAVA5_09350	conserved hypothetical protein	Hypothetical proteins
27f8	11371	MAVA5_09405	cytochrome P450 superfamily	Cellular processes
44g4[b]	10422	intergenic	106bp upstream from MAVA5_09465	N/A
37c7[b]	9100	MAVA5_09495	conserved hypothetical protein	Hypothetical proteins
18b11	11722	MAVA5_09590	pyruvate dehydrogenase E1 component	Energy metabolism
41e1	10274	MAVA5_09740	glutamate-ammonia-ligase adenylyltransferase	Amino acid biosynthesis
23d4[b,c]	18640	MAVA5_10205	5,10-methylenetetrahydro-methanopterin reductase	Energy metabolism
40h2[b,c]	7581	MAVA5_10220	conserved hypothetical protein	Hypothetical proteins
26e12[a,b]	10357	MAVA5_10275	metal-dependent hydrolase	Cellular processes
29b11[a,b]	8659	MAVA5_10275	metal-dependent hydrolase	Cellular processes
7d3[a,b]	9918	MAVA5_10275	metal-dependent hydrolase	Cellular processes
37h6[b,c]	9801	MAVA5_10295	flavin-binding monooxygenase	Unknown function
43f8[a,b,c]	9153	MAVA5_10310	monooxygenase	Energy metabolism
5d3[a,b,c]	9876	MAVA5_10310	monooxygenase	Energy metabolism
37d4[b,c]	10315	MAVA5_10315	cytochrome P450	Central intermediary metabolism
29e7	6619	MAVA5_10575	ABC-transporter integral membrane protein	Transport and binding proteins
1e5	7871	MAVA5_10615	PimT protein	Unclassified
41b1	7313	intergenic	180bp upstream from MAVA5_10720	N/A
26b3	9015	MAVA5_10770	precorrini-3B synthase	Biosynthesis of cofactors
38c11	7352	intergenic	16bp upstream from MAVA5_11070	N/A
22g7	6850	intergenic	non-CDS region. Nearest is MAVA5_11210	N/A
24c7	9529	MAVA5_11225	oxidoreductase	Central intermediary metabolism
5f6	9914	MAVA5_11355	PapA2 protein	Cellular processes
46a1	8707	MAVA5_11495	catalase/peroxidase HPI	Cellular processes
33f5	10169	MAVA5_11535	glycosyl hydrolases family 16	Energy metabolism
29a4	11193	MAVA5_11595	hyp.	Hypothetical proteins
16g11	10059	MAVA5_11885	antigen 85-C	Central intermediary metabolism
6g5	17241	MAVA5_12060	short chain dehydrogenase	Energy metabolism
30e6[b]	8683	intergenic	11 bp upstream from MAVA5_12130	N/A

[a] the same gene is interrupted between these mutants, however the locations are unique

[b] this mutant is within 10 genes proximity of the mutant before and/or after it

[c] the mutants and all genes between them are in the same orientation, potentially in an operon

Supplemental Table 4.3 (Continued)

Mutant	d7/ O.D.	A5 gene	Description	JCVI functional category
44b10[b]	8667	MAVA5_12135	transcriptional repressor, CopY family	Regulatory functions
34g9[b]	10443	intergenic	67 bp upstream from MAVA5_12190	N/A
37e2[b]	9103	MAVA5_12205	glycine dehydrogenase	Energy metabolism
39f5[b]	8697	MAVA5_12405	ppe family protein	Unknown function
11c2[b]	8293	MAVA5_12450	4-alpha-glucanotransferase	Energy metabolism
28c4	8430	MAVA5_12985	gnat-family acetyltransferase	Unknown function
21d5[b,c]	8566	MAVA5_13175	conserved hypothetical protein	Hypothetical proteins
36f9[b,c]	7932	MAVA5_13185	glucose-methanol-choline oxidoreductase	Central intermediary metabolism
39d10[b,c]	8000	MAVA5_13215	P450 heme-thiolate protein	Energy metabolism
7b10	13985	intergenic	18 bp upstream from MAVA5_13345	N/A
7b5[b,c]	14055	MAVA5_13410	excinuclease ABC, B subunit	DNA metabolism
9e11[b,c]	19286	MAVA5_13430	PknF protein	Unclassified
25g7[b]	8135	intergenic	57 bp downstream from MAVA5_13635	N/A
42c3[b]	6654	MAVA5_13685	Hypothetical protein	Hypothetical proteins
32d2[b]	7237	MAVA5_13725	adenosylmethionine-8-amino-7-oxononanoate transaminase	Biosynthesis of cofactors
24b7[b]	7719	MAVA5_13740	putative acyltransferase domain protein	Unknown function
24d3[b,c]	7105	MAVA5_13900	Hypothetical protein	Hypothetical proteins
12b8[b,c]	8694	MAVA5_13915	syringomycin synthetase	Cellular processes
6f4	11695	MAVA5_14420	acyltransferase domain protein	Cell envelope
35h2	9269	MAVA5_14570	conserved hypothetical protein	Hypothetical proteins
31a3	11338	intergenic	67 bp downstream from MAVA5_14995	N/A
27c4[b]	10722	MAVA5_15290	conserved hypothetical protein	Hypothetical proteins
39f9[b]	8372	MAVA5_15295	integrase	Mobile element functions
14a1	14085	MAVA5_15645	TrkA protein	Transport and binding proteins
11d6	9083	MAVA5_15780	conserved hypothetical protein	Unclassified
40f8	7184	intergenic	100 bp upstream from MAVA5_15795	N/A
7e2	8024	MAVA5_16155	conserved hypothetical protein	Hypothetical proteins
13f3	16446	intergenic	106 bp upstream from MAVA5_16800	
6c11	9679	MAVA5_16900	conserved hypothetical protein	Hypothetical proteins
9d7	20389	MAVA5_17275	carbon starvation protein A	Cellular processes
30e2	9158	MAVA5_17720	hypothetical protein	Hypothetical proteins
45f9	8512	MAVA5_17915	protein-glutamate methylesterase	Cellular processes
3d8	9793	MAVA5_18030	UDP-glucose 6-dehydrogenase	Cell envelope

[a] the same gene is interrupted between these mutants, however the locations are unique
[b] this mutant is within 10 genes proximity of the mutant before and/or after it
[c] the mutants and all genes between them are in the same orientation, potentially in an operon

Supplemental Table 4.3 (Continued)

Mutant	d7/ O.D.	A5 gene	Description	JCVI functional category
23e7	9292	MAVA5_18190	Hypothetical protein	Hypothetical proteins
36c1[b,c]	11491	intergenic	67 bp upstream from MAVA5_18275	N/A
32h1[b,c]	10187	MAVA5_18280	ATP-dependent DNA helicase	DNA metabolism
19c2[b]	12186	intergenic	non-CDS region. Nearest is MAVA5_18430	N/A
46d2[b,c]	11179	intergenic	41 bp upstream from MAVA5_18465	N/A
30f1[b,c]	10740	MAVA5_18475	Hypothetical protein	Hypothetical proteins
13f6	8596	MAVA5_19045	succinate dehydrogenase hydrophobic membrane anchor protein SdhD	Energy metabolism
2e3	6432	MAVA5_19115	conserved hypothetical protein	Hypothetical proteins
44e11	8961	MAVA5_19400	glutamate decarboxylase	Energy metabolism
32e6	16012	MAVA5_19430	conserved hypothetical protein	Unclassified
5d9	7737	intergenic	47 bp upstream from MAVA5_19495	N/A
1c3[b]	14839	MAVA5_19910	metal ion transporter, nramp family	Transport and binding proteins
40c10[b]	6941	MAVA5_19945	Carbonic anhydrase	Cellular processes
4b8[b,c]	10861	MAVA5_20270	conserved hypothetical protein	Hypothetical proteins
39e5[b,c]	6798	MAVA5_20295	cyclopropane-fatty-acyl-phospholipid synthase 2	Fatty acid and phospholipid metabolism
11d3	8857	MAVA5_20565	glyoxalase family protein	Unknown function
11c8	9382	MAVA5_20630	cell division protein 48, N- domain	Cellular processes
40e7	8775	MAVA5_20915	O-succinylhomoserine sulfhydrylase	Amino acid biosynthesis
8c10[b]	10371	MAVA5_21435	ATPase, AAA family	Unknown function
1a2[b]	8252	MAVA5_21480	conserved hypothetical protein	Hypothetical proteins
24g3[b]	17619	MAVA5_21530	acyl-CoA synthase	Fatty acid and phospholipid metabolism
12g6	11542	intergenic	119 bp upstream from MAVA5_21540	N/A
29c4[b]	9369	MAVA5_21610	succinate dehydrogenase	Energy metabolism
29f12[b]	9305	MAVA5_21635	putative acyl-CoA dehydrogenase	Fatty acid and phospholipid metabolism
15f7[b]	11277	intergenic	7 bp upstream from MAVA5_21660	N/A
4c2[b]	10781	MAVA5_21735	transcriptional regulator, TetR family protein	Regulatory functions
26a3[b]	10085	MAVA5_21745	phosphotriesterase homology protein	Central intermediary metabolism

[a] the same gene is interrupted between these mutants, however the locations are unique
[b] this mutant is within 10 genes proximity of the mutant before and/or after it
[c] the mutants and all genes between them are in the same orientation, potentially in an operon

Supplemental Table 4.3 (Continued)

Mutant	D7/ O.D.	A5 gene	Description	JCVI functional category
38g8[b]	7037	intergenic	58 bp upstream from MAVA5_21955	N/A
8e7[b]	9087	MAVA5_21960	membrane protein	Cell envelope
39c3[b]	6953	intergenic	58 bp upstream from MAVA5_21970	N/A
31g1[b,c]	12622	intergenic	85 bp upstream from MAVA5_22270	N/A
32a4[b,c]	10238	MAVA5_22290	transcriptional regulator, TetR family protein	Regulatory functions
43f4	13302	MAVA5_22665	TetR-family transcriptional regulator, putative	Regulatory functions
20e5	10005	MAVA5_22765	carbonic anhydrase	Cellular processes
2h7[b]	10246	MAVA5_22885	conserved hypothetical protein, putative	Hypothetical proteins
45c6[b]	14360	MAVA5_22890	fructose-bisphosphate aldolase class-I	Energy metabolism

[a] the same gene is interrupted between these mutants, however the locations are unique
[b] this mutant is within 10 genes proximity of the mutant before and/or after it
[c] the mutants and all genes between them are in the same orientation, potentially in an operon

Supplemental Table 4.4. Unique *M. avium* subsp. *hominissuis* strain A5 genomic region that nine eDNA deficient mutants were located within.

Gene	Predicted protein
MAVA5_10140	hypothetical protein
MAVA5_10145	zinc-containing alcohol dehydrogenase
MAVA5_10150	acetyl-CoA acetyltransferase
MAVA5_10155	hypothetical protein
MAVA5_10160	putative transcriptional regulator, TetR
MAVA5_10165	phenylacetic acid degradation-related protein
MAVA5_10170	putative hydrolase (alpha/beta fold)
MAVA5_10175	TetR family transcriptional regulator
MAVA5_10180	ferredoxin reductase
MAVA5_10185	cytochrome P450
MAVA5_10190	ferredoxin
MAVA5_10195	HTH-type transcriptional regulator AraC
MAVA5_10200	hypothetical protein
MAVA5_10205	luciferase-like
MAVA5_10210	hypothetical protein
MAVA5_10215	MaoC-like dehydratase
MAVA5_10220	hypothetical protein
MAVA5_10225	hypothetical protein
MAVA5_10230	enoyl-CoA dehydratase/isomerase
MAVA5_10235	hypothetical protein
MAVA5_10240	hypothetical protein, disrupted
MAVA5_10245	TetR family transcriptional regulator
MAVA5_10250	acid-CoA ligase
MAVA5_10255	acyl-CoA dehydrogenase FadE
MAVA5_10260	acetyl/propionyl carboxylase alpha subunit
MAVA5_10265	acetyl/propionyl carboxylase beta subunit
MAVA5_10270	putative transcriptional regulator
MAVA5_10275	hypothetical protein
MAVA5_10280	putative transcriptional regulator
MAVA5_10285	short-chain dehydrogenase
MAVA5_10290	hypothetical protein
MAVA5_10295	putative monooxygenase
MAVA5_10300	putative monooxygenase
MAVA5_10305	acetyl hydrolase
MAVA5_10310	monooxygenase
MAVA5_10315	cytochrome P450
MAVA5_10320	hypothetical protein
MAVA5_10325	long-chain-fatty-acid--CoA ligase
MAVA5_10330	acyl CoA dehydrogenase
MAVA5_10335	hypothetical protein
MAVA5_10340	hypothetical protein
MAVA5_10345	zinc-type alcohol dehydrogenase AdhD
MAVA5_10350	acyl CoA dehydrogenase
MAVA5_10355	metal-dependent phosphohydrolase
MAVA5_10360	putative MutT/NUDIX-like protein
MAVA5_10365	hypothetical protein
MAVA5_10370	putative regulatory protein
MAVA5_10375	cell division FtsK/SpoIIIE protein
MAVA5_10380	putative plasmid replication initiator protein

Chapter 5

Discussion and Conclusions

Sasha J. Rose

Overview

Nontuberculous mycobacteria (NTM) are ubiquitous in the environment and many species cause disease in humans. NTM infections disproportionally affect individuals with immune or respiratory defects, and the prevalence of NTM infections worldwide is rising. The overwhelming majority of NTM infections are caused by members of the *Mycobacterium avium* complex (MAC), primarily *M. avium* subsp. *hominissuis* (MAH) and *M. intracellulare*, but infections by other NTM including *M. abscessus* and *M. kansasii* are also clinically important. NTM infection in the respiratory tract is both intracellular, in macrophages mainly, but also extracellular in the form of biofilms. Though there is a growing connection between NTM biofilms and respiratory infection, the interaction of these biofilms and the immune system are incompletely understood. Furthermore, even though it has been shown that the mycobacterial cell wall contributes to biofilm formation, it is still largely unknown what other bacterial products and effectors are being produced by these biofilms, and how they are regulated. The work conducted and presented in this dissertation have furthered the knowledge in these areas of NTM biofilm biology and host interaction.

The Interaction Between *M. avium* Biofilm and the Host

In Chapter 2, I developed an in vitro model representing the interaction between an established MAH biofilm and surveilling immune cells. Macrophages in contact with the biofilm produced a robust amount of TNFα early during infection, which is distinct from the interaction with planktonic bacteria, or even planktonic bacteria centrifuged to the bottom surface of the microplate, resembling a biofilm. TNFα is associated with mycobacterial killing, so I assessed if these hyper-stimulated macrophages had increased anti-MAH killing capabilities. To our surprise, there was no reduction of MAH in the biofilms, even when the macrophages were pre-stimulated or co-incubated with natural killer cells. A large percentage of these macrophages were undergoing early TNFα-driven apoptosis within hours of this interaction, which is also peculiar, as apoptosis usually occurs several days after MAH infection.

In other biofilm-associated respiratory pathogens, it has been described that the biofilms shield the bacteria from the immune response, and can even elicit anti-inflammatory mediators (Thurlow, Hanke et al. 2011; Daw, Baghdayan et al. 2012). My findings contrast from those, as I see a large proinflammatory response from the macrophages, however, the end result of attenuation of killing is still observed. Despite eliciting different initial host responses, biofilm infections generally are helping bacteria evade immune killing over their planktonic counterparts, which could offer an explanation why many bacterial genera form biofilms during respiratory infection, where alveolar macrophages and other immune cells are commonly encountered.

My model looked at the interaction between established biofilm and macrophages, however this cannot be the only scenario found in the respiratory tract of a patient. NTM form robust biofilms in showerheads and other common plumbing surfaces, and bacteria from these biofilms are readily aerosolized into the respiratory tract during showering, for example. While it is certainly plausible that pieces of intact biofilm are being inhaled and deposited in the respiratory tract, individual bacteria (either separated from the biofilm from the sheer forces of the showerhead for example, or naturally released planktonic bacteria from the biofilm developmental cycle) are also being introduced to the respiratory tract. In the latter case, work conducted primarily by Lmar Babrak from my laboratory has also investigated this early stage of respiratory infection with single cell suspensions of planktonic MAH and found that the bacteria form microaggregates within 48 hours of exposure to respiratory epithelial cells, in vitro (See Appendix 2.5 and 2.6). Our current hypothesis is that NTM microaggregate formation is a prelude to biofilm formation, based off of strong global transcriptional similarities between early microaggregates formed on cells and established biofilms (Babrak, Danelishvili et al. 2015). Since MAH within microaggregates share more traits with biofilm than planktonic, laboratory cultured bacteria, it is interesting to speculate if a similar immune response would be observed from this population. Future work will be needed to determine if

microaggregates are effectively killed by surveilling macrophages, or if they cause similar hyper-stimulation and early apoptosis as established biofilms.

After observing the initial results of hyper-stimulation from the macrophages, I started to think about what exactly was eliciting the response, i.e. what specifically is different between the biofilm and planktonic bacteria. To test this, I exposed macrophages to acellular biofilm supernatant and assessed TNFα production. Of the two strains tested, the supernatant from MAH A5 (biofilm overproducer) elicited a strong TNFα response, but the supernatant from MAH 104 (standard biofilm producer, reference strain) failed to do so. It is known that there is more substantial biofilm matrix in MAH A5, which is visually apparent when working with these biofilms, and was observed by electron microscopy in Chapter 3. It can be assumed that components from this biofilm matrix are also being shed into the biofilm supernatant. eDNA from the biofilm supernatants of these two strains was quantified in Chapter 3, and eDNA was found in the MAH A5 supernatant, but barely detectable in the MAH 104 supernatant. The eDNA in the MAH A5 biofilm supernatant could be eliciting, at least in part, the TNFα response, since it is known that unmethylated bacterial DNA triggers multiple inflammatory receptors. Purified eDNA out of the MAH A5 biofilm extracted matrix indeed elicited a strong TNFα response when incubated with the macrophages (unpublished data). Additionally, in Chapter 2, I tested UV-sterilized MAH A5 biofilm against live biofilm, and noticed almost identical TNFα production, further demonstrating that acellular biofilm components (including eDNA) contribute to the response I observed. This does not exclude the possibility that biofilm-associated bacteria themselves do not have a differential phenotype from planktonic bacteria. Our model only examined TNFα, but there could be other cytokines and/or chemokines produced during exposure to MAH biofilms that might have been differentially produced between the live and UV-sterilized biofilms. I have preliminary data showing that washed and DNase-treated MAH A5 from an established biofilm infects and survives in macrophages at a higher level than their planktonic counterparts. Current work is looking further at this aspect of the

interaction, with focus on the actual bacteria in this biofilm state, after subtracting the matrix from the interaction.

Extracellular DNA in NTM Biofilms

My original finding of eDNA occurred serendipitously when we were following up on the work from Chapter 2, starting to investigate secreted products in MAH biofilms. When I was processing biofilm protein samples from the proteins localized on the bacterial surface and in the biofilm matrix, I consistently encountered a 'contaminant' in the MAH A5 samples. Using a shotgun approach to assess the contaminant, I found it was DNA by strong ethidium bromide fluorescence with DNA gel electrophoresis. The fluorescent quantifications of eDNA in Chapters 3 and 4 were all conducted with propidium iodide, as a result of extensive preliminary work that tested multiple DNA stains on MAH A5 biofilms including syto9, SYBR green, ethidium bromide, YO-PRO, Hoechst, and DAPI. Since the mycobacterial cell envelope is such a unique structure compared to normal cell membranes and cell walls, I encountered inconsistent and non-specific staining with some of these stains. Other stains gave high background fluorescence, lowering the sensitivity of the stain. Out of all of the stains tested, I obtained the most reliable results with lowest background with propidium iodide.

When I visualized the eDNA in MAH A5 biofilms with immunogold labelling and electron microscopy in Chapter 3, there were abundant extracellular fibrous structures that were consistent with eDNA reports in other bacteria as well as in neutrophil extracellular traps (Bockelmann, Janke et al. 2006; Barnes, Ballering et al. 2012; Brinkmann and Zychlinsky 2012), however the DNA labelling was not as pronounced as others have published (Barnes, Ballering et al. 2012). The immunogold particles were most abundant near the ends of eDNA strands and at exposed channels in the biofilm. Since various lipids have been implicated with NTM biofilms, it was assumed that lipid abundance was potentially interfering with the antibody accessibility and binding to the eDNA. I did biologically repeat the SEM with the small modification of increased antibody concentrations, and did observe

more pronounced labelling, but it still was limited comparably to other work. I also attempted to corroborate the SEM results with fluorescent microscopy, but with the limitation of 1,000x magnification on the fluorescent microscope made it difficult to visually discern individual eDNA fibers.

To determine if the eDNA observed in MAH A5 was an artifact of the strain or a more widespread trait of NTM, I surveyed multiple MAH species for eDNA, as well as other NTM that were available in the laboratory. The levels of eDNA extracted and quantified in these biofilms was variable, ranging from very little or none to the *M. abscessus* and *M. chelonae* isolates tested that produced eDNA comparable to MAH A5. This is interesting, considering these species in particular form very robust biofilm in the laboratory that shares similarities to MAH A5 biofilms. An important limitation to my survey was that in all the NTM species tested, biofilms were formed under a single set of variables, determined from my work on eDNA in MAH A5. In some of these strains that didn't produce eDNA (or produced little eDNA) under my conditions, there might be the need for other requirements (surfaces, nutrients, oxygenation, temperature, etc.) to promote eDNA production. Since I am the first to report eDNA in mycobacterial biofilms, there is not any other published work to compare these results to. It is important to retain the possibility that other strains might actually produce more eDNA under different conditions from that I tested for.

eDNA Produced by an Active Mechanism

Between what is presented in Chapters 3 and 4, I have convincing evidence for eDNA production in MAH, and potentially other NTM, being an active mechanism. One of the biggest questions that kept lingering throughout this work was, where does the eDNA come from? The bacteria in the biofilms are not actively replicating, demonstrated by CFU assessments and the lack of elongated, dividing bacilli in the SEM (Chapter 3), however I found many eDNA attenuated clones in my transposon library screen with mutations in genes involved with metabolism and energy production (Chapter 4). It has been speculated that in a given bacterium at any

given time, there are two copies of the chromosome, as vegetative bacteria are typically in a state of replication. If this is the case, and the bacteria I seed the biofilms with do, on average, possess an extra chromosome, then it still takes significant energy to export this DNA extracellularly. I hypothesize that when forming a biofilm, these bacteria focus the available energy on matrix production (and subsequently eDNA production) over vegetative replication, which would help explain why so many eDNA deficient mutants were involved in metabolism and related functions. An alternative hypothesis to the bacteria having pre-synthesized DNA is that the bacteria within the biofilm could be synthesizing the DNA during biofilm formation, and then exporting it. I explored this by assessing if sub-inhibitory concentrations of moxifloxacin, a fluoroquinolone that prevents DNA synthesis, would affect eDNA production in MAH A5 biofilms. There was no inhibition of eDNA production using 0.5x, 0.25x, or 0.125x of the MIC of moxifloxacin against MAH A5 (unpublished data). This preliminary experiment suggests that eDNA production in MAH A5 biofilm is occurring independently of DNA synthesis, however there are limitations in this assay. My system relies on biofilms formed with 10^7 bacteria. If the seeded bacteria carryover pre-synthesized DNA into the biofilms, then even if DNA synthesis is occurring during biofilm formation and being effectively blocked by moxifloxacin, I might have not seen that reduction due to the other reservoir of eDNA. I have tried eDNA quantification experiments with less than this inoculum, but the sensitivity of the eDNA quantification diminishes quickly. In reality, both pre-synthesized DNA and DNA synthesized during biofilm formation are more than likely contributing to eDNA production. More work will be needed to fully elucidate the regulation, synthesis, and export of eDNA in NTM biofilms.

Relevance of Bicarbonate as an eDNA Trigger

The connection found between bicarbonate stimulation and eDNA production in Chapter 4 made me start thinking about the evolution of this response and in what niches for NTM would this be advantageous. It is first important to clarify that I am unsure whether bicarbonate, carbon dioxide, or both are actually triggering eDNA

production. The biofilm surface proteomics results coupled with the ethoxzolamide treatment and the eDNA transposon screen show that surface-exposed carbonic anhydrases are directly involved with eDNA. These enzymes catalyze the reversible reaction between carbon dioxide and the bicarbonate anion. It is unclear whether *M. avium* and other NTM are actually responding to bicarbonate, or carbon dioxide that the carbonic anhydrases converted bicarbonate into. The literature describes pathogens responding directly to both bicarbonate (Yang, Hart et al. 2008; Abuaita and Withey 2009; Maddox, Coburn et al. 2012) and carbon dioxide (Mogensen, Janbon et al. 2006; Hammerstrom, Roh et al. 2011; Burghout, Zomer et al. 2013). The bicarbonate buffering system in humans is the major buffering system for the blood and tissues. The intricate interplay between carbon dioxide and bicarbonate, influenced by eukaryotic carbonic anhydrases, is important for maintaining buffered pH in the human body. Combining this with my observations of bicarbonate acting as a trigger for NTM suggests that bicarbonate sensing could be a bacterial response evolved to allow NTM to adapt to the host. An important consideration however, is that NTM are environmental organisms. It is unclear whether eDNA is associated with environmental NTM biofilms. In Chapter 3 I formed biofilms at 22˚C vs 37˚C to see if eDNA was specific to the host temperature, but significant eDNA was produced at both temperatures. This concluded that temperature does not seem to be a critical factor for eDNA production. Bicarbonate and carbon dioxide can be found in potable or naturally-occurring water at low concentrations, as well as in the proximity of other environmental organisms. My work does not show eDNA production or significant biofilm formation in deionized water, but NTM eDNA has not been specifically investigated in potable or naturally occurring water. Other laboratories have formed robust NTM biofilms in potable water (Williams, Yakrus et al. 2009; Mullis and Falkinham 2013), so it can be speculated that the concentrations of carbon dioxide and/or bicarbonate could be enough to stimulate eDNA in these models.

Improved Genetic Manipulation of *M. avium*

Once I determined that eDNA could be produced by active processes, the next step was identifying genes responsible. I first attempted transposon mutagenesis with the TN5367 transposon inside of the pTNGJC plasmid, that has been used previously in the laboratory. The inherent challenge when manipulating MAH genetically is plasmid stability and retention. We have shown in recent years that expression plasmids transformed into MAH work best immediately after transformation. Each passage of the bacteria after this, even when plated on very high concentrations of selectable antibiotic, reduces expressed protein levels substantially. This problem makes working with stable plasmids in MAH a real challenge, and limits the range of genetic manipulations available. The pTNGJC system works by first transforming the plasmid into MAH, PCR screening transformants for positive clones, growing up a positive clone to high numbers, and then heat-shocking the population at 40˚C for one week to activate the transposases that insert the transposon randomly into each individual clone in the population. I tried creating a transposon library in MAH A5 using pTNGJC for this work, and every positive transformant turned negative after growing the bacteria up for heat-shock and integration (similar to our problem with expression plasmids).

In the fall of 2014, I received the MycomarT7 phagemid from Eric Rubin, that had previously been used to produce transposon libraries in *M. tuberculosis*, *M. smegmatis*, and *M. marinum*. The transposon in this phagemid is a highly active Himar1-based transposon that possesses good stability once inserted. The phagemid is lytic when transduced and propagated at 30˚C (to harvest phagemid), but is integrative to deliver transposon into the chromosome when transduced and grown at 37˚C. I successfully produced transposon libraries not only in MAH A5, but also MAH 104, MAH 100, MAH 109, MAH 101, MAA Chester, MAP K10, *M. abscessus* 19977, and *M. tuberculosis* h37Rv with this phagemid. Since the transposon is delivered directly into the chromosome during transduction, I did not observe anything resembling plasmid loss during growth. Initially, 60 random clones of MAH A5 and *M. abscessus* were serially passaged three times with no selectable antibiotic

in the media, and the retention rate remained 100% throughout the passages. For each of the strains transduced, I obtained between 5,000 and 50,000 positive mutants, representing between 1 to 10x coverage of the typical mycobacterial genome. These stable, robust libraries helped me finish the work presented in Chapter 4, but have also allowed multiple other experiments to be conducted in the laboratory that are allowing us to find new interesting mutants and accomplish more with these mutants than was previously possible.

In addition to creating new transposon libraries, I spent significant time optimizing and implementing a more robust system for transposon identification than our laboratory previously used, which was not always reliable, and was very time and cost intensive. Our old nested PCR technique uses two increasingly stringent PCR steps with non-specific primers to amplify flanking sequence from the inserted transposon, however the second PCR yields many bands on a DNA gel, that all need to be individually extracted and sequenced, with still no guarantee of obtaining a positive sequence that contains transposon and flanking sequence. I conducted a literature search looking for new methods found an innovative method for transposon identification called ligation-mediated PCR (LMPCR), which was originally published for bacterial transposon identification by the Pasteur Institute in 1998. This technique has not become popular since this report, because I imagine that the molecular reagents almost 20 years ago when it was published were not of the quality of todays, so it was harder to repeat this technique independently. The method relies on digesting the entire genome of the mutant with a restriction endonuclease, ligating an artificial oligo adapter with a complementary restriction site, and then conducting PCR between the transposon and the adapter that is bound to the nearest restriction site from the random transposon insertion. This method works best with enzymes with many cut sites in mycobacteria, and SalI was utilized because it has roughly 6,000 cut sites in the average mycobacterial genome. I have had great success with this method since implementing it in the spring of 2015. Ninety percent of the mutants submitted to this approach have been successfully sequenced within 48 hours and for a minimal cost. I was able to readily sequence over 150 mutants in Chapter 4,

which gave a better picture the true range of mutated genes that are implicated with eDNA attenuation, compared to older identification methods that due to cost and time would only allow for a handful of mutants to be successfully identified. This method has also allowed me to sequence close to 100 other mycobacterial mutants for our laboratory since its application, significantly improving the results interpretation from the genetic systems and networks involved with particular phenotypes.

As mentioned briefly, plasmids are not maintained well in MAH, which is unfortunate, as it didn't allow me to create targeted gene disruptions of genes found in the transposon library screen (to confirm them) or for genes of interest that weren't found in my eDNA library screen (AraC regulator, for example). The two principal methods for targeted gene disruption in mycobacteria are the ts-*sacB* system and the newer plasmid-based phage recombinase system (Medjahed and Reyrat 2009). Though these systems have worked in other mycobacterial species, they do not work well in MAH due to plasmid retention. In other mycobacteria, the phage recombinase system has shown much higher efficiencies of recombination over the ts-*sacB* systems, so that is what I attempted for allelic exchange in MAH A5, but all attempts were unsuccessful. Knowing how unstable MAH can be with plasmids, I decided on the pMV306 integrative plasmid that integrates into the L5 site in the mycobacterial genome (Stover, de la Cruz et al. 1991) for the complementation work done in Chapter 4. I observed strong restorative phenotypes in PCR positive mutants and repeated PCR confirmation of plasmid retention, demonstrating that this plasmid backbone can be an effective tool for future MAH engineering.

Conclusions and Future Directions

The relationship between NTM biofilm formation and respiratory infection is becoming more evident, but many aspects of these infections are not well understood. In this dissertation, I determined that MAH biofilms can persist in the host because they elicit an atypical hyper-stimulation and early TNFα-driven apoptosis in surveilling phagocytes. I discovered extracellular DNA (eDNA) as an important component of MAH and other NTM biofilms that has structural and protective

properties. Lastly, I found that bicarbonate is a trigger for eDNA production and identified many genes important for eDNA production. The work described here introduces new areas for future research and potentially two important novel virulence factors in NTM: bicarbonate sensing and eDNA production.

The initial eDNA work in Chapter 3 illustrated the importance of eDNA in biofilm integrity and tolerance to antibiotics. DNase I treatment was very effective at removing established MAH biofilm and significantly reduced the tolerance of MAH biofilms to clinically used antibiotics. This is attractive as a new treatment option because there is an already an FDA approved inhaled DNase I solution (Pulmozyme) for cystic fibrosis. It will be worthwhile to evaluate if there is added benefit of adding Pulmozyme as an adjuvant to the new topical therapies for mycobacterial infection that are showing promise experimentally and in clinical trials (see Appendix 1).

The work described in Chapter 4 suggests surface-exposed carbonic anhydrases and downstream bicarbonate signaling as potentially important targets to prevent biofilm formation and eDNA production in NTM. It is particularly interesting how co-incubation with a small concentration of the carbonic anhydrase inhibitor ethoxzolamide significantly reduced eDNA in MAH biofilms. Carbonic anhydrases are also showing to be important for *M. tuberculosis* as carbonic anhydrase treatment with ethoxzolamide also inhibited ESX1 secretion, the PhoPR system, and attenuated virulence in vivo (Johnson, Colvin et al. 2015). More work needs to be conducted in MAH and other NTM to further investigate the link between bicarbonate sensing, eDNA, and virulence. An important experiment that should be carried out is to determine if eDNA deficient mutants are attenuated during respiratory infection. Since MAH is an environmental organism, and biofilm is classically an environmental adaptation, I am also very interested in investigating if any of these genes implicated in the bicarbonate response and eDNA production are associated with intracellular infection and pathogenesis. Preliminary in vitro experiments suggest that this is occurring, as the majority of tested eDNA mutants appear attenuated during in vitro macrophage infection. Multiple groups have recently defined the host response to DNA that *M. tuberculosis* is secreting intracellularly that

is essential for virulence, however the mechanisms of DNA secretion remain unknown. Since NTM and *M. tuberculosis* share many traits during intracellular infection, it is tempting to hypothesize that some of the genes found in our eDNA/bicarbonate system could be involved with *M. tuberculosis* intracellular DNA production.

BIBLIOGRAPHY

Abdallah, A. M., N. C. Gey van Pittius, et al. (2007). "Type VII secretion--mycobacteria show the way." Nat Rev Microbiol **5**(11): 883-891.

Abdallah, A. M., T. Verboom, et al. (2006). "A specific secretion system mediates PPE41 transport in pathogenic mycobacteria." Mol Microbiol **62**(3): 667-679.

Abuaita, B. H. and J. H. Withey (2009). "Bicarbonate Induces Vibrio cholerae virulence gene expression by enhancing ToxT activity." Infect Immun **77**(9): 4111-4120.

Adjemian, J., K. N. Olivier, et al. (2012). "Prevalence of nontuberculous mycobacterial lung disease in U.S. Medicare beneficiaries." Am J Respir Crit Care Med **185**(8): 881-886.

Aitken, M. L., A. Limaye, et al. (2012). "Respiratory outbreak of Mycobacterium abscessus subspecies massiliense in a lung transplant and cystic fibrosis center." Am J Respir Crit Care Med **185**(2): 231-232.

Allesen-Holm, M., K. B. Barken, et al. (2006). "A characterization of DNA release in Pseudomonas aeruginosa cultures and biofilms." Mol Microbiol **59**(4): 1114-1128.

Appelberg, R., A. G. Castro, et al. (1995). "Susceptibility of beige mice to Mycobacterium avium: role of neutrophils." Infect Immun **63**(9): 3381-3387.

Appelberg, R. and I. M. Orme (1993). "Effector mechanisms involved in cytokine-mediated bacteriostasis of Mycobacterium avium infections in murine macrophages." Immunology **80**(3): 352-359.

Asally, M., M. Kittisopikul, et al. (2012). "Localized cell death focuses mechanical forces during 3D patterning in a biofilm." Proc Natl Acad Sci U S A **109**(46): 18891-18896.

Aung, T. T., J. Y. Hoong, et al. (2015). "Biofilms of pathogenic nontuberculous mycobacteria targeted by new therapeutic approaches." Antimicrob Agents Chemother.

Babrak, L., L. Danelishvili, et al. (2015). "Microaggregate-associated protein involved in invasion of epithelial cells by Mycobacterium avium subsp. hominissuis." Virulence **6**(7): 694-703.

Babrak, L., L. Danelishvili, et al. (2015). "The environment of "Mycobacterium avium subsp. hominissuis" microaggregates induces synthesis of small proteins associated with efficient infection of respiratory epithelial cells." Infect Immun **83**(2): 625-636.

Balcewicz-Sablinska, M. K., H. Gan, et al. (1999). "Interleukin 10 produced by macrophages inoculated with Mycobacterium avium attenuates mycobacteria-induced apoptosis by reduction of TNF-alpha activity." J Infect Dis **180**(4): 1230-1237.

Bardarov, S., J. Kriakov, et al. (1997). "Conditionally replicating mycobacteriophages: a system for transposon delivery to Mycobacterium tuberculosis." Proc Natl Acad Sci U S A **94**(20): 10961-10966.

Barnes, A. M., K. S. Ballering, et al. (2012). "Enterococcus faecalis produces abundant extracellular structures containing DNA in the absence of cell lysis during early biofilm formation." MBio **3**(4): e00193-00112.

Begg, K. J., S. J. Dewar, et al. (1995). "A new Escherichia coli cell division gene, ftsK." J Bacteriol **177**(21): 6211-6222.

Begun, J., J. M. Gaiani, et al. (2007). "Staphylococcal biofilm exopolysaccharide protects against Caenorhabditis elegans immune defenses." PLoS Pathog **3**(4): e57.

Ben Salah, I. and M. Drancourt (2010). "Surviving within the amoebal exocyst: the Mycobacterium avium complex paradigm." BMC Microbiol **10**: 99.

Bermudez, L. E. (1993). "Differential mechanisms of intracellular killing of Mycobacterium avium and Listeria monocytogenes by activated human and murine macrophages. The role of nitric oxide." Clin Exp Immunol **91**(2): 277-281.

Bermudez, L. E., M. Petrofsky, et al. (1992). "An animal model of Mycobacterium avium complex disseminated infection after colonization of the intestinal tract." J Infect Dis **165**(1): 75-79.

Bermudez, L. E., M. Petrofsky, et al. (1998). "Treatment with recombinant granulocyte colony-stimulating factor (Filgrastin) stimulates neutrophils and tissue macrophages and induces an effective non-specific response against Mycobacterium avium in mice." Immunology **94**(3): 297-303.

Bermudez, L. E., K. Shelton, et al. (1995). "Comparison of the ability of Mycobacterium avium, M. smegmatis and M. tuberculosis to invade and replicate within HEp-2 epithelial cells." Tuber Lung Dis **76**(3): 240-247.

Bermudez, L. E., M. Wu, et al. (1995). "Interleukin-12-stimulated natural killer cells can activate human macrophages to inhibit growth of Mycobacterium avium." Infect Immun **63**(10): 4099-4104.

Bermudez, L. E. and L. S. Young (1988). "Tumor necrosis factor, alone or in combination with IL-2, but not IFN-gamma, is associated with macrophage killing of Mycobacterium avium complex." J Immunol **140**(9): 3006-3013.

Bermudez, L. E. and L. S. Young (1990). "Killing of Mycobacterium avium: insights provided by the use of recombinant cytokines." Res Microbiol **141**(2): 241-243.

Bermudez, L. E. and L. S. Young (1990). "Recombinant granulocyte-macrophage colony-stimulating factor activates human macrophages to inhibit growth or kill Mycobacterium avium complex." J Leukoc Biol **48**(1): 67-73.

Bermudez, L. E. and L. S. Young (1991). "Natural killer cell-dependent mycobacteriostatic and mycobactericidal activity in human macrophages." J Immunol **146**(1): 265-270.

Bermudez, L. E. and L. S. Young (1994). "Factors affecting invasion of HT-29 and HEp-2 epithelial cells by organisms of the Mycobacterium avium complex." Infect Immun **62**(5): 2021-2026.

Bermudez, L. E., L. S. Young, et al. (1991). "Interaction of Mycobacterium avium complex with human macrophages: roles of membrane receptors and serum proteins." Infect Immun **59**(5): 1697-1702.

Bockelmann, U., A. Janke, et al. (2006). "Bacterial extracellular DNA forming a defined network-like structure." FEMS Microbiol Lett **262**(1): 31-38.

Boleij, A., R. M. Schaeps, et al. (2009). "Surface-exposed histone-like protein a modulates adherence of Streptococcus gallolyticus to colon adenocarcinoma cells." Infect Immun **77**(12): 5519-5527.

Brinkmann, V. and A. Zychlinsky (2012). "Neutrophil extracellular traps: is immunity the second function of chromatin?" J Cell Biol **198**(5): 773-783.

Brown-Elliott, B. A., D. E. Griffith, et al. (2002). "Newly described or emerging human species of nontuberculous mycobacteria." Infect Dis Clin North Am **16**(1): 187-220.

Bryant, J. M., D. M. Grogono, et al. (2013). "Whole-genome sequencing to identify transmission of Mycobacterium abscessus between patients with cystic fibrosis: a retrospective cohort study." Lancet **381**(9877): 1551-1560.

Bryceson, Y. T., M. E. March, et al. (2006). "Activation, coactivation, and costimulation of resting human natural killer cells." Immunol Rev **214**: 73-91.

Burghout, P., A. Zomer, et al. (2013). "Streptococcus pneumoniae folate biosynthesis responds to environmental CO2 levels." J Bacteriol **195**(7): 1573-1582.

Camacho, L. R., D. Ensergueix, et al. (1999). "Identification of a virulence gene cluster of Mycobacterium tuberculosis by signature-tagged transposon mutagenesis." Mol Microbiol **34**(2): 257-267.

Carta, F., A. Maresca, et al. (2009). "Carbonic anhydrase inhibitors. Characterization and inhibition studies of the most active beta-carbonic anhydrase from Mycobacterium tuberculosis, Rv3588c." Bioorg Med Chem Lett **19**(23): 6649-6654.

Carter, G., M. Wu, et al. (2003). "Characterization of biofilm formation by clinical isolates of Mycobacterium avium." J Med Microbiol **52**(Pt 9): 747-752.

Chen, J. M., G. J. German, et al. (2006). "Roles of Lsr2 in colony morphology and biofilm formation of Mycobacterium smegmatis." J Bacteriol **188**(2): 633-641.

Cirillo, J. D., S. Falkow, et al. (1997). "Interaction of Mycobacterium avium with environmental amoebae enhances virulence." Infect Immun **65**(9): 3759-3767.

Conover, M. S., M. Mishra, et al. (2011). "Extracellular DNA is essential for maintaining Bordetella biofilm integrity on abiotic surfaces and in the upper respiratory tract of mice." PLoS One **6**(2): e16861.

Covert, T. C., M. R. Rodgers, et al. (1999). "Occurrence of nontuberculous mycobacteria in environmental samples." Appl Environ Microbiol **65**(6): 2492-2496.

Crowle, A. J., R. Dahl, et al. (1991). "Evidence that vesicles containing living, virulent Mycobacterium tuberculosis or Mycobacterium avium in cultured human macrophages are not acidic." Infect Immun **59**(5): 1823-1831.

Danelishvilli, L. and L. E. Bermudez (2003). "Role of Type I Cytokines in Host Defense Against Mycobacterium avium Infection." Current Pharmaceutical Design **9**(1): 61-65.

Das, T., B. P. Krom, et al. (2011). "DNA-mediated bacterial aggregation is dictated by acid-base interactions." Soft Matter **7**(6): 2927-2935.

Das, T., S. K. Kutty, et al. (2013). "Pyocyanin facilitates extracellular DNA binding to Pseudomonas aeruginosa influencing cell surface properties and aggregation." PLoS One **8**(3): e58299.

Das, T. and M. Manefield (2012). "Pyocyanin promotes extracellular DNA release in Pseudomonas aeruginosa." PLoS One **7**(10): e46718.

Daw, K., A. S. Baghdayan, et al. (2012). "Biofilm and planktonic Enterococcus faecalis elicit different responses from host phagocytes in vitro." FEMS Immunol Med Microbiol **65**(2): 270-282.

Doi, T., M. Ando, et al. (1993). "Resistance to nitric oxide in Mycobacterium avium complex and its implication in pathogenesis." Infect Immun **61**(5): 1980-1989.

Early, J., K. Fischer, et al. (2011). "Mycobacterium avium uses apoptotic macrophages as tools for spreading." Microb Pathog **50**(2): 132-139.

Falkinham, J. O., 3rd (1996). "Epidemiology of infection by nontuberculous mycobacteria." Clin Microbiol Rev **9**(2): 177-215.

Falkinham, J. O., 3rd (2011). "Nontuberculous mycobacteria from household plumbing of patients with nontuberculous mycobacteria disease." Emerg Infect Dis **17**(3): 419-424.

Falkinham, J. O., 3rd, M. D. Iseman, et al. (2008). "Mycobacterium avium in a shower linked to pulmonary disease." J Water Health **6**(2): 209-213.

Falkinham, J. O., 3rd, C. D. Norton, et al. (2001). "Factors influencing numbers of Mycobacterium avium, Mycobacterium intracellulare, and other Mycobacteria in drinking water distribution systems." Appl Environ Microbiol **67**(3): 1225-1231.

Feazel, L. M., L. K. Baumgartner, et al. (2009). "Opportunistic pathogens enriched in showerhead biofilms." Proc Natl Acad Sci U S A **106**(38): 16393-16399.

Feller, M., K. Huwiler, et al. (2007). "Mycobacterium avium subspecies paratuberculosis and Crohn's disease: a systematic review and meta-analysis." Lancet Infect Dis **7**(9): 607-613.

Flemming, H. C. and J. Wingender (2010). "The biofilm matrix." Nat Rev Microbiol **8**(9): 623-633.

Freeman, R., H. Geier, et al. (2006). "Roles for cell wall glycopeptidolipid in surface adherence and planktonic dispersal of Mycobacterium avium." Appl Environ Microbiol **72**(12): 7554-7558.

Frehel, C., C. de Chastellier, et al. (1986). "Evidence for inhibition of fusion of lysosomal and prelysosomal compartments with phagosomes in macrophages infected with pathogenic Mycobacterium avium." Infect Immun **52**(1): 252-262.

Garcia-Contreras, L., J. Fiegel, et al. (2007). "Inhaled large porous particles of capreomycin for treatment of tuberculosis in a guinea pig model." Antimicrob Agents Chemother **51**(8): 2830-2836.

Garcia-Contreras, L., V. Sethuraman, et al. (2006). "Evaluation of dosing regimen of respirable rifampicin biodegradable microspheres in the treatment of tuberculosis in the guinea pig." J Antimicrob Chemother **58**(5): 980-986.

Gloag, E. S., L. Turnbull, et al. (2013). "Self-organization of bacterial biofilms is facilitated by extracellular DNA." Proc Natl Acad Sci U S A **110**(28): 11541-11546.

Godeke, J., M. Heun, et al. (2011). "Roles of two Shewanella oneidensis MR-1 extracellular endonucleases." Appl Environ Microbiol **77**(15): 5342-5351.

Gomes, M. S., M. Florido, et al. (1999). "Improved clearance of Mycobacterium avium upon disruption of the inducible nitric oxide synthase gene." J Immunol **162**(11): 6734-6739.

Gonzalez-Juarrero, M., L. K. Woolhiser, et al. (2012). "Mouse model for efficacy testing of antituberculosis agents via intrapulmonary delivery." Antimicrob Agents Chemother **56**(7): 3957-3959.

Goodman, S. D., K. P. Obergfell, et al. (2011). "Biofilms can be dispersed by focusing the immune system on a common family of bacterial nucleoid-associated proteins." Mucosal Immunol **4**(6): 625-637.

Grande, R., M. Di Giulio, et al. (2011). "Extracellular DNA in Helicobacter pylori biofilm: a backstairs rumour." J Appl Microbiol **110**(2): 490-498.

Greendyke, R. and T. F. Byrd (2008). "Differential antibiotic susceptibility of Mycobacterium abscessus variants in biofilms and macrophages compared to that of planktonic bacteria." Antimicrob Agents Chemother **52**(6): 2019-2026.

Griffith, D. E. (2011). "The talking Mycobacterium abscessus blues." Clin Infect Dis **52**(5): 572-574.

Griffith, D. E., T. Aksamit, et al. (2007). "An official ATS/IDSA statement: diagnosis, treatment, and prevention of nontuberculous mycobacterial diseases." Am J Respir Crit Care Med **175**(4): 367-416.

Guerin, I. and C. de Chastellier (2000). "Pathogenic mycobacteria disrupt the macrophage actin filament network." Infect Immun **68**(5): 2655-2662.

Halstrom, S., P. Price, et al. (2015). "Review: Environmental mycobacteria as a cause of human infection." International Journal of Mycobacteriology **4**(2): 81-91.

Hammerstrom, T. G., J. H. Roh, et al. (2011). "Bacillus anthracis virulence regulator AtxA: oligomeric state, function and CO(2) -signalling." Mol Microbiol **82**(3): 634-647.

Hannan, S., D. Ready, et al. (2010). "Transfer of antibiotic resistance by transformation with eDNA within oral biofilms." FEMS Immunol Med Microbiol **59**(3): 345-349.

Harmsen, M., M. Lappann, et al. (2010). "Role of extracellular DNA during biofilm formation by Listeria monocytogenes." Appl Environ Microbiol **76**(7): 2271-2279.

Harriff, M. and L. E. Bermudez (2009). "Environmental amoebae and mycobacterial pathogenesis." Methods Mol Biol **465**: 433-442.

Hartmann, P., R. Becker, et al. (2001). "Phagocytosis and killing of Mycobacterium avium complex by human neutrophils." J Leukoc Biol **69**(3): 397-404.

Hellyer, T. J., I. N. Brown, et al. (1991). "Plasmid analysis of Mycobacterium avium-intracellulare (MAI) isolated in the United Kingdom from patients with and without AIDS." J Med Microbiol **34**(4): 225-231.

Henkle, E., K. Hedberg, et al. (2015). "Population-based Incidence of Pulmonary Nontuberculous Mycobacterial Disease in Oregon 2007 to 2012." Ann Am Thorac Soc **12**(5): 642-647.

Hoefsloot, W., J. van Ingen, et al. (2013). "The geographic diversity of nontuberculous mycobacteria isolated from pulmonary samples: an NTM-NET collaborative study." Eur Respir J **42**(6): 1604-1613.

Honda, J. R., V. Knight, et al. (2015). "Pathogenesis and risk factors for nontuberculous mycobacterial lung disease." Clin Chest Med **36**(1): 1-11.

Howard, S. T., E. Rhoades, et al. (2006). "Spontaneous reversion of Mycobacterium abscessus from a smooth to a rough morphotype is associated with reduced expression of glycopeptidolipid and reacquisition of an invasive phenotype." Microbiology **152**(Pt 6): 1581-1590.

Hymes, S. R., T. M. Randis, et al. (2013). "DNase inhibits Gardnerella vaginalis biofilms in vitro and in vivo." J Infect Dis **207**(10): 1491-1497.

Ignatov, D., E. Kondratieva, et al. (2012). "Mycobacterium avium-triggered diseases: pathogenomics." Cell Microbiol **14**(6): 808-818.

Jesaitis, A. J., M. J. Franklin, et al. (2003). "Compromised host defense on Pseudomonas aeruginosa biofilms: characterization of neutrophil and biofilm interactions." J Immunol **171**(8): 4329-4339.

Johnson, B. K., C. J. Colvin, et al. (2015). "The Carbonic Anhydrase Inhibitor Ethoxzolamide Inhibits the Mycobacterium tuberculosis PhoPR Regulon and Esx-1 Secretion and Attenuates Virulence." Antimicrob Agents Chemother **59**(8): 4436-4445.

Johnson, M. M. and J. A. Odell (2014). "Nontuberculous mycobacterial pulmonary infections." J Thorac Dis **6**(3): 210-220.

Jurcisek, J. A. and L. O. Bakaletz (2007). "Biofilms formed by nontypeable Haemophilus influenzae in vivo contain both double-stranded DNA and type IV pilin protein." J Bacteriol **189**(10): 3868-3875.

Kahana, L. M., J. M. Kay, et al. (1997). "Mycobacterium avium complex infection in an immunocompetent young adult related to hot tub exposure." Chest **111**(1): 242-245.

Kaplan, J. B., K. LoVetri, et al. (2012). "Recombinant human DNase I decreases biofilm and increases antimicrobial susceptibility in staphylococci." J Antibiot (Tokyo) **65**(2): 73-77.

Karakousis, P. C., R. D. Moore, et al. (2004). "Mycobacterium avium complex in patients with HIV infection in the era of highly active antiretroviral therapy." Lancet Infect Dis **4**(9): 557-565.

Kiehn, T. E., F. F. Edwards, et al. (1985). "Infections caused by Mycobacterium avium complex in immunocompromised patients: diagnosis by blood culture and fecal examination, antimicrobial susceptibility tests, and morphological and seroagglutination characteristics." J Clin Microbiol **21**(2): 168-173.

Kieser, K. J. and E. J. Rubin (2014). "How sisters grow apart: mycobacterial growth and division." Nat Rev Microbiol **12**(8): 550-562.

Kirschner, R. A., Jr., B. C. Parker, et al. (1992). "Epidemiology of infection by nontuberculous mycobacteria. Mycobacterium avium, Mycobacterium intracellulare, and Mycobacterium scrofulaceum in acid, brown-water swamps of the southeastern United States and their association with environmental variables." Am Rev Respir Dis **145**(2 Pt 1): 271-275.

Kobashi, Y., K. Yoshida, et al. (2006). "Relationship between clinical efficacy of treatment of pulmonary Mycobacterium avium complex disease and drug-sensitivity testing of Mycobacterium avium complex isolates." J Infect Chemother **12**(4): 195-202.

Kullavanijaya, P., S. Sirimachan, et al. (1997). "Primary cutaneous infection with Mycobacterium avium intracellulare complex resembling lupus vulgaris." Br J Dermatol **136**(2): 264-266.

Kunisch, R., E. Kamal, et al. (2012). "The role of the mycobacterial DNA-binding protein 1 (MDP1) from Mycobacterium bovis BCG in host cell interaction." BMC Microbiol **12**: 165.

Lai, C. C., C. K. Tan, et al. (2010). "Increasing incidence of nontuberculous mycobacteria, Taiwan, 2000-2008." Emerg Infect Dis **16**(2): 294-296.

Lappann, M., H. Claus, et al. (2010). "A dual role of extracellular DNA during biofilm formation of Neisseria meningitidis." Mol Microbiol **75**(6): 1355-1371.

Lavollay, M., M. Arthur, et al. (2008). "The peptidoglycan of stationary-phase Mycobacterium tuberculosis predominantly contains cross-links generated by L,D-transpeptidation." J Bacteriol **190**(12): 4360-4366.

Le Cabec, V., C. Cols, et al. (2000). "Nonopsonic phagocytosis of zymosan and Mycobacterium kansasii by CR3 (CD11b/CD18) involves distinct molecular determinants and is or is not coupled with NADPH oxidase activation." Infect Immun **68**(8): 4736-4745.

Lee, E. S., T. H. Yoon, et al. (2010). "Inactivation of environmental mycobacteria by free chlorine and UV." Water Res **44**(5): 1329-1334.

Liao, S., M. I. Klein, et al. (2014). "Streptococcus mutans extracellular DNA is upregulated during growth in biofilms, actively released via membrane vesicles, and influenced by components of the protein secretion machinery." J Bacteriol **196**(13): 2355-2366.

Liu, R., Z. Yu, et al. (2012). "Pyrosequencing analysis of eukaryotic and bacterial communities in faucet biofilms." Sci Total Environ **435-436**: 124-131.

Lumb, R., R. Stapledon, et al. (2004). "Investigation of spa pools associated with lung disorders caused by Mycobacterium avium complex in immunocompetent adults." Appl Environ Microbiol **70**(8): 4906-4910.

Maddox, S. M., P. S. Coburn, et al. (2012). "Transcriptional regulator PerA influences biofilm-associated, platelet binding, and metabolic gene expression in Enterococcus faecalis." PLoS One **7**(4): e34398.

Mangione, E. J., G. Huitt, et al. (2001). "Nontuberculous mycobacterial disease following hot tub exposure." Emerg Infect Dis **7**(6): 1039-1042.

Manzanillo, P. S., M. U. Shiloh, et al. (2012). "Mycobacterium tuberculosis activates the DNA-dependent cytosolic surveillance pathway within macrophages." Cell Host Microbe **11**(5): 469-480.

Marsollier, L., P. Brodin, et al. (2007). "Impact of Mycobacterium ulcerans biofilm on transmissibility to ecological niches and Buruli ulcer pathogenesis." PLoS Pathog **3**(5): e62.

Martinez, A., S. Torello, et al. (1999). "Sliding motility in mycobacteria." J Bacteriol **181**(23): 7331-7338.

McNabe, M., R. Tennant, et al. (2011). "Mycobacterium avium ssp. hominissuis biofilm is composed of distinct phenotypes and influenced by the presence of antimicrobials." Clin Microbiol Infect **17**(5): 697-703.

McNamara, M., S. C. Tzeng, et al. (2012). "Surface proteome of "Mycobacterium avium subsp. hominissuis" during the early stages of macrophage infection." Infect Immun **80**(5): 1868-1880.

Medjahed, H. and J. M. Reyrat (2009). "Construction of Mycobacterium abscessus defined glycopeptidolipid mutants: comparison of genetic tools." Appl Environ Microbiol **75**(5): 1331-1338.

Mijs, W., P. de Haas, et al. (2002). "Molecular evidence to support a proposal to reserve the designation Mycobacterium avium subsp. avium for bird-type isolates and 'M. avium subsp. hominissuis' for the human/porcine type of M. avium." Int J Syst Evol Microbiol **52**(Pt 5): 1505-1518.

Mogensen, E. G., G. Janbon, et al. (2006). "Cryptococcus neoformans senses CO2 through the carbonic anhydrase Can2 and the adenylyl cyclase Cac1." Eukaryot Cell **5**(1): 103-111.

Moscoso, M., E. Garcia, et al. (2006). "Biofilm formation by Streptococcus pneumoniae: role of choline, extracellular DNA, and capsular polysaccharide in microbial accretion." J Bacteriol **188**(22): 7785-7795.

Mullis, S. N. and J. O. Falkinham, 3rd (2013). "Adherence and biofilm formation of Mycobacterium avium, Mycobacterium intracellulare and Mycobacterium abscessus to household plumbing materials." J Appl Microbiol **115**(3): 908-914.

Nash, K. A., B. A. Brown-Elliott, et al. (2009). "A novel gene, erm(41), confers inducible macrolide resistance to clinical isolates of Mycobacterium abscessus but is absent from Mycobacterium chelonae." Antimicrob Agents Chemother **53**(4): 1367-1376.

Nessar, R., J. M. Reyrat, et al. (2011). "Deletion of the mmpL4b gene in the Mycobacterium abscessus glycopeptidolipid biosynthetic pathway results in loss of surface colonization capability, but enhanced ability to replicate in human macrophages and stimulate their innate immune response." Microbiology **157**(Pt 4): 1187-1195.

Nishiuchi, Y., R. Maekura, et al. (2007). "The recovery of Mycobacterium avium-intracellulare complex (MAC) from the residential bathrooms of patients with pulmonary MAC." Clin Infect Dis **45**(3): 347-351.

Nishiuchi, Y., A. Tamura, et al. (2009). "Mycobacterium avium complex organisms predominantly colonize in the bathtub inlets of patients' bathrooms." Jpn J Infect Dis **62**(3): 182-186.

Noguchi, H., M. Hiruma, et al. (1998). "A pediatric case of atypical Mycobacterium avium infection of the skin." J Dermatol **25**(6): 384-390.

Novotny, L. A., A. O. Amer, et al. (2013). "Structural stability of Burkholderia cenocepacia biofilms is reliant on eDNA structure and presence of a bacterial nucleic acid binding protein." PLoS One **8**(6): e67629.

Oberley-Deegan, R. E., Y. M. Lee, et al. (2009). "The antioxidant mimetic, MnTE-2-PyP, reduces intracellular growth of Mycobacterium abscessus." Am J Respir Cell Mol Biol **41**(2): 170-178.

Oh, Y. K. and R. M. Straubinger (1996). "Intracellular fate of Mycobacterium avium: use of dual-label spectrofluorometry to investigate the influence of bacterial viability and opsonization on phagosomal pH and phagosome-lysosome interaction." Infect Immun **64**(1): 319-325.

Ojha, A., M. Anand, et al. (2005). "GroEL1: a dedicated chaperone involved in mycolic acid biosynthesis during biofilm formation in mycobacteria." Cell **123**(5): 861-873.

Ojha, A. K., A. D. Baughn, et al. (2008). "Growth of Mycobacterium tuberculosis biofilms containing free mycolic acids and harbouring drug-tolerant bacteria." Mol Microbiol **69**(1): 164-174.

Okshevsky, M., V. R. Regina, et al. (2015). "Extracellular DNA as a target for biofilm control." Curr Opin Biotechnol **33**: 73-80.

Orange, J. S. and Z. K. Ballas (2006). "Natural killer cells in human health and disease." Clin Immunol **118**(1): 1-10.

Orme, I. M. and D. J. Ordway (2014). "Host response to nontuberculous mycobacterial infections of current clinical importance." Infect Immun **82**(9): 3516-3522.

Parks, Q. M., R. L. Young, et al. (2009). "Neutrophil enhancement of Pseudomonas aeruginosa biofilm development: human F-actin and DNA as targets for therapy." J Med Microbiol **58**(Pt 4): 492-502.

Peyron, P., C. Bordier, et al. (2000). "Nonopsonic phagocytosis of Mycobacterium kansasii by human neutrophils depends on cholesterol and is mediated by CR3 associated with glycosylphosphatidylinositol-anchored proteins." J Immunol **165**(9): 5186-5191.

Pillai, S. R., B. M. Jayarao, et al. (2001). "Identification and sub-typing of Mycobacterium avium subsp. paratuberculosis and Mycobacterium avium subsp. avium by randomly amplified polymorphic DNA." Vet Microbiol **79**(3): 275-284.

Prados-Rosales, R., A. Baena, et al. (2011). "Mycobacteria release active membrane vesicles that modulate immune responses in a TLR2-dependent manner in mice." J Clin Invest **121**(4): 1471-1483.

Prod'hom, G., B. Lagier, et al. (1998). "A reliable amplification technique for the characterization of genomic DNA sequences flanking insertion sequences." FEMS Microbiol Lett **158**(1): 75-81.

Qin, Z., Y. Ou, et al. (2007). "Role of autolysin-mediated DNA release in biofilm formation of Staphylococcus epidermidis." Microbiology **153**(Pt 7): 2083-2092.

Qvist, T., S. Eickhardt, et al. (2015). "Chronic pulmonary disease with Mycobacterium abscessus complex is a biofilm infection." Eur Respir J **46**(6): 1823-1826.

Ramasoota, P., N. Chansiripornchai, et al. (2001). "Comparison of Mycobacterium avium complex (MAC) strains from pigs and humans in Sweden by random amplified polymorphic DNA (RAPD) using standardized reagents." Vet Microbiol **78**(3): 251-259.

Rao, S. P., K. Ogata, et al. (1993). "Mycobacterium avium-M. intracellulare binds to the integrin receptor alpha v beta 3 on human monocytes and monocyte-derived macrophages." Infect Immun **61**(2): 663-670.

Recht, J. and R. Kolter (2001). "Glycopeptidolipid acetylation affects sliding motility and biofilm formation in Mycobacterium smegmatis." J Bacteriol **183**(19): 5718-5724.

Recht, J., A. Martinez, et al. (2000). "Genetic analysis of sliding motility in Mycobacterium smegmatis." J Bacteriol **182**(15): 4348-4351.

Recht, J., A. Martinez, et al. (2001). "[Sliding motility and biofilm formation in mycobacteria]." Acta Cient Venez **52 Suppl 1**: 45-49.

Reddy, V. M. and B. Kumar (2000). "Interaction of Mycobacterium avium complex with human respiratory epithelial cells." J Infect Dis **181**(3): 1189-1193.

Ren, H., L. G. Dover, et al. (2007). "Identification of the lipooligosaccharide biosynthetic gene cluster from Mycobacterium marinum." Mol Microbiol **63**(5): 1345-1359.

Rice, K. C., E. E. Mann, et al. (2007). "The cidA murein hydrolase regulator contributes to DNA release and biofilm development in Staphylococcus aureus." Proc Natl Acad Sci U S A **104**(19): 8113-8118.

Ricketts, W. M., T. C. O'Shaughnessy, et al. (2014). "Human-to-human transmission of Mycobacterium kansasii or victims of a shared source?" Eur Respir J **44**(4): 1085-1087.

Roecklein, J. A., R. P. Swartz, et al. (1992). "Nonopsonic uptake of Mycobacterium avium complex by human monocytes and alveolar macrophages." J Lab Clin Med **119**(6): 772-781.

Rose, S. J., L. M. Babrak, et al. (2015). "Mycobacterium avium Possesses Extracellular DNA that Contributes to Biofilm Formation, Structural Integrity, and Tolerance to Antibiotics." PLoS One **10**(5): e0128772.

Rose, S. J. and L. E. Bermudez (2014). "Mycobacterium avium biofilm attenuates mononuclear phagocyte function by triggering hyperstimulation and apoptosis during early infection." Infect Immun **82**(1): 405-412.

Rose, S. J., M. E. Neville, et al. (2014). "Delivery of aerosolized liposomal amikacin as a novel approach for the treatment of nontuberculous mycobacteria in an experimental model of pulmonary infection." PLoS One **9**(9): e108703.

Russell, D. G., J. Dant, et al. (1996). "Mycobacterium avium- and Mycobacterium tuberculosis-containing vacuoles are dynamic, fusion-competent vesicles that are accessible to glycosphingolipids from the host cell plasmalemma." J Immunol **156**(12): 4764-4773.

Sahu, P. K., P. S. Iyer, et al. (2012). "Characterization of eDNA from the clinical strain Acinetobacter baumannii AIIMS 7 and its role in biofilm formation." ScientificWorldJournal **2012**: 973436.

Salah, I. B., E. Ghigo, et al. (2009). "Free-living amoebae, a training field for macrophage resistance of mycobacteria." Clin Microbiol Infect **15**(10): 894-905.

Sangari, F. J., J. Goodman, et al. (2001). "Mycobacterium avium invades the intestinal mucosa primarily by interacting with enterocytes." Infect Immun **69**(3): 1515-1520.

Sani, M., E. N. Houben, et al. (2010). "Direct visualization by cryo-EM of the mycobacterial capsular layer: a labile structure containing ESX-1-secreted proteins." PLoS Pathog **6**(3): e1000794.

Sarmento, A. and R. Appelberg (1996). "Involvement of reactive oxygen intermediates in tumor necrosis factor alpha-dependent bacteriostasis of Mycobacterium avium." Infect Immun **64**(8): 3224-3230.

Sarmento, A. M. and R. Appelberg (1995). "Relationship between virulence of Mycobacterium avium strains and induction of tumor necrosis factor alpha production in infected mice and in in vitro-cultured mouse macrophages." Infect Immun **63**(10): 3759-3764.

Sassetti, C. M., D. H. Boyd, et al. (2001). "Comprehensive identification of conditionally essential genes in mycobacteria." Proc Natl Acad Sci U S A **98**(22): 12712-12717.

Saunders, B. M. and C. Cheers (1996). "Intranasal infection of beige mice with Mycobacterium avium complex: role of neutrophils and natural killer cells." Infect Immun **64**(10): 4236-4241.

Schulze-Robbecke, R. and K. Buchholtz (1992). "Heat susceptibility of aquatic mycobacteria." Appl Environ Microbiol **58**(6): 1869-1873.

Seper, A., V. H. Fengler, et al. (2011). "Extracellular nucleases and extracellular DNA play important roles in Vibrio cholerae biofilm formation." Mol Microbiol **82**(4): 1015-1037.

Shao, Y., C. Chen, et al. (2015). "The epidemiology and geographic distribution of nontuberculous mycobacteria clinical isolates from sputum samples in the eastern region of China." PLoS Negl Trop Dis **9**(3): e0003623.

Silva, M. T., M. N. Silva, et al. (1989). "Neutrophil-macrophage cooperation in the host defence against mycobacterial infections." Microb Pathog **6**(5): 369-380.

Skriwan, C., M. Fajardo, et al. (2002). "Various bacterial pathogens and symbionts infect the amoeba Dictyostelium discoideum." Int J Med Microbiol **291**(8): 615-624.

Slosarek, M., M. Kubin, et al. (1993). "Water-borne household infections due to Mycobacterium xenopi." Cent Eur J Public Health **1**(2): 78-80.

Steed, K. A. and J. O. Falkinham, 3rd (2006). "Effect of growth in biofilms on chlorine susceptibility of Mycobacterium avium and Mycobacterium intracellulare." Appl Environ Microbiol **72**(6): 4007-4011.

Stoodley, P., K. Sauer, et al. (2002). "Biofilms as complex differentiated communities." Annu Rev Microbiol **56**: 187-209.

Stover, C. K., V. F. de la Cruz, et al. (1991). "New use of BCG for recombinant vaccines." Nature **351**(6326): 456-460.

Sturgill-Koszycki, S., U. E. Schaible, et al. (1996). "Mycobacterium-containing phagosomes are accessible to early endosomes and reflect a transitional state in normal phagosome biogenesis." EMBO J **15**(24): 6960-6968.

Sturgill-Koszycki, S., P. H. Schlesinger, et al. (1994). "Lack of acidification in Mycobacterium phagosomes produced by exclusion of the vesicular proton-ATPase." Science **263**(5147): 678-681.

Sugita, Y., N. Ishii, et al. (2000). "Familial cluster of cutaneous Mycobacterium avium infection resulting from use of a circulating, constantly heated bath water system." Br J Dermatol **142**(4): 789-793.

Swart, R. M., J. van Ingen, et al. (2009). "Nontuberculous mycobacteria infection and tumor necrosis factor-alpha antagonists." Emerg Infect Dis **15**(10): 1700-1701.

Swartz, R. P., D. Naai, et al. (1988). "Differences in uptake of mycobacteria by human monocytes: a role for complement." Infect Immun **56**(9): 2223-2227.

Takayama, K., C. Wang, et al. (2005). "Pathway to synthesis and processing of mycolic acids in Mycobacterium tuberculosis." Clin Microbiol Rev **18**(1): 81-101.

Taylor, R. H., J. O. Falkinham, 3rd, et al. (2000). "Chlorine, chloramine, chlorine dioxide, and ozone susceptibility of Mycobacterium avium." Appl Environ Microbiol **66**(4): 1702-1705.

Tetz, G. V., N. K. Artemenko, et al. (2009). "Effect of DNase and antibiotics on biofilm characteristics." Antimicrob Agents Chemother **53**(3): 1204-1209.

Thegerstrom, J., V. Friman, et al. (2008). "Clinical features and incidence of Mycobacterium avium infections in children." Scand J Infect Dis **40**(6-7): 481-486.

Thomas, V. C., L. R. Thurlow, et al. (2008). "Regulation of autolysis-dependent extracellular DNA release by Enterococcus faecalis extracellular proteases influences biofilm development." J Bacteriol **190**(16): 5690-5698.

Thomson, R., C. Tolson, et al. (2013). "Isolation of nontuberculous mycobacteria (NTM) from household water and shower aerosols in patients with pulmonary disease caused by NTM." J Clin Microbiol **51**(9): 3006-3011.

Thomson, R., C. Tolson, et al. (2013). "Mycobacterium abscessus isolated from municipal water - a potential source of human infection." BMC Infect Dis **13**: 241.

Thurlow, L. R., M. L. Hanke, et al. (2011). "Staphylococcus aureus biofilms prevent macrophage phagocytosis and attenuate inflammation in vivo." J Immunol **186**(11): 6585-6596.

Tortoli, E. (2003). "Impact of genotypic studies on mycobacterial taxonomy: the new mycobacteria of the 1990s." Clin Microbiol Rev **16**(2): 319-354.

Torvinen, E., S. Suomalainen, et al. (2004). "Mycobacteria in water and loose deposits of drinking water distribution systems in Finland." Appl Environ Microbiol **70**(4): 1973-1981.

Tuffley, R. E. and J. D. Holbeche (1980). "Isolation of the Mycobacterium avium-M. intracellulare-M. scrofulaceum complex from tank water in Queensland, Australia." Appl Environ Microbiol **39**(1): 48-53.

Turenne, C. Y., D. M. Collins, et al. (2008). "Mycobacterium avium subsp. paratuberculosis and M. avium subsp. avium are independently evolved pathogenic clones of a much broader group of M. avium organisms." J Bacteriol **190**(7): 2479-2487.

van Gennip, M., L. D. Christensen, et al. (2012). "Interactions between polymorphonuclear leukocytes and Pseudomonas aeruginosa biofilms on silicone implants in vivo." Infect Immun **80**(8): 2601-2607.

Vilain, S., J. M. Pretorius, et al. (2009). "DNA as an adhesin: Bacillus cereus requires extracellular DNA to form biofilms." Appl Environ Microbiol **75**(9): 2861-2868.

von Reyn, C. F., J. N. Maslow, et al. (1994). "Persistent colonisation of potable water as a source of Mycobacterium avium infection in AIDS." Lancet **343**(8906): 1137-1141.

Wassermann, R., M. F. Gulen, et al. (2015). "Mycobacterium tuberculosis Differentially Activates cGAS- and Inflammasome-Dependent Intracellular Immune Responses through ESX-1." Cell Host Microbe **17**(6): 799-810.

Weiss, C. H. and J. Glassroth (2012). "Pulmonary disease caused by nontuberculous mycobacteria." Expert Rev Respir Med **6**(6): 597-612; quiz 613.

Whiley, H., A. Keegan, et al. (2012). "Mycobacterium avium complex--the role of potable water in disease transmission." J Appl Microbiol **113**(2): 223-232.

Whitchurch, C. B., T. Tolker-Nielsen, et al. (2002). "Extracellular DNA required for bacterial biofilm formation." Science **295**(5559): 1487.

WHO (2015). Global tuberculosis report, World Health Organization.

Williams, M. M., M. A. Yakrus, et al. (2009). "Structural analysis of biofilm formation by rapidly and slowly growing nontuberculous mycobacteria." Appl Environ Microbiol **75**(7): 2091-2098.

Winters, B. D., N. Ramasubbu, et al. (1993). "Isolation and characterization of a Streptococcus pyogenes protein that binds to basal laminae of human cardiac muscle." Infect Immun **61**(8): 3259-3264.

Winthrop, K., A. Rivera, et al. (2016). "A Rhesus Macaque Model of Pulmonary Nontuberculous Mycobacterial Disease." Am J Respir Cell Mol Biol **54**(2): 170-176.

Winthrop, K. L., E. Chang, et al. (2009). "Nontuberculous mycobacteria infections and anti-tumor necrosis factor-alpha therapy." Emerg Infect Dis **15**(10): 1556-1561.

Winthrop, K. L., E. McNelley, et al. (2010). "Pulmonary nontuberculous mycobacterial disease prevalence and clinical features: an emerging public health disease." Am J Respir Crit Care Med **182**(7): 977-982.

Wu, C. W., S. K. Schmoller, et al. (2009). "A novel cell wall lipopeptide is important for biofilm formation and pathogenicity of Mycobacterium avium subspecies paratuberculosis." Microb Pathog **46**(4): 222-230.

Wu, U. I. and S. M. Holland (2015). "Host susceptibility to non-tuberculous mycobacterial infections." Lancet Infect Dis **15**(8): 968-980.

Yamazaki, Y., L. Danelishvili, et al. (2006). "The ability to form biofilm influences Mycobacterium avium invasion and translocation of bronchial epithelial cells." Cell Microbiol **8**(5): 806-814.

Yamazaki, Y., L. Danelishvili, et al. (2006). "Mycobacterium avium genes associated with the ability to form a biofilm." Appl Environ Microbiol **72**(1): 819-825.

Yang, J., E. Hart, et al. (2008). "Bicarbonate-mediated transcriptional activation of divergent operons by the virulence regulatory protein, RegA, from Citrobacter rodentium." Mol Microbiol **68**(2): 314-327.

Zambrano, M. M. and R. Kolter (2005). "Mycobacterial biofilms: a greasy way to hold it together." Cell **123**(5): 762-764.

Zhang, L., T. A. Ignatowski, et al. (1999). "Streptococcal histone induces murine macrophages To produce interleukin-1 and tumor necrosis factor alpha." Infect Immun **67**(12): 6473-6477.

Appendices

Appendix 1

Delivery of Aerosolized Liposomal Amikacin as a Novel Approach for the Treatment of Nontuberculous Mycobacteria in an Experimental Model of Pulmonary Infection

Sasha J. Rose, Mary E. Neville, Renu Gupta, and Luiz E. Bermudez

PLOS ONE

2014 **9**(9): e108703

PMID 25264757

Abstract

Pulmonary infections caused by nontuberculous mycobacteria (NTM) are an increasing problem in individuals with chronic lung conditions and current therapies are lacking. We investigated the activity of liposomal amikacin for inhalation (LAI) against NTM *in vitro* as well as in a murine model of respiratory infection. Macrophage monolayers were infected with three strains of *Mycobacterium avium*, two strains of *Mycobacterium abscessus*, and exposed to LAI or free amikacin for 4 days before enumerating bacterial survival. Respiratory infection was established in mice by intranasal inoculation with *M. avium* and allowing three weeks for the infection to progress. Three different regimens of inhaled LAI were compared to inhaled saline and parenterally administered free amikacin over a 28 day period. Bacteria recovered from the mice were analyzed for acquired resistance to amikacin. *In vitro*, liposomal amikacin for inhalation was more effective than free amikacin in eliminating both intracellular *M. avium* and *M. abscessus*. *In vivo*, inhaled LAI demonstrated similar effectiveness to a ~25% higher total dose of parenterally administered amikacin at reducing *M. avium* in the lungs when compared to inhaled saline. Additionally, there was no acquired resistance to amikacin observed after the treatment regimen. The data suggest that LAI has the potential to be an effective therapy against NTM respiratory infections in humans.

Introduction

Pulmonary infections caused by nontuberculous mycobacteria (NTM), specifically *Mycobacterium avium* subsp. *hominissuis* (MAH) and *Mycobacterium abscessus* (Ma), are increasing in incidence. MAH infection of the airways (and likely Ma as well), has been associated with the formation of biofilm (Carter, Wu et al. 2003; Yamazaki, Danelishvili et al. 2006; Greendyke and Byrd 2008). Disease in patients with underlying lung pathology, such as cystic fibrosis and bronchiectasis, is especially difficult to treat, because the basic lung condition significantly affects the ability of the host to clear the pathogens. Treatment with macrolides, such as clarithromycin or azithromycin, in combination with ethambutol and rifampin is typically effective against MAH pulmonary infections (Griffith, Aksamit et al. 2007; Johnson and Odell 2014). Streptomycin and amikacin can also be supplemented with the MAH regimen unless tolerability and toxicity become an issue. Macrolides are generally ineffective against Ma because it possesses *erm*, an inducible macrolide-resistance gene (Nash, Brown-Elliott et al. 2009; Griffith 2011). Ma pulmonary infection is typically treated with cefoxitime, imipenem, and amikacin. Newer drugs, such as tigecycline and linezolid, show good *in vitro* effectiveness against Ma and are used in some instances (Griffith, Aksamit et al. 2007). The described treatment regimens for MAH and Ma are very long, many of the drugs require parenteral administration, and bacterial resistance to these drugs is a concern. Therefore, the limited activity of regimens and the lack of alternative therapeutic options make the treatment of these infections challenging.

NTM reside and multiply in both macrophages in the airway submucosa as well as in alveolar macrophages, which requires that compounds achieve bacteriostatic or bactericidal activity intracellularly (Iseman 1989; Kilby, Gilligan et al. 1992). Being able to deliver high concentrations of a compound intracellularly might be crucial for the ability to effectively treat the infection (Horsburgh 1991; Griffith, Aksamit et al. 2007). Liposomes are an attractive drug delivery system that can allow drugs with typically poor membrane penetration (e.g. aminoglycosides) to accomplish these objective.

The use of aminoglycosides encapsulated in liposomes has been shown to be effective as anti-*M. avium* both in macrophages *in vitro* and in mice when delivered intravenously (Bermudez, Yau-Young et al. 1990). Liposomal encapsulation also permits sustained release of high concentrations of the aminoglycoside, which translates into less frequent administration. Amikacin is particularly active against both MAH and Ma, but the narrow toxicity index for the compound and the need for parenteral administration make its current application limited (Griffith, Aksamit et al. 2007).

A new experimental liposome preparation, liposomal amikacin for inhalation (LAI), composed of dipalmitoylphosphatidilcholine (DPPC) and cholesterol containing encapsulated amikacin, has been developed for aerosol delivery for respiratory infection. Inhalation of LAI to the respiratory tract lowers the potential for ototoxicity and nephrotoxicity compared to systemic administration of amikacin and maintains higher concentration of drug in the lung and at the site of infection (Meers, Neville et al. 2008). LAI was effective for the treatment of *Pseudomonas aeruginosa* infection in a model of cystic fibrosis in rats and was shown to penetrate the *P. aeruginosa* biofilm (Meers, Neville et al. 2008). Recently, a phase II study using LAI for the treatment of *P. aeruginosa* in cystic fibrosis patients was reported, demonstrating the short-term efficacy, safety, and tolerability of the drug (Clancy, Dupont et al. 2013). In this current study, we established the efficacy of LAI against both intracellular MAH and Ma *in vitro* as well as in an experimental murine MAH respiratory infection.

Materials and Methods

Ethical statement. All the performed experiments were carried out according to the guidelines for animal ethics. All the experiments were reviewed and approved by the IACUC committee of Oregon State University (ACUP # 4257).

Bacteria. *M. avium* subsp. *hominissuis* strains MAH 104 and MAH A5 are blood isolates from patients with AIDS. MAH 3388 is a lung isolate from a patient with chronic pulmonary disease (kindly provided by Dr. Richard Wallace, University of Texas Health Science Center at Tyler, Tyler TX). *M. abscessus* subsp. *bolletii* Ma 26 and Ma 36 lung isolates were kindly provided by Dr. Steve Holland (National Institutes of Health). Each of the isolates was identified as MAH and Ma by using a commercially available DNA probe (Gen-Probe, San Diego CA). Ma 26 and 36 were further identified as subsp. *bolletii* by amplification and direct sequencing of the *erm*(41), *rpoB,* and *23s* genes by standard procedures and the primers used were sourced from Teng *et al.*(Teng, Chen et al. 2013). MAH 104 and A5 have been shown to be virulent in mice, but he other strains have not been tested in experimental models to date. MAH and Ma were cultured on Middlebrook 7H10 agar (Hardy Diagnostics, Santa Maria, CA), supplemented with oleic acid, albumin, dextrose, and catalase (OADC; Hardy Diagnostics, Santa Maria, CA) for 10 and 4 days, respectively, at 37°C. Only pure clones (transparent colonies) were used in the study.

Antimicrobial agents. Amikacin sulfate was purchased from Hospira, Inc. (Lake Forest, IL) and LAI (Lot #232-012-015 for *in vitro* experiments, Lot #3-NFF-0184 for *in vivo* experiments) was provided by Insmed Incorporated (Monmouth Junction, NJ). LAI is a liquid dispersion consisting of 70 mg/ml amikacin encapsulated in liposomes prepared from dipalmitoylphosphatidilcholine (DPPC) and cholesterol (2:1 mole ratio at a total lipid concentration of 40 mg/ml) in 1.5% NaCl. Placebo liposomes were made of DPPC and cholesterol at the same mole ratio and concentrations as LAI but contained no amikacin.

Macrophage test system. The source of macrophages was the THP-1 human monocyte cell line (ATCC, Manassas, VA) cultured in RPMI-1640 medium (Gibco, Chicago, IL) supplemented with 5% fetal bovine serum (Gemini, Sacramento, CA)

and 2 mM of L-glutamine. THP-1 cells were maintained at 37°C in an atmosphere of 5% CO_2. Assays were performed as previously described, with minor modifications (Bermudez, Inderlied et al. 2001). Monocytes were grown to 5 x 10^6 cells per ml, washed and resuspended to a concentration of 1 x 10^6 cells per ml, and 1 ml was seeded into a 24 well tissue culture plate (Costar, Cambridge, MA). Monolayers were then treated with 0.5 μg of phorbol myristate acetate per ml for 24 hours to stimulate the maturation of the monocytes.

Bacteria were prepared for infection by resuspension in Hank's buffered salt solution (HBSS) to concentrations of 3 x 10^8 CFU/ml by comparison with a McFarland #1 turbidity standard. Prior to the infection of macrophage monolayers, the suspension was vortex agitated for 2 minutes and passed through a 23-gauge needle ten times to disperse clumps. Microscopic observation confirmed the dispersion of the inoculum. Suspensions were serially diluted and plated onto 7H10 agar to confirm the concentration of the inoculum.

The monolayers were infected with MAH or Ma at a multiplicity of infection of 10:1. After 1 hour of infection, the extracellular bacteria were removed with 3 HBSS washes, and the intracellular infection was allowed to incubate for 24 hours. Following the establishment of the infection baseline, the addition of LAI or controls was performed once daily for 4 days. Lysis of THP-1 cells was carried out with a 10 minute incubation in 0.1% Triton X-100 in sterile H_2O followed by mixing, diluting, and plating onto 7H10 agar plates for CFU enumeration.

Mice. Six week-old female C57BL/6 mice were purchased from The Jackson Laboratory (Bar Harbor, ME) and delivered to the Laboratory Animal Research Center at Oregon State University, where they were acclimated for 7 days prior to experimentation.

Experimental respiratory infection of mice. Mice were infected intranasally with 2.25 x 10^7 CFU of MAH strain 104. To minimize sneezing or aspirating, each mouse was lightly sedated with brief exposure to isoflorane prior to inoculation. Infection was allowed to establish for three weeks, where at that point 12 mice were euthanized to determine the pre-treatment infection burden. Five groups of 12 mice

were used for treatment, including: 1 hour of saline inhalation every day for 28 days; 1 hour of LAI inhalation every day for 28 days; 2 hours of LAI inhalation every day for 14 days, then 14 days of no treatment; 2 hours of LAI inhalation every other day for 28 days; IP injected free amikacin IP administered once every day for 28 days. A 12 port Jaeger-NYU nose-only directed flow inhalation system (CH Technologies, Westwood, NJ) was used in conjunction with a Devilbiss 8650d compressor (Devilbiss, Jackson, TN) and LC Star nebulizers (Pari, Midlothian, VA), connected by flexible tubing (supplied with the nebulizers). The mice are fully conscious and not anesthetized while in the plastic restrainers for the duration of treatment. Five (5) ml of test article (either 1.5% NaCl or LAI) was placed inside a nebulizer and the system ran for 20 minutes at 30 psi. This was performed 3 times consecutively to achieve an inhalation time of 1 hour and 6 times consecutively to achieve an inhalation time of 2 hours. The nebulizers were weighed before and after every 20 minute cycle to assure consistent nebulization. The actual dose of delivered LAI into the plastic restrainers was determined multiple times throughout the 28 day treatment regimen, following a previously published protocol (Wolff and Dorato 1993). Amikacin sulfate was diluted in sterile HBSS to 100 mg/kg and administered intraperitoneally (IP) using a 28 gauge needle and restraining the non-anesthetized animal by a scruff grip.

Extraction and enumeration of bacteria from mice. Necropsies were performed and the lungs (containing bronchus and 0.5 cm of trachea) were aseptically excised and homogenized using a Bullet Blender (Next Advance, Averill Park, NY) following the manufacturer protocol for bacterial isolation from host tissue. Homogenized samples were then serially diluted and plated onto 7H10 agar plates for CFU enumeration.

Measuring amikacin resistance of bacteria recovered from mice. Two methods were employed to assess resistance of bacteria to amikacin. First, homogenate was serially diluted and plated onto 7H10 to allow individual colonies to grow. Individual colonies from three mice of each group were transferred into 7H9 broth to 3 x 10^8 CFU per ml using visual turbidity. Individual colonies from lab-

maintained MAH 104 were used to assess the baseline minimum inhibitory concentration (MIC) of the strain. Final solutions of 3 x 10^5 CFU per ml in 0.5 through 64 µg/ml of amikacin, in 7H9 broth, were shaken at 37˚C for 5 days. At this point, MICs were determined by assessing visual turbidity. Second, sample homogenates from groups all treatment groups were plated directly onto 7H10 agar with no antibiotic, 7H10 containing 32 µg/ml of amikacin, and 7H10 containing 64 µg/ml of amikacin. Plates were incubated at 37˚C for 14 days and CFU data was compared between the antibiotic and no antibiotic plates.

Statistical analysis. Pairwise comparisons made for the *in vitro* experiments were determined by the Mann-Whitney non-parametric test. Comparisons between multiple groups were conducted with ANOVA. Graph Pad Prism (La Jolla, CA) was used for statistical analyses and graphical outputs.

Results

LAI is more effective than free amikacin against intracellular mycobacteria in vitro. Previous work has demonstrated the effectiveness of LAI against extracellular *P. aeruginosa* in a rat model of respiratory infection (Meers, Neville et al. 2008). The aim of this study was to assess the efficacy of LAI against intracellular mycobacteria. It has been found that fluorescently labeled LAI is internalized by macrophages, via co-localization of it with the intracellular environment (unpublished data), which introduces the possibility of testing it against intracellular pathogens. We first investigated the effectiveness of LAI against *Mycobacterium avium* subsp. *hominissuis* (MAH) and *Mycobacterium abscessus* (Ma) *in vitro*. Monolayers of adherent THP-1 macrophages were infected with approximately 1 x 10^7 MAH for 1 hour. The extracellular (non-phagocytized) bacteria were removed by multiple washes, and the macrophages containing intracellular bacteria were incubated at 37°C for 24 hours and then treated with either compounds or controls. Free amikacin was used at 10 μg/ml and LAI was used at 1, 2, 4, 8, and 10 μg/ml of amikacin. MAH strains 104 (blood isolate), A5 (blood isolate; biofilm overproducer), and 3388 (lung isolate), were significantly inhibited by free amikacin and LAI, compared to the day 4 control and empty liposome treatment (Appendix Figure 1.1 A-C). At the concentration of 10 μg/ml, LAI treatment of MAH A5 and MAH 3388 was associated with significantly more killing compared with 10 μg/ml of free amikacin (Appendix Figure 1.1 B and C, respectively).

Macrophages infected with the strains Ma 36 and Ma 24 were treated with both amikacin and LAI leading to the killing of the intracellular Ma (Appendix Figure 1.1 D and E). LAI at 10 μg/ml was significantly more effective than free amikacin for both strains. Reductions in Ma CFUs appeared to show a linear dose dependence for LAI. Collectively, this demonstrates the effectiveness of LAI *in vitro* against intracellular NTM infection of macrophages.

LAI is comparable to parenterally administered free amikacin against intracellular mycobacteria in a murine respiratory infection. Due to the effectiveness of LAI against intracellular mycobacteria *in vitro*, an established murine

model was used to evaluate the efficacy of LAI for treatment of an experimental MAH respiratory infection (Yamazaki, Danelishvili et al. 2006; Bermudez, Motamedi et al. 2008). Mice were inoculated intranasally with MAH strain 104 and infection was allowed to establish for three weeks. Three different inhaled treatment regimens of LAI were compared with inhaled saline and 100 mg/kg/day free amikacin by IP injection. The three LAI treatment groups included 76 mg/kg/day (1 hour) for 28 consecutive days, 152 mg/kg/day (2 hours) for 14 consecutive days (and then 14 days of no treatment), and 152 mg/kg/day (2 hours) every other day over 28 days. Importantly, all three groups received the same cumulative amount of LAI by the end of the 28 day period. LAI was delivered at a lower daily dose (76 mg/kg/day) compared to injected soluble amikacin (100 mg/kg/day) based on data collected throughout the treatment regimen that determined the delivered dose. After 28 days of therapy, all mice were euthanized and lungs were processed for CFU.

All amikacin treatment groups significantly reduced the MAH burden in the mice, when compared with the inhaled saline control group (Appendix Figure 1.2). Furthermore, the groups that received one hour daily LAI inhalation and two hours every other day cleared more MAH than the group that received IP injected amikacin, despite the fact that these animals received 32% less amikacin over the course of the study (p not significant). The group that received two hours of LAI inhalation every other day also had more animals without culturable MAH than the IP injected amikacin group (42% and 25% of animals, respectively; Appendix Figure 1.2).

Bacteria recovered from lung homogenates were assessed for acquired resistance to amikacin, using two methods. First, homogenate from saline and LAI treated mice were plated onto 7H10 agar without antibiotic, and 7H10 containing 32 or 64 µg/ml of amikacin. No bacteria grew at either amikacin concentration for any of the homogenates tested (Appendix Table 1.1). Second, a broth dilution method was used to determine the actual minimum inhibitory concentration of MAH from various treatment groups to amikacin, which also yielded no differences from the saline treated and laboratory-maintained bacteria (Appendix Table 1.2). Both of these experiments indicate that resistance to amikacin was not acquired by MAH during the

28 days of therapy. Taken together, this data suggests that inhaled LAI treatment is effective against MAH infection of the airways in mice, and resistance to amikacin was not observed after the treatment regimen.

Discussion

Nontuberculous mycobacteria (NTM) are a cause of serious infection in patients with chronic pulmonary conditions. These infections progress slowly and in many cases have unsatisfactory response to antibiotic therapy (Griffith, Aksamit et al. 2007). Although MAH infections appear to respond to therapy initially, both the course of MAH and Ma infections are known to progress in despite of antimicrobial therapy. Therefore, new forms of therapy with limited toxicity are urgently needed. Inhaled preparations of aminoglycosides, that are active in the lung but have limited distribution in other tissues and that are associated with less toxicity than the free drug, are potentially a useful approach for new therapy.

In this study, liposomal amikacin for inhalation (LAI) showed significant activity against both intracellular MAH and Ma in a macrophage model *in vitro*. Notably, LAI was superior to comparable concentrations of free amikacin. The dynamic conditions in the lungs should favor LAI because of its deposition of higher local concentrations of amikacin. In fact, LAI reduced and eradicated *P. aeruginosa* in a rat lung model more effectively than inhaled free amikacin (Meers, Neville et al. 2008). However, this is the first time that the activity of LAI has been evaluated in an established *in vivo* system against an intracellular pathogen versus parenterally injected amikacin. In the present murine model, both inhaled LAI and parenteral administration of amikacin were very effective in reducing the CFU of MAH in the lungs of mice compared to inhaled saline. In a recent report describing a new experimental murine *M. tuberculosis* model for testing aerosolized drugs (Gonzalez-Juarrero, Woolhiser et al. 2012), the authors demonstrated that aerosolized amikacin was comparable to subcutaneously injected amikacin at reducing *M. tuberculosis* in the lungs, even with a lower dose used and less frequent administration. This data agrees with our results showing the efficacy of LAI against MAH in mice. Inhaled dry powder containing antibiotic has also shown promise for the treatment of *M. tuberculosis* infection (Garcia-Contreras, Sethuraman et al. 2006; Garcia-Contreras, Fiegel et al. 2007), and has even been recently evaluated in a phase I study in healthy individuals (Dharmadhikari, Kabadi et al. 2013). Collectively, this recent work

indicates that topical treatment of pulmonary mycobacterial infections could be feasible as a future treatment approach.

The *in vivo* effectiveness of LAI was comparable to injected free amikacin, even though a smaller dose of LAI was delivered. Although there was not a statistically significant difference in CFU reduction between the free amikacin group and two of the three LAI groups (one hour inhalation every day for 28 days and two hours inhalation every other day for 28 days), the mean CFU recovered in these two experimental groups were both smaller than the group treated with free amikacin, despite receiving 32% less drug. The data suggests that LAI might be more effective than the free amikacin in reducing MAH, which concurs with the observation *in vitro*.

It is well known that liposomal preparations achieve a greater intracellular concentration in phagocytes than free compounds (Briones, Colino et al. 2008). It is more evident in the case of aminoglycosides, which have limited ability to cross membranes of mammalian cells (Luedtke, Carmichael et al. 2003), therefore only achieving a small fraction of the extracellular concentration intracellularly. Liposomal preparations can efficiently penetrate cell membranes, but the ability to cross and concentrate within phagosomes can vary with the preparation. Liposomal amikacin and gentamicin preparations have been evaluated against MAH and have shown to be as active or more active than the free drug, both in a macrophage system, as well as in mice when delivered intravenously (Bermudez, Yau-Young et al. 1990). A possible advantage of achieving high concentrations of a compound at the site of infection, beyond the greater anti-bacterial activity, is the decreased chance for the development of antibiotic resistance. In this current study, development of resistance to amikacin was not observed in bacteria recovered from both mice treated with LAI or free amikacin (Appendix Table 1.1 and 1.2).

LAI was generally well tolerated in mice infected with NTM; however two animals were preemptively euthanized, following IACUC guidelines, due to adverse stress and subsequent weight loss (greater than 20% reduction from starting weight). These animals were in the group that received two hours of LAI daily for 14 days, and then no treatment for 14 days, even though they were euthanized before day 14.

Both animals displayed abnormal posture, rough hair coat, reduced mobility, decreased alertness, and labored breathing. The attending veterinarian determined that these symptoms were a result of the weight loss. There did not appear to be any gross pathology upon necropsy. Even though they were not included in the data presented in this study, the CFU in the lung of one of these animals was obtained and was at a level consistent with the other animals in the group, ruling out that an adverse response to infection was the source of the weight loss. All of the other mice receiving LAI in all three LAI treatment regimens actually gained weight over the course of the study and had a higher average weight than the inhaled saline group at the end of the study, suggesting that LAI was not the cause of the weight loss either. Thus the stress of two hours of daily confinement in the inhalation chamber may have led to an eating disorder in these two animals, which has been seen in mice that are merely restrained and not treated with any test articles (Laugero and Moberg 2000).

In summary, this study demonstrated that LAI is active against MAH and Ma *in vitro* at concentrations easily achieved in the airways and respiratory mucosa. Additionally, a lower dose of LAI administered topically via inhalation was comparable to parenterally administered amikacin in the treatment of MAH lung infection in mice, with no resistance to amikacin observed in bacteria recovered after the various treatment regimens. These data suggest that LAI be further investigated as a new treatment option for NTM respiratory infection. Currently, a phase 2 clinical trial with LAI for the treatment of patients with NTM infection is underway in the US, including at the National Institutes of Health and Infectious Diseases (ClinicalTrials.gov Identifier: NCT01315236).

Acknowledgements

We thank Nicholas Milani, Zhili Li, and Conor Zoebelein for their technical assistance with the animal study. This work was supported by Insmed Incorporated.

Appendix Figure 1.1. Efficacy of LAI against intracellular mycobacteria *in vitro*. LAI, a liposome-encapsulated amikacin compound, was tested against intracellular *M. avium* subsp. *hominissuis* (MAH) and *M. abscessus* (Ma) *in vitro*. THP-1 human cells (that were first differentiated and adhered with PMA) were infected with a 10:1 MOI of MAH strains 104 and A5, which are blood isolates (A and B, respectfully), MAH 3388, a lung isolate (C), and Ma strains 26 and 36, which are also lung isolates (D and E, respectively) for 1 hour. Extracellular bacteria were removed and cells containing internalized bacteria were incubated at 37˚C for 24 hours. Wells were either plated for CFU (day 0 control) or treated daily with HBSS (day 4 control), empty liposome, 10 μg/ml amikacin sulfate, or between 10 and 1 μg/ml of LAI for 4 days. Cells were disrupted, diluted, and plated to obtain CFUs of surviving bacteria. Bars represent means of CFU counts and error bars represent standard deviation. Statistical comparisons: 1 = $p < 0.05$ compared to day 0 control; 2 = $p < 0.05$ compared to day 4 control; 3 = $p < 0.05$ compared to empty liposome; 4 = $p < 0.05$ compared to free amikacin.

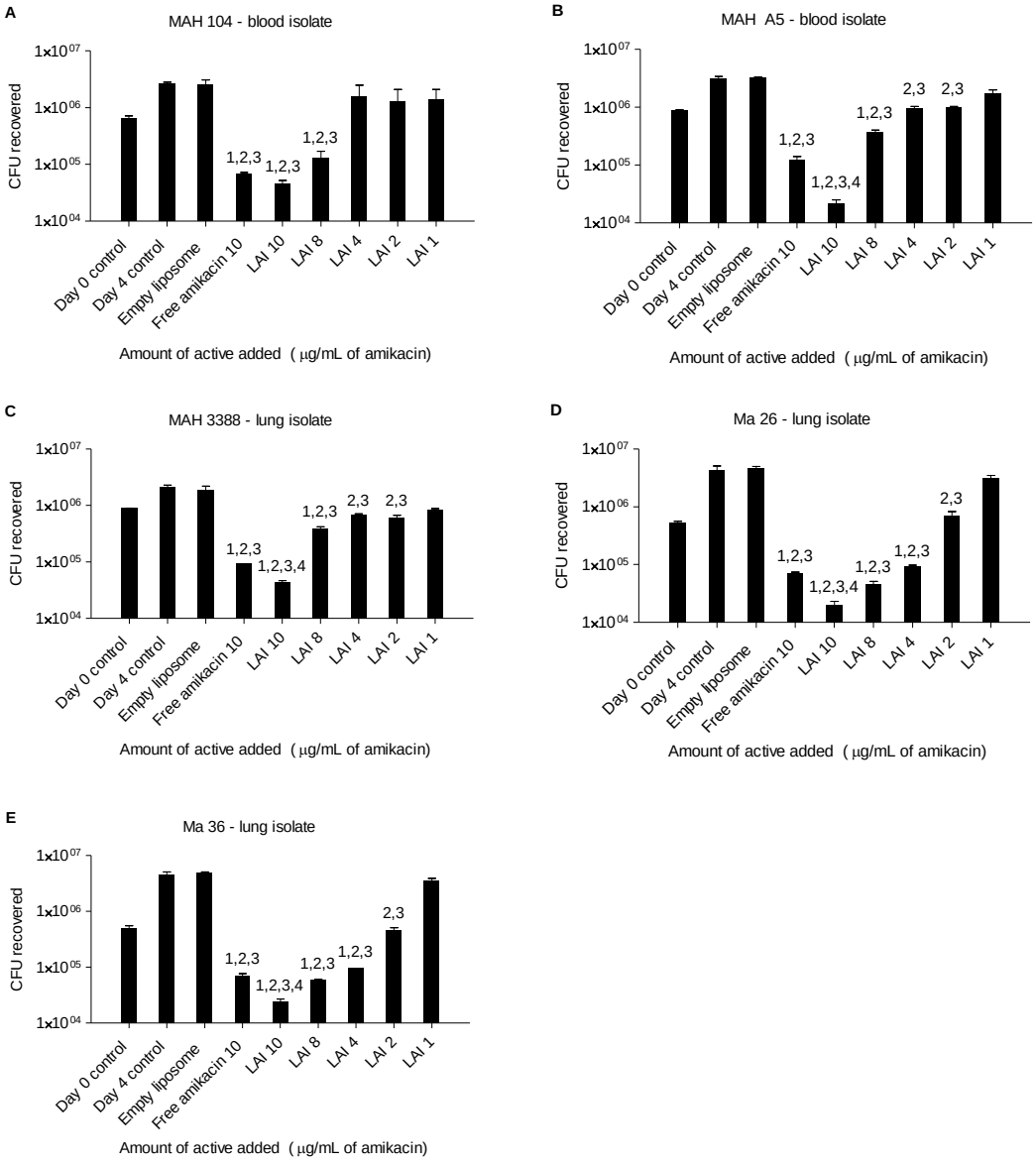

Appendix Figure 1.1. Efficacy of LAI against intracellular mycobacteria *in vitro*.

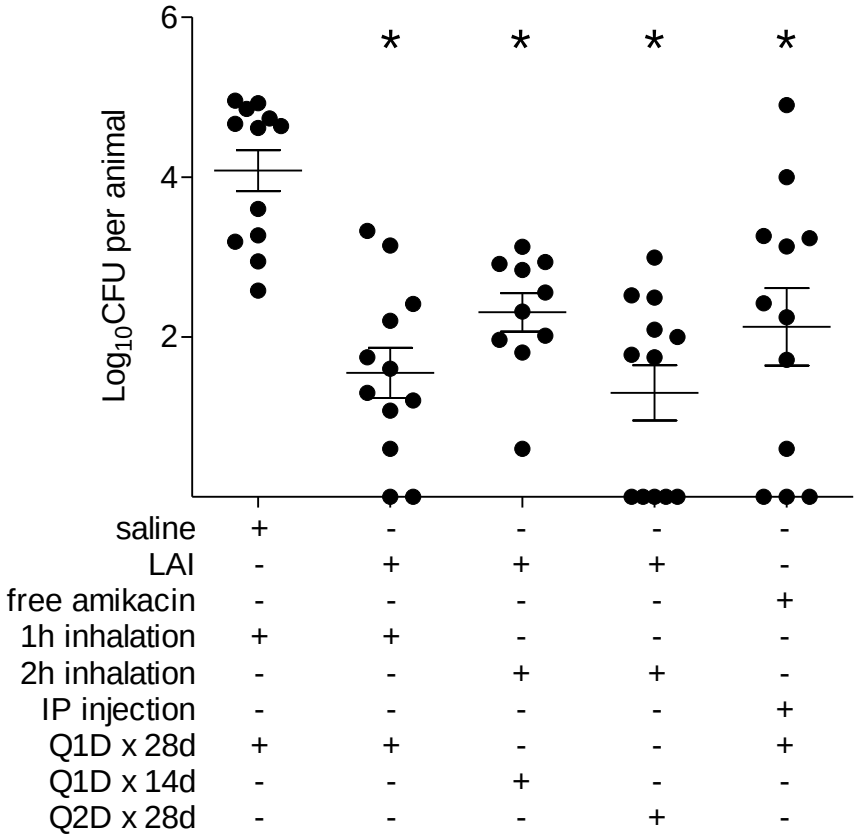

Appendix Figure 1.2. Efficacy of inhaled LAI compared to parenterally administered free amikacin in murine respiratory infection. Six groups of 12 mice were intranasally infected with MAH 104 and a respiratory infection was allowed to establish for three weeks. At this point, an initial group of 12 mice were euthanized to determine the pre-treatment burden of MAH 104 in the respiratory tract. The other 5 groups received either saline, LAI, or amikacin sulfate by various delivery routes and treatment regimens, as listed in the figure. Twenty-eight days after the initiation of treatment, all mice were euthanized and lungs were processed to determine the post-treatment MAH 104 burden. Dots resting on the x-axis are animals that had no culturable MAH in their lungs. Abbreviations: QID x 28d = treatment every day for 28d; Q1D x 14d = treatment every other day for 14d, then no treatment for 14d; Q2D x 28d = treatment every other day for 28d. Horizontal lines represent the mean and SEM. Statistical comparisons: * = $p < 0.05$ compared with inhaled saline control.

Appendix Table 1.1. Amikacin resistance testing on bacteria grown from lung homogenate after treatment regimen.

Source of bacteria		Bacterial growth (Y/N)		
Treatment regimen	**# of mice sampled**	**0ug/ml**	**32ug/ml**	**64ug/ml**
Saline 1h Q1D x 28d	5	Y	N	N
LAI 1h Q1D x 28d	5	Y	N	N
LAI 2h Q1D x 14d	3	Y	N	N
LAI 2h Q2D x 28d	1	Y	N	N

Appendix Table 1.2. Amikacin minimum inhibitory concentration determination on colonies isolated from lung homogenate after treatment regimen.

Treatment regimen	# of mice sampled	# of colonies tested*	MIC (µg/ml)
Saline 1h Q1D x 28d	2	6	4
LAI 1h Q1D x 28d	2	6	4
LAI 2h Q1D x 14d	2	6	4
LAI 2h Q2D x 28d	2	6	4
IP amikacin Q1D x 28d	2	6	4
lab-maintained control†	N/A	3	4

* three (3) colonies were isolated and tested from each mouse lung homogenate

† lab-maintained MAH 104 (not recovered from infected mice) was used as a baseline

References

Bermudez, L. E., C. B. Inderlied, et al. (2001). "Telithromycin is active against *Mycobacterium avium* in mice despite lacking significant activity in standard *in vitro* and macrophage assays and is associated with low frequency of resistance during treatment." Antimicrob Agents Chemother **45**(8): 2210-2214.

Bermudez, L. E., N. Motamedi, et al. (2008). "The efficacy of clarithromycin and the bicyclolide EDP-420 against Mycobacterium avium in a mouse model of pulmonary infection." J Infect Dis **197**(11): 1506-1510.

Bermudez, L. E., A. O. Yau-Young, et al. (1990). "Treatment of disseminated *Mycobacterium avium* complex infection of beige mice with liposome-encapsulated aminoglycosides." J Infect Dis **161**(6): 1262-1268.

Briones, E., C. I. Colino, et al. (2008). "Delivery systems to increase the selectivity of antibiotics in phagocytic cells." J Control Release **125**(3): 210-227.

Carter, G., M. Wu, et al. (2003). "Characterization of biofilm formation by clinical isolates of Mycobacterium avium." J Med Microbiol **52**(Pt 9): 747-752.

Clancy, J. P., L. Dupont, et al. (2013). "Phase II studies of nebulised Arikace in CF patients with Pseudomonas aeruginosa infection." Thorax **68**(9): 818-825.

Dharmadhikari, A. S., M. Kabadi, et al. (2013). "Phase I, single-dose, dose-escalating study of inhaled dry powder capreomycin: a new approach to therapy of drug-resistant tuberculosis." Antimicrob Agents Chemother **57**(6): 2613-2619.

Garcia-Contreras, L., J. Fiegel, et al. (2007). "Inhaled large porous particles of capreomycin for treatment of tuberculosis in a guinea pig model." Antimicrob Agents Chemother **51**(8): 2830-2836.

Garcia-Contreras, L., V. Sethuraman, et al. (2006). "Evaluation of dosing regimen of respirable rifampicin biodegradable microspheres in the treatment of tuberculosis in the guinea pig." J Antimicrob Chemother **58**(5): 980-986.

Gonzalez-Juarrero, M., L. K. Woolhiser, et al. (2012). "Mouse model for efficacy testing of antituberculosis agents via intrapulmonary delivery." Antimicrob Agents Chemother **56**(7): 3957-3959.

Greendyke, R. and T. F. Byrd (2008). "Differential antibiotic susceptibility of *Mycobacterium abscessus* variants in biofilms and macrophages compared to that of planktonic bacteria." Antimicrob Agents Chemother **52**(6): 2019-2026.

Griffith, D. E. (2011). "The talking Mycobacterium abscessus blues." Clin Infect Dis **52**(5): 572-574.

Griffith, D. E., T. Aksamit, et al. (2007). "An official ATS/IDSA statement: diagnosis, treatment, and prevention of nontuberculous mycobacterial diseases." Am J Respir Crit Care Med **175**(4): 367-416.

Horsburgh, C. R., Jr. (1991). "*Mycobacterium avium* complex infection in the acquired immunodeficiency syndrome." N Engl J Med **324**(19): 1332-1338.

Iseman, M. D. (1989). "*Mycobacterium avium* complex and the normal host: the other side of the coin." N Engl J Med **321**(13): 896-898.

Johnson, M. M. and J. A. Odell (2014). "Nontuberculous mycobacterial pulmonary infections." J Thorac Dis **6**(3): 210-220.

Kilby, J. M., P. H. Gilligan, et al. (1992). "Nontuberculous mycobacteria in adult patients with cystic fibrosis." Chest **102**(1): 70-75.

Laugero, K. D. and G. P. Moberg (2000). "Energetic response to repeated restraint stress in rapidly growing mice." Am J Physiol Endocrinol Metab **279**(1): E33-43.

Luedtke, N. W., P. Carmichael, et al. (2003). "Cellular uptake of aminoglycosides, guanidinoglycosides, and poly-arginine." J Am Chem Soc **125**(41): 12374-12375.

Meers, P., M. Neville, et al. (2008). "Biofilm penetration, triggered release and in vivo activity of inhaled liposomal amikacin in chronic Pseudomonas aeruginosa lung infections." J Antimicrob Chemother **61**(4): 859-868.

Nash, K. A., B. A. Brown-Elliott, et al. (2009). "A novel gene, erm(41), confers inducible macrolide resistance to clinical isolates of Mycobacterium abscessus but is absent from Mycobacterium chelonae." Antimicrob Agents Chemother **53**(4): 1367-1376.

Teng, S. H., C. M. Chen, et al. (2013). "Matrix-assisted laser desorption ionization-time of flight mass spectrometry can accurately differentiate between Mycobacterium masilliense (M. abscessus subspecies bolletti) and M. abscessus (sensu stricto)." J Clin Microbiol **51**(9): 3113-3116.

Wolff, R. K. and M. A. Dorato (1993). "Toxicologic testing of inhaled pharmaceutical aerosols." Crit Rev Toxicol **23**(4): 343-369.

Yamazaki, Y., L. Danelishvili, et al. (2006). "The ability to form biofilm influences Mycobacterium avium invasion and translocation of bronchial epithelial cells." Cell Microbiol **8**(5): 806-814.

Appendix 2. Abstracts of Additional Manuscripts

Appendix 2.1

Beta-Lactam Antibiotic Resistance Among *Enterobacter* spp. Isolated from Infection in Animals

Authors: M.S. Wilberger*, K.E. Anthony*, S. Rose, M. McClain, and L.E. Bermudez
*These authors contributed equally to this work

Journal: Advances in Microbiology. 2012. 2:129-137.

Abstract:
Nosocomial infections are frequent complications of hospitalization, caused by opportunistic pathogens that gain access to hosts undergoing invasive procedures, such as surgery, intubation, and placement of deep vein lines. Nosocomial infections in animal hospitals can infect other animals, as well as be transmitted to human personnel. *Enterobacter* is a genus of common gram-negative bacteria, which can be associated with antibiotic resistant hospital infections. Because of an outbreak in antibiotic resistance in the genus, we decided to investigate five years of *Enterobacter* infections in the Large Animal Services of the Lois Bates Acheson Veterinary Teaching Hospital (LBAVTH) at Oregon State University. The demographics from 37 *Enterobacter*-infected patients of the LBAVTH were obtained from charts and analyzed. The identified clusters of infections suggested possible patient-environment sources of infection. The environment of the hospital was sampled in an attempt to determine the source of infection. Although *Enterobacter* was not isolated, three of the collected samples contained bacteria with resistance to third-generation cephalosporins. *Enterobacter* isolates from six of the 37 patients were further analyzed for presence of specific ESBL resistance genes. All six of the isolates harbored multiple extended-spectrum beta-lactamase genes, i.e., CTX-M-15, TEM-80, SHV-2 and AmpC. In summary, *Enterobacter* infection in the veterinary hospital

was caused by beta-lactam-resistant strains, carrying ESBL-resistant genes. Veterinary hospital personnel should be aware of the potential for transmission, to both humans and animals, of ESBL-gene-containing bacteria.

Appendix 2.2

Imported Ornamental Fish are Colonized with Antibiotic-Resistant Bacteria

Authors: S. Rose*, R. Hill*, L.E. Bermudez, and T. Miller-Morgan
*These authors contributed equally to this work

Journal: Journal of Fish Diseases. 2013. 36:533-542.

Abstract:
There has been growing concern about the overuse of antibiotics in the ornamental fish industry and its possible effect on the increasing drug resistance in both commensal and pathogenic organisms in these fish. The aim of this study was to carry out an assessment of the diversity of bacteria, including pathogens, in ornamental fish species imported into North America and to assess their antibiotic resistance. Kidney samples were collected from 32 freshwater ornamental fish of various species, which arrived to an importing facility in Portland, Oregon from Colombia, Singapore and Florida. Sixty-four unique bacterial colonies were isolated and identified by PCR using bacterial 16S primers and DNA sequencing. Multiple isolates were identified as bacteria with potential to cause disease in both fish and humans. The antibiotic resistance profile of each isolate was performed for nine different antibiotics. Among them, cefotaxime (16% resistance among isolates) was the antibiotic associated with more activity, while the least active was tetracycline (77% resistant). Knowing information about the diversity of bacteria in imported ornamental fish, as well as the resistance profiles for the bacteria will be useful in more effectively treating clinical infected fish, and also potential zoonoses in the future.

Appendix 2.3

Evaluation of Eight Live Attenuated Vaccine Candidates for Protection Against Challenge with Virulent *Mycobacterium avium* subspecies *paratuberculosis* in Mice

Authors: J.P. Bannantine, J.L. Everman, S. Rose, L. Babrak, R. Katani, R.G. Barletta, A.M. Talaat, Y.T. Grohn, Y. Chang, V. Kapur, and L.E. Bermudez

Journal: Frontiers in Cellular and Infection Microbiology. 2014. 4:84.

Abstract:
Johne's disease is caused by *Mycobacterium avium* subsp. *paratuberculosis* (MAP), which results in serious economic losses worldwide in farmed livestock such as cattle, sheep, and goats. To control this disease, an effective vaccine with minimal adverse effects is needed. In order to identify a live vaccine for Johne's disease, we evaluated eight attenuated mutant strains of MAP using a C57BL/6 mouse model. The persistence of the vaccine candidates was measured at 6, 12, and 18 weeks post vaccination. Only strains 320, 321, and 329 colonized both the liver and spleens up until the 12-week time point. The remaining five mutants showed no survival in those tissues, indicating their complete attenuation in the mouse model. The candidate vaccine strains demonstrated different levels of protection based on colonization of the challenge strain in liver and spleen tissues at 12 and 18 weeks post vaccination. Based on total MAP burden in both tissues at both time points, strain 315 (MAP1566::Tn5370) was the most protective whereas strain 318 (intergenic Tn5367 insertion between MAP0282c and MAP0283c) had the most colonization. Mice vaccinated with an undiluted commercial vaccine preparation displayed the highest bacterial burden as well as enlarged spleens indicative of a strong infection. Selected vaccine strains that showed promise in the mouse model were moved forward into a goat challenge model. The results suggest that the mouse trial, as conducted, may have a relatively poor predictive value for protection in a ruminant host such as goats.

Appendix 2.4

Mycobacterium tuberculosis Alters the Metalloprotease Activity of the COP9 Signalosome

Authors: L. Danelishvili, L. Babrak*, S.J. Rose*, J. Everman, and L.E. Bermudez
*These authors contributed equally to this work

Journal: mBio. 2014. 5:e01278-14.

Abstract:
Inhibition of apoptotic death of macrophages by *Mycobacterium tuberculosis* represents an important mechanism of virulence that results in pathogen survival both in vitro and in vivo. To identify *M. tuberculosis* virulence determinants involved in the modulation of apoptosis, we previously screened a transposon bank of mutants in human macrophages, and an *M. tuberculosis* clone with a nonfunctional Rv3354 gene was identified as incompetent to suppress apoptosis. Here, we show that the Rv3354 gene encodes a protein kinase that is secreted within mononuclear phagocytic cells and is required for *M. tuberculosis* virulence. The Rv3354 effector targets the metalloprotease (JAMM) domain within subunit 5 of the COP9 signalosome (CSN5), resulting in suppression of apoptosis and in the destabilization of CSN function and regulatory cullin-RING ubiquitin E3 enzymatic activity. Our observation suggests that alteration of the metalloprotease activity of CSN by Rv3354 possibly prevents the ubiquitin-dependent proteolysis of *M. tuberculosis*-secreted proteins.

Appendix 2.5

The Environment of *Mycobacterium avium* subsp. *hominissuis* Microaggregates Induces the Synthesis of Small Proteins Associated with Efficient Infection of the Respiratory Epithelial Cells

Authors: L. Babrak, L. Danelishvili, S.J. Rose, T. Kornberg, and L.E. Bermudez

Journal: Infection and Immunity. 2014. 83(2): 625-636.

Abstract:

Mycobacterium avium subsp. *hominissuis* is an opportunistic environmental pathogen that causes respiratory illness in immunocompromised patients, such as those with cystic fibrosis as well as other chronic respiratory diseases. Currently, there is no efficient approach to prevent or treat *M. avium* subsp. *hominissuis* infection in the lungs. During initial colonization of the airways, *M. avium* subsp. *hominissuis* forms microaggregates composed of 3 to 20 bacteria on human respiratory epithelial cells, which provides an environment for phenotypic changes leading to efficient mucosal invasion in vitro and in vivo. DNA microarray analysis was employed to identify genes associated with the microaggregate phenotype. The gene encoding microaggregate-binding protein 1 (MBP-1) (MAV_3013) is highly expressed during microaggregate formation. When expressed in noninvasive *Mycobacterium smegmatis*, MBP-1 increased the ability of the bacteria to bind to HEp-2 epithelial cells. Using anti-MBP-1 immune serum, microaggregate binding to HEp-2 cells was significantly reduced. By far-Western blotting, and verified by coimmunoprecipitation, we observed that MBP-1 interacts with the host cytoskeletal protein vimentin. As visualized by confocal microscopy, microaggregates, as well as MBP-1, induced vimentin polymerization at the site of bacterium-host cell contact. Binding of microaggregates to HEp-2 cells was inhibited by treatment with an antivimentin antibody, suggesting that MBP-1 expression is important for *M. avium* subsp. *hominissuis* adherence to the host cell. MBP-1 immune serum significantly

inhibited *M. avium* subsp. *hominissuis* infection throughout the respiratory tracts of mice. This study characterizes a pathogenic mechanism utilized by *M. avium* subsp. *hominissuis* to bind and invade the host respiratory epithelium, suggesting new potential targets for the development of antivirulence therapy.

Appendix 2.6

Microaggregate-associated Protein Involved in Invasion of Epithelial Cells by *Mycobacterium avium* subsp. *hominissuis*

Authors: L. Babrak, L. Danelishvili, S.J. Rose, and L.E. Bermudez

Journal: Virulence. 2015. 6(7): 694-703.

Abstract:
The environmental opportunistic pathogen *Mycobacterium avium* subsp *hominissuis* (MAH), a member of the nontuberculous mycobacteria (NTM) cluster, causes respiratory as well as disseminated disease in patients such as those with chronic respiratory illnesses or AIDS. Currently, there is no effective method to prevent NTM respiratory infections. The formation of mycobacterial microaggregates comprises of phenotypic changes that lead to efficient adherence and invasion of the respiratory mucosa in vitro and in vivo. Microaggregate adhesion to the respiratory epithelium is mediated in part through the mycobacterial protein, MAV_3013 (MBP-1). Through DNA microarray analysis, the small hypothetical gene MAV_0831 (Microaggregate Invasion Protein-1, MIP-1) was identified as being upregulated during microaggregate formation. When MIP-1 was overexpressed in poorly-invasive *Mycobacterium smegmatis*, it provided the bacterium the ability to bind and enter epithelial cells. In addition, incubating microaggregates with recombinant MIP-1 protein enhanced the ability of microaggregates to invade HEp-2 cells, and exposure to anti-MIP-1 immune serum reduced the invasion of the host epithelium. Through protein-protein interaction assays, MIP-1 was found to bind to the host protein filamin A, a cytoskeletal actin-binding protein integral to the modulation of host cell shape and migration. As visualized by immunofluorescence, filamin A was able to co-localize with microaggregates and to a lesser extent planktonic bacteria. Invasion of HEp-2 cells by microaggregates and planktonic bacteria was also inhibited by the addition of anti-filamin A antibody suggesting that filamin A plays an important role

during infection. In addition, at earlier time points binding and invasion assay results suggest that MBP-1 participates significantly during the first interactions with the host cell while MIP-1 becomes important once the bacteria adhere to the host epithelium. In summary, we have unveiled one more step associated with MAH crossing the respiratory mucosa.

Appendix 2.7

A Rhesus Macaque Model of Pulmonary Nontuberculous Mycobacterial Disease

Authors: K. Winthrop, A. Rivera, F. Engelmann, S. Rose, A. Lewis, J. Ku, L. Bermudez, and I. Messaoudi

Journal: American Journal of Respiratory Cell and Molecular Biology. 2016. 54(2): 170-176.

Abstract:
In this study, we sought to develop a nonhuman primate model of pulmonary Mycobacterium avium complex (MAC) disease. Blood and bronchoalveolar lavage fluid were collected from three female rhesus macaques infected intrabronchially with escalating doses of *M. avium* subsp. *hominissuis*. Immunity was determined by measuring cytokine levels, lymphocyte proliferation, and antigen-specific responses. Disease progression was monitored clinically and microbiologically with serial thoracic radiographs, computed tomography scans, and quantitative mycobacterial cultures. The animal subjected to the highest inoculum showed evidence of chronic pulmonary MAC disease. Therefore, rhesus macaques could provide a robust model in which to investigate host–pathogen interactions during MAC infection.

Appendix 2.8

Comparative Genomic Analysis of Four *Mycobacterium avium* subsp. *hominissuis* Isolates

Authors: B. Jeffrey, S.J. Rose, K. Gilbert, and L.E. Bermudez

Journal: Submitted to the Journal of Medical Microbiology.

Abstract:
Mycobacterium avium subsp. *hominissuis* is a member of the *Mycobacterium avium* complex (MAC). *M. avium* is isolated causing lung infection or disseminated infection in patients with immunosuppression or chronic disease. *M. avium* is a heterogeneous group of bacteria and virulence can vary substantially depending on the strain. In this work, the genomic sequences of four *M. avium* subsp. *hominissuis* isolates obtained from clinical specimens were completed. MAC101, MAC100 and MACA5 were isolates from the blood of patients with AIDS, while MAC3388 was isolated from the lungs of a patient with chronic lung disease. The sequences were also annotated using the MAC104 isolate sequence blueprint existing in the Database. The results showed that while MAC101 is very similar to MAC104, the other strains genomes when compared express signs of significant divergence. Several of the virulence-related genes are expressed differently among the isolates. The sequences not only provide important information about *M. avium* heterogenicity and evolution as a pathogen, but also offer the chance to augment the understanding about virulence determinants in *M. avium*.

Appendix 2.9

The Identification of *Mycobacterium avium* subsp. *hominissuis* Intracellular Secreted Proteins Using an In Vitro System Mimicking the Phagosomal Environment

Authors: J.J. Chinison*, L.M. Babrak*, S.J. Rose*, R. Gupta, L. Danelishvili, and L.E. Bermudez

*These authors contributed equally to this work

Journal: Submitted to the journal Scientific Reports.

Abstract:

Mycobacteria, like many other intracellular pathogens, use diverse mechanisms to alter phagosome maturation and survive inside of host cells. In *Mycobacterium avium*, however, what proteins are secreted, how they are secreted, and what host processes they interact with remain largely elusive. Since secretion of bacterial proteins intracellularly may be triggered by phagosomal environment cues, we utilized a previously established in vitro system that mimics the metal ion concentrations and pH of the *M. avium* phagosome at 24 hours post-infection, to study secreted proteins unique to this environment. *M. avium* was exposed to this metal mixture for 4 and 24 hours and exported proteins were compared it to proteins secreted by bacteria exposed to control 7H9 broth. Mass spectrometric analysis of the secreted proteome identified 55 total proteins, with 46 of those being unique to bacteria in the metal mixture. Ten of these proteins were selected and tracked during THP-1 phagocyte infection using a beta-lactamase FRET-based reporter system. All ten proteins were confirmed to be secreted intracellularly. The gene expression of the 10 selected genes was comparable between the metal mixture and the 7H9 broth, indicating that instead of or besides production, the metal mixture likely stimulates secretion of these pre-made proteins. In conclusion, we established an in vitro system for studying intracellular M. avium protein secretion and revealed that the metal mixture triggers protein secretion mechanism(s) that have yet to be determined.